Two Dimensional Genetic Approach to the Development of a Controllable Lytic Phage Display System

by

Katlyn A. Sheldon

A thesis
presented to the University of Waterloo
in fulfillment of the
thesis requirement for the degree of
Master of Science
in
Biology

Waterloo, Ontario, Canada, 2013

AUTHOR'S DECLARATION

I hereby declare that I am the sole author of this thesis. This is a true copy of the thesis, including any required final revisions, as accepted by my examiners.

I understand that my thesis may be made electronically available to the public.

Abstract

Bacteriophage Lambda (λ) has played a historical role as an essential model contributing to our current understanding of molecular genetics. Lambda's major capsid protein "gpD" occurs on each capsid at 405 to 420 copies per phage in homotrimeric form and functions to stabilize the head and likely to compact the genomic DNA. The interesting conformation of this protein allows for its exploitation through the genetic fusion of peptides or proteins to either the amino or carboxy terminal end of gpD, while retaining phage assembly functionality and viability. The lytic nature of λ and the conformation of gpD in capsid assembly makes this display system superior to other display options.

Despite previous reports of λ as a phage display candidate, decorative control of the phage remains an elusive concept. The primary goal of this study was to design and construct a highly controllable head decoration system governed by two genetic conditional regulation systems; plasmid-mediated temperature sensitive repressor expression and bacterial conditional amber mutation suppression.

The historical λ *Dam15* conditional allele results in a truncated gpD fragment when translated in nonsuppressor, wild-type *E. coli* cells, resulting in unassembled, nonviable progeny. I sequenced the *Dam15* allele, identifying an amber (UAG) translational stop at the 68th codon. Employing this mutant in combination with a newly created isogenic cellular background utilizing the amber suppressors SupD (Serine), SupE (Glutamine), SupF (Tyrosine) and Sup^{-} (wild type), we sought to control the level of incorporation of undecorated gpD products. As a second dimension, I constructed two separate temperature-inducile plasmids whereby expression of either *D* or *D::eGFP* was governed by the λ strong λ CI[Ts]857 temperature-sensitive repressor and expressed from the λ P_L strong promoter.

Our aim was to measure the decoration of the λ capsid by a *D::gfp* fusion under varying conditions regulated by both temperature and presence of suppression. This was achieved utilizing this controllable system, enabling the measurement of a variable number of fusions per phage based on diverse genetic and physical environments without significantly compromising phage viability. Surprisingly, both SupE and SupF showed similar levels of *Dam15* suppression, even though sequencing data indicated that only SupE could restore the native gpD sequence at amino acid 68 (Q). In contrast, SupD (S), conferred very weak levels of suppression, but imparted an environment for very high decoration of gpD::eGFP per capsid, even at lower (repressed) temperatures. The presence of albeit few wild-type gpD molecules allowed for an even greater display than that of the perceived "100%" decoration scenario provided by the nonsuppressor strain. It appears that the lack of wild-type gpD does not allow for the space required to display the maximum number of fusions and in turn creates an environment that affects both phage assembly and therefore phage viability. Finally, the use of Western blotting, confirmed the presence of gpD::eGFP fusion decoration by employing a polyclonal anti-eGFP antibody.

The significance of this work relates to the unique structure of λ's capsid and its ability to exploit gpD in the design of controlled expression, which is guiding future research examining the fusion of different therapeutic peptides and proteins. Furthermore this approach has important implications specifically for the design of novel vaccines and delivery vehicles for targeted gene

therapy in which steric hindrance and avidity are important concerns.

The execution of this project employed basic bacterial genetics, phage biology and molecular biology techniques in the construction of bacterial strains and plasmids and the characterization of the phage display system.

Acknowledgements

I would like to extend a huge thank you to Dr. Roderick Slavcev for the opportunity to work in his lab, I have learned a great deal about scientific research and phage biology over the past four years and have seen tremendous growth and development in myself.

I would also like to thank my committee members Dr. Christine Dupont, Dr. John Honek and Dr. Barbara Moffat for their guidance, input and overall assistance throughout my graduate degree.

A special thanks to Jeff Kruk and the Beazely lab for their assistance with the fluorescent exposures and Dr. Sang Lee and the Moffatt lab for their help with the Western Blotting, I could not have completed my experiments without your aid.

Another big thank you to Nafiseh Nafissi for your constant and consistent friendship, humour and warmth and for being the wall I could bounce things off of over the past four years and to Dr. Tranum Kaur and Dr. Ola Wasfi for their help and suggestions along the way. In addition, thank you to Alex Kerstens, Gary Tran and Brandon Wong for helping with experiments and allowing me to practice my mentorship skills, hopefully you were able to learn some science in the process. Also, thank you to all of the graduate students at the School of Pharmacy for making my graduate studies interesting and eventful, we all have had a unique experience, which we will undoubtedly remember for many years to come.

Lastly, I would like to thank my parents, family and friends for their love, support and constant encouragement throughout my entire university studies.

Dedication

To Mom and Dad, for always being there.

Table of Contents

List of Figures

List of Tables

List of Abbreviations

a.a.	Amino acid
Ap	Ampicillin
AS	Amber Suppressor
bp	Base pair
$CaCl_2$	Calcium Chloride
cDNA	Complementary DNA
cfu	Colony forming unit
$CHCl_3$	Chloroform
ddH_2O	Double-distilled water
DNA	Deoxyribonucleic acid
ds	Double stranded
EDTA	Ethylenediaminetetraacetic acid
eGFP	Enhance Green Fluorescent Protein
ELISA	Enzyme-linked immunosorbent assay
eop	Efficiency of Plating
GFP	Green Fluorescent Protein
HCV	Hepatitis C Virus
HIV	Human Immunodeficiency Virus
Hoc	Head Outer Capsid protein (Enterobacteria phage T4)
kb	Kilobase
Kn	Kanamycin
λ	Lambda
LB	Luria broth
luc	Luciferase enzyme
Mg^{2+}	Magnesium
pfu	Plaque forming unit
PIII	Minor coat protein (Filamentous phage)
PVIII	Major coat protein (Filamentous phage)
RSV	Human Respiratory Syncytial Virus
SDS	Sodium dodecyl sulfate
shp	Head decoration protein (Enterobacteria phage P21)
Soc	Small Outer Capsid Protein (Enterobacteria phage T4)
SPA	Sequential Peptide Affinity
TAT	Trans-Activator of Transcription protein (Human Immunodeficiency Virus)
Tc	Tetracyline
Tn*10,* Tc^R	Transposon *10* (conferring) Tetracycline Resistance
tRNA	Transfer RNA

Chapter 1 General Introduction

1.1 Discovery of Bacteriophages and Bacteriophage λ

The term Bacteriophage (phage) was first derived from the word bacteria and the Greek word *phagein* meaning "to eat". Phage number in the range of 10^{31} total on the planet and have long been exploited as a founding piece in the fields of molecular and microbial biology. Simply defined as viruses that infect bacteria, they have been part of a continuing dialogue throughout the last century (d'Herelle, Smith 1926). Discovered independently in 1915 and 1917 by two separate researchers; British bacteriologist Frederick Twort and French-Canadian microbiologist Félix d'Hérelle, phage have continued to play a significant role in our early understanding of microbial genetics (d'Herelle, Smith 1926, Twort 1915, Duckworth 1976).

One of the first papers published on bacteriophages (Twort, 1915) described what he called “ultra-microscopic viruses”. His initial experiments involved the filtration of phage, where he found it difficult to obtain proof of their existence aside from their antibacterial effects and was unable to show growth on many types of media or show the infection of a variety of different animal species. Here he also recorded the first observation of plaques, which he explained as “transparent colonies” (Twort 1915).

In 1926 d'Hérelle published a book entitled “The Bacteriophage and Its Behavior”, where he examined many aspects of phage and recounted his discoveries in using phage to treat dysentery. He chronicled these stories in “On an Invisible Microbe Antagonistic to Dysentery Bacteria", where he ran into many of the initial culturing problems of Twort (Duckworth 1976, d'Herelle, Smith 1926). D'Hérelle makes reference to the work done by Twort, and the use of ultrafiltration and presence of plaques referring to them as “dissolution of the bacterial cell”. D'Hérelle also examined the minimum and maximum amount of bacteriophage required to induce “bacteriophagy” and went on to test the effects of many substances and conditions on viability of phage (d'Herelle, Smith 1926).

Among the earliest studies of phage, bacteriophage λ has played an essential role in the development and understanding of bacterial genetics and has long been used in the development of biological tools. Decades after phage were first isolated, the structure of λ was beginning to be understood using electron microscopy, it was also determined that if phage were heated or dialyzed against a chelating agent, they would eject their DNA, resulting in particles referred to as ghost particles. It was through work using electron microscopy that A.D. Kaiser (1966) was able to determine the structure, the capsid size and shape and the genomic compaction of λ DNA, which led him to suggest the hypothetical structure of the phage, which consists of a coat and a core that was surrounded by DNA. He commented on the geometric shape of a phage and the appearance of the tail structure, which is not very dissimilar from the head structure that we know today, comprised of an outer coat, DNA wrapped around a core and a tail (Kaiser 1966).

1.1.1 Bacteriophage λ Capsid Morphology and Major Capsid Protein gpD

The capsid of λ was determined to be icosahedral in shape, approximately 60 nm in diameter, with a shell thickness of 4 nm that accommodates a genome of approximately 47 kb in length (Witkiewicz, Schweiger 1982, Hohn, Katsura 1977). Empty, the capsid has a molecular weight of 21 x 10^6 Daltons;the genome adds an additional 31 x 10^6 Daltons (Hohn, Katsura 1977).

Phage λ's capsid is made up of two major proteins, gpE and gpD, arranged in a hexagonal lattice in equimolar quantities, where the bottom side of gpD binds to the gpE arrangement (Wurtz, Kistler & Hohn 1976, Yang et al. 2000). The gpD, capsid protein has a molecular mass of 11.4 kDa, and like its counterpart gpE is present in approximately 405-420 copies in a mature phage head as strongly protruding thimble-shaped trivalent spikes. Unlike its arrangement on the mature capsid, λ major capsid proteins exist as monomers in solution (Mikawa, Maruyama & Brenner 1996, Witkiewicz, Schweiger 1982, Dokland, Murialdo 1993, Yang et al. 2000). GpD function is related to the stabilization of the phage head as it fills with DNA and is essential for phage head morphology, but only when packaged with a full-length wild-type genome (Mikawa, Maruyama & Brenner 1996, Sternberg, Hoess 1995, Lankes et al. 2007). In the absence of gpD only mutants packaging less than 82% of DNA can form mature phage (Sternberg, Hoess 1995, Mikawa, Maruyama & Brenner 1996, Katsura 1983, Imber et al. 1980, Sternberg, Weisberg 1977). The gpD protein possesses similar properties to eukaryotic chromosomal proteins and has been shown to cross-react immunologically with eukaryotic histones (Witkiewicz, Schweiger 1982). This similarity may further help to predict gpD's function involving the stabilization and compaction of phage DNA. One such study replaced D with phage 21's *shp* gene, which is homologous to D and shares 49% amino acid identity. Results showed that *shp* can stabilize the λ head shell, but virions were strictly dependent on the presence of Mg^{2+} and were very sensitive to chelating agents (Wendt, Feiss 2004).

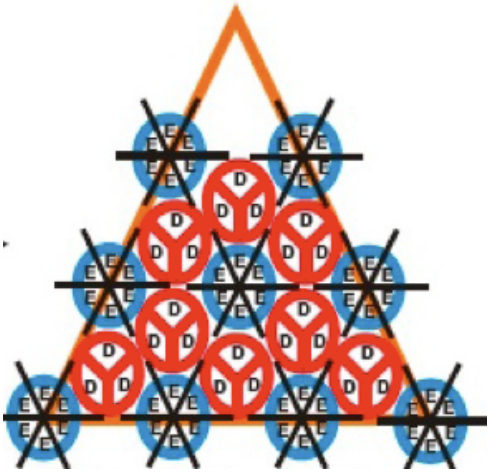

Figure 1: Single face of Bacteriophage Lambda displaying major capsid proteins gpD and gpE

Schemtic of a single face of λ illustrating the arrangement and position of the two major capsid proteins, gpD (arranged in trimers) and gpE (arranged in hexamers). Approximately 405-420 copies of each protein are found per capsid.

1.2 Initial Phage Display

Phage display is defined as the "process by which a peptide or protein is expressed as an exterior fusion to a surface protein of the phage particle" (Lindqvist 2005). This revolutionary technique is based on the genetic fusion, which creates a physical link between phenotype, where the fused protein is expressed on the phage coat and genotype where its corresponding gene is inserted into the phage genome (Jestin 2008). The first indications that phage could potentially be used as display vectors came from the work of Makela and Haimovich and Sela in the mid 1960s. Makela et al. (1966) was able to couple phage T2 with 3-iodo-4-hydroxy-5-nitrophenylacetic acid chloride (NIP) and then inactivate the phage with an anti-NIP antibody while working to produce a sensitive assay for an anti-hapten antibody. It was found that a very low concentration of antibody was required to inactivate the coupled phage. In a similar study Haimovich and Sela were able to react phage T4B with N-earhoxy-DL-alanine anhydride to yield poly-DL-alanyl bacteriophage and then inactivate the phage antisera (Haimovich, Sela 1969a). Haimovich and Sela were also able to demonstrate the covalent attachment of proteins to phage T4 employed to quantitatively measure the antigens and detect their antibodies (Haimovich, Sela 1969b). This application is of major importance to phage display in current research since the ability to fuse foreign molecules especially antibodies to the phage coat has greatly increased the ability to scan large peptide libraries and identify novel binding targets. However, the techniques to append these foreign molecules to the surface of the phage have become much more advanced since the time of this initial study (Vaccaro et al. 2006)

The first evidence of a translational capsid gene fusion was observed by G.P. Smith (1985) when he successfully inserted an external gene into a phage genome. This construct consisted of the *Eco*RI endonuclease gene product being displayed on the filamentous phage fd minor coat protein pIII (Smith 1985). Based on this research it was envisioned that lytic and temperate phage could potentially be used as fusion vectors and this premise has since been explored (Garufi et al. 2005). The lytic phages T4 and T7 and the temperate phage λ, have been shown to express both amino or carboxy terminal fusions to major and/or minor capsid proteins (Lindqvist 2005).

While filamentous phages are not a focus of this study, the principles of their early use govern phage display advances, and hence, are worth reviewing here. The most extensively used phage are derived from the *E. coli* Ff (filamentous) class, where the most commonly explored species include M13, fd and f1. The basic structure of these phage consists of a circular single stranded DNA genome that is encased in a long tube composed of thousands of copies of a single major coat protein with four additional minor capsid proteins at the tips. The two major coat proteins are pVIII and pIII respectively, where the most common fusions to these proteins are N-terminal and the average phage can be found to have approximately 2700 copies of pVIII and 3-5 copies of pIII, depending on the size of genome. Traditionally filamentous phages require the use of a *phagemid* or helper phage to participate in phage display of foreign peptides or proteins. A phagemid is a hybrid of a phage and plasmid vector, where it contains two origins of replication (one from the phage and one from the bacterial host), one of the coat proteins, a multiple cloning site and an antibiotic resistance gene, but lacks all other phage genes that encode structural and non-structural proteins required to produce a viable phage. These phagemids can then be grown as plasmids in a bacterial cell and packaged with the aid of a helper phage, which provides the remainder of the necessary machinery to produce functional phage (Mullen et al. 2006). In addition to the use of phagemids and helper phage,

filamentous display systems, usually also employ peptide linkers in between the foreign peptides and the coat protein, so that the recombinant can maintain its native structure and function normally; the phage protein acts only as an anchor (Bratkovic 2010).

Initially, phage display was developed to create phage display libraries. Two types of libraries are commonly created: random peptide libraries and natural peptide libraries. Peptide libraries contain synthetic random degenerate oligonucleotide inserts that are used almost exclusively to identify linear antigenic epitopes. These have a universal nature and are used for many applications. Natural peptide libraries on the other hand are composed of randomly fragmented DNA from the genomes of selected organisms. These libraries are important alternatives to the random peptide library that are used for identification of vaccine components and bacterial adhesins but unfortunately the majority of clones are nonfunctional, since many are not in the correct orientation or coding frame (Mullen et al. 2006).

While filamentous phage played an essential role in the establishment of phage display and their application in biotechnology, they possess some major limitations that are overcome by lytic display. Firstly, they require the fusion to be translocated across the plasma membrane and therefore many hydrophilic cytoplasmic proteins cannot be extruded as fusion proteins. Secondly, there is a significant limitation to the size of fusions (Garufi et al. 2005, Mikawa, Maruyama & Brenner 1996, Sternberg, Hoess 1995) and thirdly, filamentous phage do not cause lysis or loss of viability to the host, which can be detrimental if the fusion is a toxic molecule and could prove harmful to the host when expressed in large quantities. Toxicity exists when the fusion is expressed in large quantities because the filamentous phage lifecycle does not lyse the cell (individual phage bud from the host) which would not allow high concentrations of toxic molecules to accumulate within the cell (Garufi et al. 2005). Due to the lytic nature of vegetative growing phage, the fusion of toxic proteins to lytic phage is no longer a concern in temperate or lytic double stranded (ds) DNA bacteriophage since they are repressed in the phage lysogenic state and are only expressed just prior to cell lysis (Garufi et al. 2005).

Soon after the finding that λ could be used in phage display, subsequent studies revealed other interesting phage platforms. The C-terminus of the minor T4 fibrous structural protein fibritin that builds the collar/whiskers complex on the neck of the phage, and the C-terminus of the T4 minor capsid proteins HOC and SOC were also found to tolerate fusions for phage display (Ren et al. 1996, Efimov, Nepluev & Mesyanzhinov 1995). More recently, phage T7 has also been used as a display platform for various GFP-based cytoplasmic proteins that showed poor expression (fluorescence) with more traditional filamentous display vectors (Dai et al. 2008). Though it was important to study the ability of lytic phages to display foreign proteins on their surfaces, the use of temperate phage λ as a display vector was investigated further.

Santini et al. (1998) developed a chimeric phage system in which C-terminal fusions to lambda's gpD were made. In this work, recombinant phage were decorated with both wild-type D and proteins from a hepatitis C virus (HCV) cDNA expression library and these recombinant phage were compared to two other libraries utilizing the cDNA expression library: N-terminal fusions to the pIII and pVIII capsid proteins of M13. HCV was chosen for this study because the immune response in humans has been heavily studied. With regard to the cDNA library, the majority of the inserts were

between 100 to 300 bp in length. In order to avoid the possibility of lambda phage containing only wild-type gpD, the vector used contained a second copy of the D gene that carried an amber mutation, and therefore the library was plated on an amber suppressor (BB4) allowing for the formation of chimeric phage. When comparing filamentous phage proteins, pVIII's display was more efficient then pIII, and when pVIII was compared to gpD display and selection of protein fragments of limited size, the two libraries showed comparable efficiencies. When larger protein fragments were tested, gpD outperformed pVIII. This can be attributed to the fact that λ does not require secretion of the fusion protein, and therefore unlike pIII/VIII, larger recombinant proteins can fold properly; do not interfere with phage assembly, and are displayed in higher densities. Non-homogeneous ligates such as human HCV-positive sera could also be used to identify positive phage after a single round or a few rounds of selection when utilizing λ. This level of specificity can be exploited to identify common immunodominant antigens in the development of new vaccines (Santini et al. 1998).

Gupta et al. (2003) designed a lambda phage display vector that expressed fusions on the C-terminus of gpD. This library was compared an M13 phage library involving N-terminal fusions to the major and minor coat proteins PVIII and PIII, respectively. The λ library displayed a 100-fold higher display for all fragments compared to filamentous phage when tested using an antibody-binding assay. In addition, no degradation of displayed products was observed, a consequence that is common when using M13. Overall, the λ system was able to display proteins of different sizes, with the number of fusions displayed on each phage particle being 2-3 orders of magnitude greater than that of M13. This high-density display became very powerful when applying it to epitope mapping; the λ system far outperformed M13, based on its higher ELISA reactivity. (Gupta et al. 2003)

1.3 λ Phage Display

One key finding that indicated interest in the use of temperate phage (λ) in an industrial setting was a patent filing in 1982, where a commercial approach was taken for the use of these modified molecules. In the claims it is suggested that a new strategy for vaccine production was possible where the foreign particle function would be preserved as well as the maintenance of viral replication. The system would then elicit an immune response *in vivo* (Dulbecco 1982). This filing helps to support the continuation of this type of research study and gives justification for its further downstream development and potential commercialization.

Early experiments of λ-fused peptides were conducted by fusing the peptide or protein of interest to the carboxy terminus of the major tail protein gpV. The initial display vector employed the carboxy terminus because this end of the protein faces outward and has previously been shown to be non-essential and therefore free to accept fusions. Dunn also demonstrated that λ gpV tolerated large multimeric proteins such as, β-galactosidase, but that the incorporation of fusions as well as the yield of phage after affinity chromatography was very low at approximately one copy per lambda tail tube and one percent recovery, respectively (Dunn 1995).

While the main application for phage display remains the screening of cDNA libraries, other more clinical applications include: antibody engineering, epitope mapping, tumour targeting, diagnostic development, identification of protein-protein interactions and drug development (Petrenko 2008).

1.3.1 Fusion to Major Capsid Protein gpD

To overcome the copy limitations imposed by gpV-mediated fusions, fusions to the major capsid protein gpD were investigated. gpD's incorporation to the λ capsid was ideal for fusions since both its amino and carboxy termini protrude outward (Mikawa, Maruyama & Brenner 1996, Witkiewicz, Schweiger 1982). Mikawa et al. (1996) determined that both the N and C termini of gpD are neither at the trimer interaction interface nor do they interact with the other major capsid protein gpE and that terminal tolerance and capacity depends on the peptide/protein that is fused. Subsequent studies demonstrated that gpD was tolerant of peptide and protein genetic fusions at either its N- or C-termini (Sternberg, Hoess 1995). Thus, the system could be used to detect binding of relatively low-affinity ligands and has the potential to be exploited to pan epitope libraries as a high avidity gene delivery vehicle.

Two unique vector features used in these initial constructs included a peptide linker and the use of conditional fusions via amber suppression strategies that permitted the fusion of multimeric proteins. Suppression was used as a crude control mechanism for capsid fusion expression, which was attempted by employing various allogenic *E. coli* suppressor strains, only a slight difference of expression was observed (SupE, SupF, SupG, Sup^{-}) (Maruyama, Maruyama & Brenner 1994, Mikawa, Maruyama & Brenner 1996). These strains allowed differing levels of expression of gpD due to the presence of mutations in the tRNA genes of the *E. coli* strains in which the phage were grown.

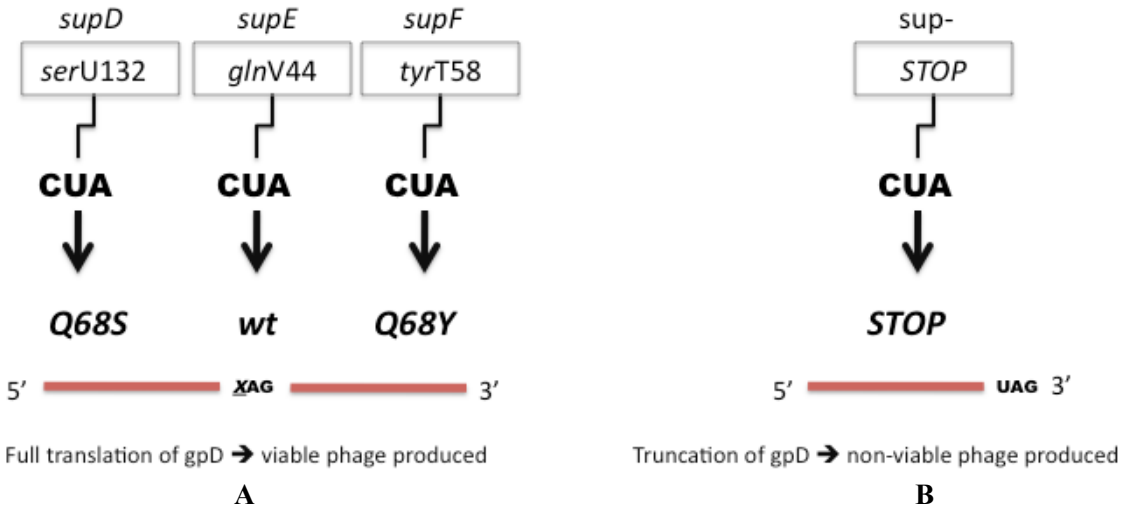

Figure 2: Schematic of Amber Suppression

The above schematic illustrates the concept of suppression as it pertains to the D*am15* mutation within λF7. **A.** When λF7 is grown on a suppressor strain an amino acid is inserted instead of a termination signal, gpD is fully translated and a viable phage is produced. **B.** In the absence of suppressor, gpD is truncated and a non-viable phage is produced. Sequencing of λDam15 determined a point mutation in the 68th codon (CAG) of gene D encoding Glutamine (Q), to an amber stop codon (UAG), this agrees with historical literature that demonstrates that supE is the strongest suppressor.

Amber suppression. The genetic phenomenon of suppression is mediated by mutant alleles of tRNA's that possess an anticodon mutation. This is complementary to a stop codon that results in the insertion of an amino acid in response to reading a termination *nonsense* codon as *sense*, thus relieving the translational truncation imparted by the original nonsense codon. In this study, a bacteriophage containing an amber stop codon within its *D* gene is suppressible on a mutant bacterial strain (Sup^{+}) that recognizes and decodes the termination signal with an amino acid, resulting in a non-truncated, full length 110 amino acid (a.a.) protein (Figure 2). Depending on the termination signal that is suppressed the suppression can either be amber (UAG), ochre (UAA), or opal (UGA). Amber suppressors are the focus of this study. These are suppressible by mutant *E. coli* strains that recognize and code the UAG stop signal as *sense*. Permissive hosts are considered suppression positive (Sup+) and non-permissive hosts are correspondingly suppression negative (Sup^{-}). If a variety of permissive hosts suppress the same type of stop codon then they belong to the same class (amber suppressors, AS, suppress the UAG stop codon), but based on the AS allele, may insert a different amino acid into the peptide chain at an encountered stop signal. The amber suppressor tRNAs that have been created *in vivo* include serine, glutamine, tyrosine and leucine; this study used serine (*supD*), glutamine (*supE*) and tyrosine (*supF*), respectively. In permissive strains both the terminated and completed peptide chain are produced, with the efficiency of suppression being dependent on which suppressor is carried by the bacterial strain (Brenner, Stretton & Kaplan 1965, Sarabhai et al. 1964). It is proposed that the *supD* amber suppressor was created by a single random nucleotide change in the anticodon from CGA (serine) to CUA, the anticodon that reads UAG (amber) stop codons (Steege 1983). The *supE* suppressor has been found to exist in two species ($tRNA_1^{Gln}$ & $tRNA_2^{Gln}$). The $tRNA_2^{Gln}$ suppressor was used in this research. It maps at 15 min on the *E. coli* chromosome, near the integration site of λ, thus complicating transduction of this gene. SupE is derived from a single base change again at the 3′ end of the anticodon altering the recognition from glutamine to amber stop (CUG to CUA) (Inokuchi et al. 1979). The third suppressor used in this research, *supF* encodes tyrosine in the place of UAG and is again derived from a single point mutation, this time a switch from GUA to CUA, allowing a tyrosine to be inserted upon reading the amber stop codon. Although all amber suppressors operate at different strengths, they are still superior to ochre suppressors. Moreover, although their complete function is not fully understood, they do allow for the expression of modified proteins in a controlled fashion when a permissive host is present, which has become very useful during the construction of this phage capsid display platform (Goodman et al. 1968).

1.3.2 Application of Phage Display in Phage Therapy

Many different applications of phage display have been employed throughout the years, with the system remaining essentially the same, but the number of applications steadily increasing. Vaccines represent one such important application. Bastien et al. (1997) investigated the use of a recombinant fd phage displaying the glycoprotein G of the human respiratory syncytial virus (RSV).

One of the major concerns surrounding λ display is the available screening for in-frame fusions especially when display is employed to screen cDNA libraries for novel compounds. Santini et al. (1998) constructed and characterized a HCV cDNA expression library displayed as a fusion to the C-terminal of gpD along with wild-type D creating a chimeric phage collection. This was used to

screen for anti-HCV human monoclonal antibodies recognizing linear or conformational epitopes, and antibodies from human sera from HCV-infected patients. The generated lytic display libraries were then also compared to similar libraries created using filamentous phage M13 (Santini et al. 1998). To increase the complexity of their screening system the same group also constructed two additional λ libraries, one containing total RNA from the human adult brain and the other made of total mouse embryos RNA and were able to show that fused polypeptides are specifically and very efficiently selected by using monoclonal antibodies and affinity selection (Santi et al. 2000).

The screening process has since been taken one step further, to target specific cells. Curiel et al. (2004) used a phage display library to identify specific dendritic cell binding peptides, which were then fused to a structural protein of hepatitis C virus for display to naive CD4+ and CD8+T cells. This work represents a novel way to use phage for vaccine development (Curiel et al. 2004).

Examples of proteins/peptides that have been fused to λ include: human peroxisome proliferator-activated receptor γ (Kong, Ma 2006), scFv antibodies (Vaccaro et al. 2006), β-galactosidase, β-lactamase and IgG-biding domains of the *Staphylococcus aureus* protein A (Mikawa, Maruyama & Brenner 1996), tumor-associated antigens (Minenkova et al. 2003) and autoantigens from HeLa and HepG2 cells (Niwa et al. 2000).

In order to simplify the process of screening cDNA libraries, specific vectors have been created that have been designed to readily accept in-frame fusions that will expedite the phage display library construction. Two such vectors are the λD-bio vector and the λKM phage The λD-bio vector utilizes the host encoded biotin ligase (Bir A) by placing its biotinylation target downstream of the C-terminal cloning site of gpD (Ansuini et al. 2002). By employing this construct only those fusions that are in frame with the target sequence are biotinylated (*in vivo* and *in vitro*) and are then selected by affinity chromatography with the high-affinity biotin ligand, streptavidin. The λKM phage possess; two unique cloning sites, a two-gene system of genomic *D* and *Dam* and a GS linker to maintain fusion-folding integrity. One phage is designed to accept N-terminal D fusions (λKM8) and the second designed for C-terminal fusions (λKM10) (Pavoni et al. 2004).

In recent years phage therapeutic practices also include the use of a T7 and λ for phage display to identify antigens eliciting B cell responses in cancer patients. Isolates were then tested for their suitability to develop a microarray system (Kalnina et al. 2008). Two important recent therapeutic applications of phage display include a study where phage display was employed for *in vivo* targeted gene therapy involving the heart vasculature (Nicol et al. 2009); the second utilized phage display to screen for potential peptides with the ability to transport molecules to the brain via the nasal passage—a viable approach in order to bypass the blood-brain barrier (Wan et al. 2009). While both of these studies utilized systems based on filamentous phage M13, a related study described the use of phage λ displaying the HIV-1 Tat peptide on the phage surface and carried mammalian marker genes in its genome was conducted (Eguchi et al. 2001). The presence of the TAT protein appears to increase the likelihood of gene transfer across the plasma membrane of mammalian cells, which could give insight into future gene delivery strategies (Eguchi et al. 2001).

1.4 Phage Therapy

While phage may be exploited for a wide array of therapeutic applications, their initial and most basic use employed their natural attributes as powerful and malleable antibacterials that co-evolve with their host(s). Here I examine one application, termed *phage therapy*.

An initial study that gave insight into the potential use of λ as a therapeutic explored the use of this phage for the elimination of foreign particles in a tissue-specific manner from non-immune germ-free animals. Geier et al. (1973) examined the accumulation of phage in various organs after intraperitoneal, intravenous and intramuscular administration. Although all organs studied contained viable phage, the spleen contained the highest titres with generally higher titres upon intraperitoneal injection. The overall observation that phage are quickly eliminated through the immune system of intact animals would become important in future studies examining the ability of phage to be used in the development of biologics and as a gene delivery tool (Geier, Trigg & Merril 1973).

With the evolution of phage display, the question that remains is, for what benefit can this technique be used therapeutically? One of the most prominent ideas for temperate and lytic phage display is their use in the generation of novel antibacterials, leveraging the natural action of phage for lysis of the host cell. One of the first studies that demonstrated the use of bacteriophage as therapeutics was done by Smith and Huggins in 1982. They showed that a single intramuscular dose of anti-K1 phage against an *E. coli* strain was more effective than multiple intramuscular doses of various antibiotics in curing mice of a potentially lethal intramuscularly or intracerebrally induced infection and was at least as effective as multiple intramuscular doses of streptomycin (Smith, Huggins 1982). Furthermore, it has been suggested that phage themselves can direct us towards novel bacterial protein targets for the development of new antibiotics, if we study their native strategies (Brown 2004). One such study that provides support for this theory sequenced 26 *Staphylococcus aureus* phages and identified 31 novel polypeptide families that inhibited host cell growth upon expression and could potentially be used as antibacterials, targeting vital components of host cell machinery (Liu et al. 2004).

Phage were used as antibacterials in many countries even before the advent of antibiotics. Today in some countries like the former Soviet Union, phage therapy is still employed to treat infections. In addition to human treatment, the use of phage in animal industries is also being explored (Coates, Hu 2007, Kropinski 2006). With the current status of antibiotics and antibiotic resistant strains, many companies are revisiting the use of phage as therapeutics. Countries such as Georgia, Poland, Germany, Portugal, Israel, UK, USA and Canada, have research programs based on the use of phage (Kropinski 2006). Even though there is much interest in using phage commercially the main research and practice regarding phage therapy is happening at Eliava Institute in Tbilisi (Georgia) and the L. Hirszfeld Institute of Immunology and Experimental Therapy in Wroclaw (Poland). The use of phage is a very promising alternative to the dilemma facing the future of infectious disease; but there is still a great deal to investigate. The principal concerns associated with phage therapy are safety and efficacy, particularly integration, resistance, and long-term effects and consequences on commensal biota and host specificity (Gorski, Weber-Dabrowska 2005). Additional questions and caveats include large-scale production where the best storage and transportation practices need to be determined; and human clinical trials, where the lack of data and potential for

exploration in children is still not well understood (Fortuna et al. 2008); lack of information regarding the pharmacokinetics of phage and discussions surround giving phage orally; phages ability to reach their site of action including the ability to cross the blood-brain barrier; and their preferential use of passive or active therapy modalities still needs much exploration (Brussow 2005).

To increase the quality control and standardization of phages for use as therapeutics, studies examining their applicability to be stored and transported have been reported. Jepson and March (2004) examined many aspects that could potentially affect the commercialization of new phage λ therapeutics. These included examining phage half-life, freeze-thaw stability, stability of desiccated phage, stability of liquid phage stocks, stability of phage in water, and effect of pH on phage stability. In general, they discovered that most phage were found to be highly stable under normal storage conditions and oral administration of phage DNA vaccines via drinking water may even be possible (Jepson, March 2004).

Potential uses for phage therapy range from decontamination of surfaces and/or environment, carcass treatment, use in the treatment of plants, aquaculture, animals and humans in an oral, intravenous or topical manner. More broad uses include; phage as vaccine delivery vehicles, targeted gene-delivery and for the detection and typing of bacteria (Clark, March 2006). In addition, Gorski et al. (2009) examined the use of phage therapy for the treatment of infections as they relate to the overall burden produced by current antibiotics. They discuss many of the issues and benefits of phage therapy as well as describe the massive repertoire of therapeutic phages housed by the Institute of Immunology and Experimental Therapy in Poland, where phage therapy has been conducted along with the distribution of therapeutic phages since 1952. In 2005 an outpatient clinic was even established there. One of the surprises surrounding phage therapy is the presence of many clinical trials taking place all over Europe, where one such formulation (PhageBioDerm) has been licensed for use since 1999 (Gorski et al. 2009).

1.5 Controllable Phage Display Systems

Although significant applications have been derived from the original work on lytic display, control of fusion copy number has generally remained quite crude. The use of amber suppression to regulate gpD fusions was first introduced by Mikawa et al. (1996) and represents the only rudimentary regulation system to date. This approach was allogeneic, qualitative and based on relative display.

Elegant and more modern approaches have been employed to generate gpD fusions *in vivo*, to generate libraries and purify functional fusions, and to increase the size and density of capsid fusions, but the issue of copy control that may have an important impact upon the different applications of this technology has yet to be resolved (Lankes et al. 2007). Variation in the number of fusions per phage particle does indeed occur, which is dependent upon the size of the fused fragment, whereby the smaller the fragment the greater the number of fusions per phage (Gupta et al. 2003). Since a differentiation in fusion number naturally exists, when comparing strategies for the development of a vaccine versus a vector for gene delivery or fusion of a peptide versus a large multimeric protein, vastly different approaches must be taken. In addition, the occurrence of overstimulation of a signal due to high affinity or high avidity interactions and the possibility of cross-reactivity and steric

hindrance impeding protein function or ligand access are also considerations that must be taken into account depending on the desired downstream application.

Since the initial lytic phage display design studies, there has been little attention paid to improving expression control, rather the focus has remained upon development of novel therapeutic or industrial applications for the system. Newer application studies that combine the genomic flexibility of phage with phage display pave the way however, for a powerful bimodal strategy that employs phage display in combination with genomic modifications for targeted gene delivery systems. Lankes et al. (2007) were the first to report the potential of phage manipulation for gene transfer *in vivo,* showing increased cellular uptake of a λ phage, modified to express firefly luciferase enzyme (*luc*), in mammalian cells by displaying an integrin-binding ligand domain on the surface of the phage to target CD51/CD61 receptors that mediate efficient endocytosis on the surface of dendritic cells. The incorporation of control over fusion decoration is a paramount concept toward the development of phage display therapeutics for clinical applications.

1.6 This Research

The primary goal of this work was to construct and characterize a λ phage display system that enables rigorous control of phage capsid fusion copy number. In order to achieve this goal, phage λ with an amber mutation in the major capsid protein, gpD, C-terminally fused to eGFP for ease of detection, was exploited. A bacterial system that contained two genetic systems for inducible control was used: host cell amber suppression and plasmid-encoded, repressor-mediated temperature sensitive repression. In the past, phage λ has been shown to accommodate C-terminal gpD fusions, but decorative control was never a focus.

1.6.1 First Level of Control: Conditional D expression via Amber Suppression

As previously introduced, "amber suppression" is a genetic conditional expression process whereby a nonsense codon is read by a complementary mutant tRNA of *E. coli* host, the binding leads to the insertion of an amino acid in place of the UAG stop signal tRNA (Benzer, Champe 1962). This conditional expression strategy was also applied to bacteriophage T4D, where nonsense mutations within the head protein were suppressed to produce a fragment of the polypeptide chain in the presence of a suppressor host (Sup^+) (Sarabhai et al. 1964). It was through this initial research that further inferences were made to predict that codons UAG and UAA were chain terminators and that in the presence of a permissive cell (Sup^+) they could be suppressed and propagation observed, albeit at a lower frequency. Correspondingly, in a nonpermissive cell (Sup^-) the amber mutations were not suppressed and propagation was absent. Furthermore, there was also a switch in amino acid observed from the wild-type sequence and different types of suppressors existed (amber, ochre) depending on the triplet present in the sequence and in fact different suppressor strains did exist for each and were mutually exclusive (Brenner, Stretton & Kaplan 1965). One caveat of amber suppression is the ability to restore original sequence functionality. With suppression, two levels of protein function occur: non-functional fragments of the protein in addition to full-length functional species. To increase the efficiency of suppressors, it has been proposed that these are created through total gene synthesis, where the inserted amino acid is equivalent to the wild type (Normanly et al. 1986).

1.6.2 Second Level of Control: Temperature-inducible Fusion Expression

The λ *cI*[Ts]*857* temperature-labile repressor has long been used to regulate downstream gene expression. Lieb (1966) first characterized the temperature-mediated lability of this protein, and discovered that it was the dissociation of this repressor complex that allowed downstream transcription to proceed (Lieb 1966, Szybalski et al. 1969). It is the controllable nature of this repressor, associated with its expression from a strong promoter that has made temperature-sensitive *cI*[Ts] alleles attractive for use in cloning vectors. In these cases a single copy of the *c1*[Ts] gene produces enough repressor to completely inhibit the strong λ P_L or P_R promoter, whether on single or multicopy replicons (Bernard et al. 1979, Remaut, Stanssens & Fiers 1981). Under this promoter's control, a downstream gene is expressed at increasing levels as temperature rises due to one of the two lesions. First,the c*I857* allele confers thermal sensitivity. Even though this high-level expression strategy may not be as effective as chemical induction approaches, it is less likely to be genotoxic and provides controllable expression—attributes that comparatively are far more advantageous. The second lesion termed Ind$^-$, renders the c*I857* repressor resistant to inactivation by the RecA protein, which when active can act as a protease and autocatalytically cleave the repressor (Mott et al. 1985, Villaverde et al. 1993). The c*I857* allele is most unstable at its denaturation point of 40-42° C, where maximal expression is thought to be observed (Hayes, Hayes 1986). Conversely, temperatures as low as 29° C may be required to fully repress transcription from P_L via the c*I857* allele, and highest protein yields can be obtained following induction at 36° C, but the latter temperature and its efficiency is still dependent on the protein being expressed and the host cell as the expression of many heterologous proteins innately affects bacterial cell growth and survival (Lowman, Bina 1990, Villaverde et al. 1993, Guzman et al. 1994, Jechlinger et al. 1999).

Strategies to avoid protein expression toxicity include: i) suppression of basal expression from leaky inducible promoters; ii) suppression of read-through transcription from cryptic promoters; iii) tight control of plasmid copy numbers; iv) protein production as inactive (but reversible) forms; and v) the creation of special expression vectors and modified *E. coli* strains (Saida et al. 2006). This repressor is also not limited to *E. coli*, but has also been shown to be effective in other Gram positive strains such as *Bacillus subtilis* where downstream expression efficiencies were similar to those reported in *E. coli*, where only minor codon bias changes needed to be made (Breitling, Sorokin & Behnke 1990).

1.6.3 Visualization of Control: Enhanced Green Fluorescent Protein

Green fluorescent protein (GFP) has long been used in protein localization because of its ability to autocatalytically form a fluorophore without the need for any external agents other than oxygen. Two major drawbacks to the use of wild-type GFP are its inability to fold at higher temperatures as well as its low intrinsic fluorescence. Due to these drawbacks, mutant versions of GFP have been created to improve its use in molecular biology. One such mutant that is commercially available is Enhanced GFP (eGFP) (Scholz et al. 2000). It is also worth noting that the properties of GFP can change depending on its fusion partner. Aoki et al. (2003) showed through sodium dodecyl sulfate (SDS) gel analysis that active and inactive GFPs migrated to different positions. In addition, a single amino acid change in the fused polypeptide segment of a GFP-fused polypeptide caused it to migrate differently through a urea containing gel (Aoki et al. 2003). GFP has also been successfully

integrated into the *E. coli* chromosome under the control of strong λ P_L and P_R promoters, regulated by c*I*857; visibly detectable levels of GFP were expressed from the single copy *gfp* gene as temperature was increased (Pinheiro et al. 2008).

1.6.4 Experimental Rationale

The goal driving this work was to develop a controllable phage capsid display system that could be employed toward biologic-based therapeutics. The scientific basis supporting this study is derived from previous findings that the major capsid protein gpD of phage λ tolerates a wide array of fusions to its amino and carboxy-termini (Mikawa 1996, Sternberg 1995). A comparison of a traditional wild-type D protein and a C-terminal D fusion is shown in the schematic below.

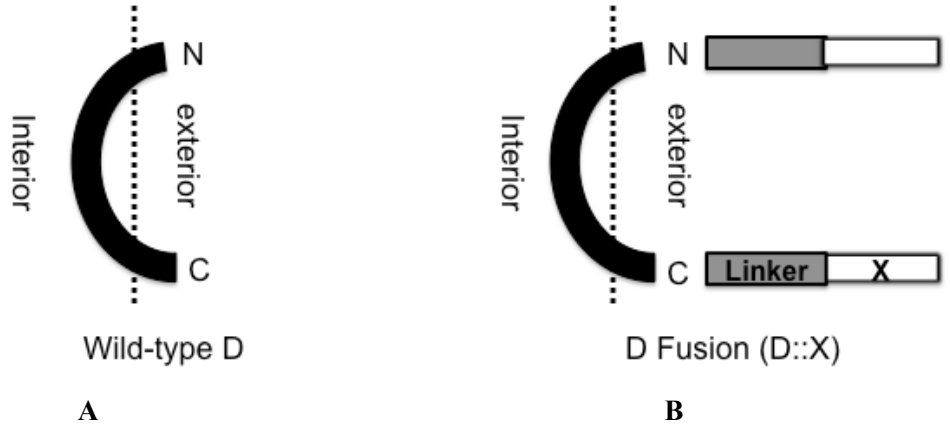

Figure 3: Schematic diagram of wild-type λ gpD and gpD::X.

A. Representation of the N and C termini of the wild-type gpD protein. **B.** Representation of a D fusion protein, with a fusion at the C-terminal end. GpD is shown in black, the translational linker in gray and the fusion X (eGFP) in white.

1.6.4.1 Research Objectives

The objectives defined by this research project included both the bacterial/phage preparative component of the work as well as the molecular design and construction.

1. Identify amber suppression allele effectiveness to suppress the λ *Dam15* mutation through the assessment of phage viability on different isogenic suppressor strains
2. Construction of a *D::eGFP* fusion within the pKS1 plasmid under the control of a temperature sensitive CI repressor and test *eGFP* expression at various temperatures
3. Measure the ability of pKS1 to complement for the λ *Dam15* mutation at various temperatures governing *D* or *D::eGFP* expression
4. Introduce both the suppressor and temperature sensitive repressor approaches in a single strain and vary both temperature and amber suppressor to determine the

number of gpD_{wt} and gpD::eGFP peptides on the capsid surface under each set of conditions

In order to complete the above objectives studies were performed that combine techniques in bacterial genetics, virology and biochemistry. The experiments designed for this research study centered on the measurement of suppressor strength and level of plasmid expression. Both qualitative and semi-quantitative methods were employed. After the initial sequencing and diagnostic tests, isogenic suppressors and eGFP expressing plasmids were created, analyzed individually and then the plasmid was transformed into each of the suppressors. From here complementation assays were performed using a plasmid expressing wild-type D along with efficiency of plating, qualitative studies analyzing both cellular expression and phage decoration with eGFP and finally protein analysis by Western blotting was carried out.

Chapter 2 Materials and Methods

2.1 Materials

2.1.1 Media Preparation

2.1.1.1 LB broth: Used for growing bacterial cultures. 10 g tryptone, 5 g yeast extract, 5 g NaCl/L of ddH_2O, pH adjusted to 7.8, Antibiotic was added as necessary [Ampicillin, (Ap), 100 μg/mL, Tetracycline (Tc), 15 μg/mL] to cooling LB and stored at 4^oC.

2.1.1.2 LB agar: Used for plating bacteria and phage. 10 g tryptone, 5 g yeast extract, 5 g NaCl and 12 g bacto agar/L of ddH_2O. After sterilization, plates were then aseptically poured into sterile Petri plates and allowed to cool. Antibiotic was added as necessary (Ap, 100 μg/mL, Tc, 15 μg/mL, Kn, 50 μg/mL) to cooling agar prior to pouring.

2.1.1.3 Top agar (used for phage overlays). 10 g tryptone, 5 g yeast extract, 5 g NaCl and 7 g bacto agar in 1 L of water. After mixing, media was poured into individual bottles and then sterilized and stored at room temperature.

TN Buffer: Used to dilute cells and phage. 0.1 M NaCl, 0.01 M Tris-HCl at pH 8.0 and sterilized.

2.1.1.4 Antibiotics:

Stock ampicillin (Ap) was prepared at a concentration of 100 mg/mL by dissolving the stock powder into sterile water and storing at -80° C. Thawed stock solution was then added to sterile media to concentration of 100 μg/mL. Tetracycline (Tc) stock was prepared at a concentration of 40 mg/mL by dissolving the stock powder into 1:1 H_2O: EtOH, filter sterilized and stored at -80° C. Thawed antibiotic was then added to final concentration of 40 μg/mL.

2.1.2 Strain Description

Summary of strains used and constructed in carrying out this work are shown in Table 1.

Table 1: Bacteriophages, Bacterial strains and Plasmids

Strain Designation	Relevant Properties	Phenotype	Source
Bacteriophages			
λF7	λ*Dam15imm21cIts*	D^-	(Mikawa, Maruyama & Brenner 1996)
λ*imm21*	λ *imm21cIts*	D^+	(NBRP-Prokaryotes(E.coli) 2009)
P1*rev6*	*rev6*	Super-transducing particle	Gift from B. Funnell (University of Toronto)
P1kc	*kc*	Super-transducing particle	Gift from B. Funnell (University of Toronto)
Bacterial Strains			
BB4	*supF58 supE44 HsdR514 galK2 galT22 trpR55 metB1 tonA* DE(lac) U169		(Minenkova et al. 2003)
W3101	F-, *galT22*, λ-, IN(*rrnD-rrnE*)1, *rph-1*		(Yale University 2011)
DS-3	F-, *phoA4*(Am), *serU132*(AS), *his-45*, *rpsL114*(strR), *valR116*		(Yale University 2011)
W3899	F-, glnV44(AS), *nadB7*		(Yale University 2011)
K1227	F-, *ompF627*(T2R), *tyrT5888*(AS), *oppC506::*Tn*10*, *fadL701*(T2R), *relA1*, *pitA10*, *spoT1*, *rrnB-2*, *mcrB1*, *creC510*		(Yale University 2011)
CAG 12077	F-, *crcA280::*Tn*10*, *λ-*, *rph-1*		(Yale University 2011)
CAG 12156	F-, *λ-*, *uvrC279::*Tn*10*, *rph-1*		(Yale University 2011)
W3101 [pKS2]	F-, *galT22*, *λ-*, IN(*rrnD-rrnE*)*1*, *rph-1*		This study.
W3101 supD	F-, *galT22*, *λ-*, IN(*rrnD-rrnE*)1, *rph-1*, *uvrC279::*Tn*10*, *serU132*(AS),		This study.
W3101 supE	F-, *galT22*, *λ-*, IN(*rrnD-rrnE*)1, *rph-1*, *crcA280::*Tn*10*, *glnV44*(AS),		This study.
W3101 supF	F-, *galT22*, *λ-*, IN(*rrnD-rrnE*)1, *rph-1*, *oppC506::*Tn*10*, *tyrT5888*(AS)		This study.

W3101 supD [pPL451]	F-, *galT22*, *λ*-, IN(*rrnD-rrnE*)1, *rph-1*, *uvrC279::*Tn*10*, *serU132*(AS),	This study.
W3101 supE [pPL451]	F-, *galT22*, *λ*-, IN(*rrnD-rrnE*)1, *rph-1*, *crcA280::*Tn*10*, *glnV44*(AS),	This study.
W3101 supF [pPL451]	F-, *galT22*, *λ*-, IN(*rrnD-rrnE*)1, *rph-1*, *oppC506::*Tn*10, tyrT5888*(AS)	This study.
W3101 supD [pKS1]	F-, *galT22*, *λ*-, IN(*rrnD-rrnE*)1, *rph-1*, *uvrC279::*Tn*10*, *serU132*(AS),	This study.
W3101 supE [pKS1]	F-, *galT22*, *λ*-, IN(*rrnD-rrnE*)1, *rph-1*, *crcA280::*Tn*10*, *glnV44*(AS),	This study.
W3101 supF [pKS1]	F-, *galT22*, *λ*-, IN(*rrnD-rrnE*)1, *rph-1*, *oppC506::*Tn*10, tyrT5888*(AS)	This study.
Plasmids		
pPL451	P_L-c*I857-tm*	(NBRP-Prokaryotes(E.coli) 2009)
pKS2 (pPL451 gpD)	P_L-c*I857-D*	This study.
pKS1 (pPL451 gpD::eGFP)	P_L-c*I857-D::eGFP*	This study.
Lysogens		
LE392 (Imm21)	(*malT supE44 supF58 hsdR514 galK2 galT22 metB1 trpR55 lacY1*)	(NBRP-Prokaryotes(E.coli) 2009)
W3899 (λF7)		This study.
W3101 (λc*I857*)		(Yale University 2011)

2.1.2.1 Phages Summary

λF7 (λ*Dam15imm21cIts*) is a lambda *D* amber mutant phage that is unable to grow in the absence of an amber suppressor, such a *supD*, *supE*, *supF*. λF7 formed the foundation of this research where viability was measured under various conditional scenarios involving suppression, temperature and complementation.

λ*imm21* was utilized as a control phage where viability was unchanged regardless of growth conditions. This phage is structurally and genetically identical to wild type λ except that the immunity region (O_LP_L-*cI857*-O_RP_R) has been recombined with the immunity region of phage 21. This heteroimmune phage is thus able to grow on a λ lysogen or any cell expressing the λ *cI* repressor.

P1*rev6* and **P1kc** are high frequency transducing particles that exploit the headful-packaging characteristic of P1 phage. P1*rev6* and P1kc were used to perform the P1-mediated transductions in order to transfer the suppressor alleles into the isogenic background (W3101). P1 has the ability to package up to 100 kb or ~2 min of the *E. coli* genome.

2.1.2.2 Bacteria Summary

BB4 (*supF58 supE44 HsdR514 galK2 galT22 trpR55 metB1 tonA* DE*(lac) U169*) served as the positive control cell to indicate viability of amber phage (λF7). Viability on BB4 was then used as the baseline (denominator) to determine efficiency of plating (eop). BB4 was utilized as 100% plating efficiency standard due to the presence of 2 amber suppressors encoded by this strain that provide plating efficiencies of λ*Dam15* that were essentially equivalent to that of the wt (λimm21).

W3101 (F-, *galT22,* λ-, IN*(rrnD-rrnE)1, rph-1*) was employed as the nonsuppressor strain and negative control for λD*am15* plating efficiency. Due to the absence of any amber suppressor (Sup^{--}) λD*am15* is phenotypically D^- on this host and inviable.

2.1.2.3 Donor Suppressor strains

DS-3 (F-, *phoA4(Am), serU132*(AS), *his-45, rpsL114*(strR), *valR116*) supplied the *supD* suppressor allele for the isogenic strain. Tet^R and suppressor alleles were selected within 1 minute of each other on the *E. coli* genome to increase the occurrence of successful transfer of both alleles creating W3101 *supD*.

W3899 (F-, *glnV44*(AS), *nadB7*) supplied the *supE* suppressor allele for the isogenic strain. Tet^R and suppressor alleles were selected within 1 minute of each other on the *E. coli* genome to increase the occurrence of successful transfer of both alleles creating W3101 *supE*.

K1227 (F-, *ompF627(T2R), tyrT5888(AS), oppC506::Tn10, fadL701(T2R), relA1, pitA10, spoT1, rrnB-2, mcrB1, creC510*) supplied the supF suppressor allele for the isogenic strain. Strain K1227 already contains a linked Tn*10* allele (Tet^R) and therefore only a single transduction was required to create W3101 *supF*.

Table 4 (below) illustrates the relative genomic address of each suppressor mutation within the *E. coli* genome and the necessary donor strain that supplied the linking Tc^R gene to permit co-transduction of the allele to W3101 background.

2.1.2.4 CAG Tn*10* linker strains

Two CAG strains were employed to link a Tc^R marker to each appropriate *sup*. The strain designation and its Tn*10* alleles are listed below. The location of the marker relative to the suppressor mutation is shown in Table 4. Note in order for the Tc^R marker to be co-transduced with an allele it must reside within 2 min (~100 kb) of the allele to be transferred.

CAG 12156 (F-, λ-, *uvrC279*::Tn*10*, *rph-1*) allowed for selection of the isogenic *supD* suppressor strain through its linked Tn*10* carrying tetracycline resistance.

CAG 12077 (F-, *crcA280*::Tn*10*, λ-, *rph-1*) allowed for selection of the isogenic supE suppressor strain through its linked *Tn10* carrying tetracycline resistance.

K1227 (F-, *ompF627*(T2R), *tyrT5888*(AS), *oppC506:*:Tn*10*, *fadL701*(T2R), *relA1*, *pitA10*, *spoT1*, *rrnB-2*, *mcrB1*, *creC510*) allowed for selection of the isogenic *supF* suppressor strain through its already linked Tn*10* conferring Tc^R..

Table 2: *E. coli* genomic positioning of *sup* alleles and their associated Tc^R markers

Suppressor Mutation	Mutation Position (min)	Tn*10* Linkage	Tn*10* Position
serU132(AS) (*supD)*	44.01	*uvrC279::Tn10*	42.91
glnV44(AS) (*supE)*	14.99	*crcA280::Tn10*	14.14
tyrT5888(AS) (*supF)*[1]	27.74	*oppC506::Tn10*	28.06

[1] The K1227 strain used for the supF isogenic suppressor contains both the suppressor allele and the Tet^R marker, therefore only a single transduction was required to co-transduce both the marker and linked suppressor from the donor to the nonsuppressor (W3101) recipient.

2.1.2.5 Isogenic Suppressor Strains

W3101 *supD*, *supE*, and *supF* derivatives were constructed by co-transducing the AS allele linked to the Tc^R marker from the donor construct into recipient W3101 cells using transducing phage, in doing so the genetic background was maintained to ensure that any differences in suppression were entirely due to the activity of the AS allele and not strain allogeneity (other potentially confounding mutations present within different strain backgrounds). It is however worth noting that the insertion of the Tn*10* marker varies in each strain and as such there is the potential (although highly improbable) that the insertion has disrupted a gene that may variably influence the function attributed solely to the transduced suppressor mutation.

2.1.2.6 Plasmids Summary

1) pUC57-D::eGFP: The translational fusion (*gpD::eGFP* 1176 bp) was first synthesized in pUC57 (2710 bp), which contains a Ap^R resistance gene and *lacZα*. In this plasmid *D::eGFP* was cloned in the reverse orientation to the P_{Lac} promoter so the fusion would not be expressed.

2) pPL451: Plasmid backbone for eGFP expression (gpD::eGFP) and complementation (gpD) cassettes. Both cassettes below were cloned into the *HpaI* and *Nco I* sites of the multiple cloning region.

3) pKS1 (pPL451-gpD::eGFP): Plasmid pKS1 was constructed by cutting the *gpD::eGFP* sequence from #1 above and cloning into the *Hpa*I and *Nco*I sites of pPL451, yielding the finalized pKS1 plasmid. The resultant sequence creates a C-terminal translational fusion with λF7 gpD (see Figure 3 below). Removing the terminal stop codon from *D* and start codon of the eGFP sequence to fuse the two genes. The two genes were also separated by an in-frame short linker (T-S-G-S-G-S-G-S-G-S-G-

S-G-S-G, T = threonine, S = serine, G = glycine) that was placed between and followed by a *Kpn*I cut site to maximize fusion functionality and also allow for additional fusions to be designed in the future. The *gpD::eGFP* sequence was then amplified and cloned into the *Hpa*I and *Nco*I sites on pPL451, placing it under the control of a temperature-inducible repressor *cI*857, conferring temperature-regulated expression.

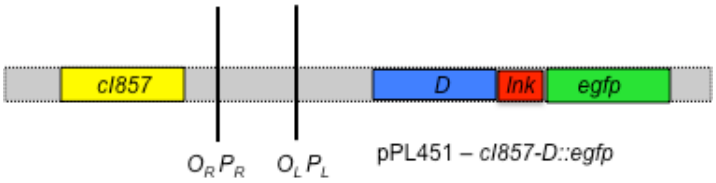

Figure 4: Schematic of pKS1 *D::eGFP* temperature-regulated fusion expression plasmid

Schematic of pKS1 expression vector in which the D::eGFP fusion is downstream of the temperature-inducible c*I857* repressor. gpD and eGFP are separated by a 15 a.a. linker to allow for correct folding of both proteins.

4) pKS2 (pPL451-gpD): To construct the pPL451 *gpD* vector, pKS1 was digested by *Kpn*I removing e*GFP* from the C-terminal of the linker to the last 36 C-terminal bp, which was then ligated back together to create pKS2.

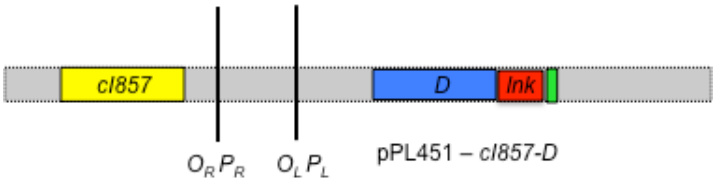

Figure 5: Schematic of pKS2 pPL451-gpD, complementation plasmid

Schematic of pKS2 expression vector in which gpD is downstream of the temperature-inducible c*I857* repressor. In addition, a short linker (15 a.a.) separates gpD from the last 36 C-terminal bp of eGFP, which include an ochre stop codon.

2.1.3 Primers

Primers to sequence the *Dam*15 mutation of λF7 were designed to base pair on the last nucleotide of the amino and carboxyl termini of gene D as follows:

KS1: Forward *D* primer: 5′CACACCAGTGTAAGGGATGTTT -3′

KS2: Reverse *D* primer: 5′CCTTTAGTGATGAAGGGTAAAG -3′

Sequencing primers KS1 and KS2 were centrifuged at maximum rpm for 2 min, re-suspended at a concentration of 100 mM in sterile molecular grade water and centrifuged for an additional 2 min to make stock solutions.

2.2 Methods

2.2.1 Transformation

Generation of Competent Cells ($CaCl_2$ Method): Cells were grown overnight in 5 mL of LB broth. A $1/100^{th}$ dilution was grown at 30°C in LB with vigorous shaking in a large flask to facilitate aeration until the cells reached an OD_{600} between 0.2 and 0.6. Cells were iced for 10 min and then centrifuged at 12 K RPM for 5 min at 4° C. The supernatant was discarded and cells were re-suspended in a half volume of sterile, ice-cold (4° C) 0.1 M NaCl and left on ice for 1 hour. Cells were then spun down as above and re-suspended in a half volume of sterile, ice-cold 50 mM $CaCl_2$ and spun down again. Cells were re-suspended in $1/10^{th}$ volume of $CaCl_2$ and stored on ice. Next a 100 µL aliquot of $CaCl_2$ competent cells was transferred from pre-frozen stock to pre-chilled 1.5 mL microfuge tubes and between 50 and 400 ng of plasmid DNA was added. Tubes were gently mixed and placed on ice for 1 hour to allow the DNA to adhere to the cells. Then, cells were heat shocked in a 42° C water bath for 45 to 60 s and immediately returned to ice for 5 min. One mL of LB was added to each tube and tubes were incubated at 30° C with gentle shaking for 60-90 min. After incubation, cells were centrifuged at 12 K RPM for 2 min and re-suspended in 100 µL of fresh LB, and plated on LB + antibiotic plates and incubated at 30° C overnight.

2.2.2 P1 Transduction

P1 Lysate Preparation: The P1 transduction methodology was adapted from Moore (2011). Briefly, 20 µL of cells carrying a Tc^R (Tn*10*) marker linked to the allele of interest were used to innoculate, 2 mL LB broth were grown for 30 min at 37° C until the culture was slightly turbid. Next, 20 µL of transducing phage lysate grown on a "wild-type" *E. coli* K-12 (W3101) strain was added. The lysate titre of minimum was 5 x 10^8 pfu/mL concentration. The mixture was grown at 37° C with shaking for approximately 2.5 hrs (or until culture is clear from lysis). Tubes were then placed on ice for 10 min and centrifuged for 15 min at 12K RPM. The supernatant was decanted to a fresh tube and 40 µL of $CHCl_3$ was added to sterilize the solution. All lysates were stored at 4° C (Moore 2011).

Generalized Transduction and screening: Freshly grown recipient cells (1.5 mL) were re-suspended in 1 mL of fresh 10 mM $MgSO_4$ + 5 mM $CaCl_2$. Next, 100 µL P1 lysate were added to 100 µL of recipient cells and the mixture was incubated at 37° C for 20 min. Next, 200 µL of 1 M Na Citrate and 1 mL LB was added to each tube. Tubes were then incubated at 37˚ C for 90 min with vigorous shaking to allow expression of the relevant antibiotic resistance marker. Cells were then centrifuged at 6 K RPM for 3 min and each pellet was re-suspended in 90 µL of LB and 10 µL of Na Citrate and the total volume was spread plated on LB plates + antibiotic. Plates were incubated at 37° C for 24 hrs and colonies were counted and screened as necessary. An LB plate was marked with a grid for each cell to be screened. On a second LB plate, loopfuls of λF7 and sterile water were spread (phage plate). A sterile loop was touched to the colony to be screened and then the phage plate, and then streaked onto the marked LB plate. Plates were incubated for 24 hrs at 37° C and then analyzed for plating capability of F7, indicating successful transfer of the *sup* allele.

2.2.3 Construction of Isogenic Suppressor Strains

Construction of isogenic suppressors was conducted by P1 transduction in two steps: 1) insertion of a Tc^R marker within 100 kb of each AS gene within the donor strain; and 2) co-transduction of both the *sup* mutation and the Tc^R marker into the recipient (W3101) strain, selecting for Tc resistance. Transductants were screened with λF7 for lysis (as above) to confirm the presence of the *sup* allele.

2.2.4 Lysate Preparation

Phage Streaking: 300 µL of indicator cells was added to 3 mL of fresh top agar and the mixture was poured evenly onto a fresh LB plate and allowed to set. Next, 10 µL of phage lysate with a titre greater than 1 x 10^8 pfu/mL was transferred onto the plate and was streaked across the plate using sterile paper strips isolating for single pfu, using a new piece of paper for each steak. The plate was then incubated O/N at the appropriate temperature and single plaques were isolated to generate new lysates.

Primary Culture Lysate Preparation: In a test tube, cofactor (0.01 M $MgCl_2$; and/or 0.01 M $CaCl_2$) was added to 300 µL of indicator cells. From a fresh overnight phage streak, a single plaque was removed and mixed with cells and incubated for 15-20 min at 37º C without shaking to allow adsorption. 10 mL of LB + 0.01 M cofactor was incubated at 37º C in flask before the contents of the test tube were added and further incubated for 2.5 – 3 hrs or until lysed (OD_{600} of 0.05 or less). The lysate was then placed on ice for 10 min before being centrifuged for 20 min at 15 K RPM at 4° C. The supernatant was decanted and 20-40 µL of $CHCl_3$ was added to sterilize.

Secondary Lysate Preparation: In a test tube, 300 µl of indicator cells, 10 µL of 1 M cofactor and 10 µL of prepared (primary) lysate with a titre of >1 x 10^8 pfu/mL was added and was incubated for 15-20 min at 37º C without shaking. In a flask 10 mL of LB and 1/100th volume of cofactor was then incubated at 37° C with vigorous shaking then mixed with the contents of the test tube and further incubated for 2.5 – 3 hrs or until lysed (OD_{600} of 0.05 or less). Once the solution was clear, the flask was placed on ice for 10 min then centrifuged at ~12 K RPM for 20 min at 4° C. The supernatant was decanted and 20-40 µL of $CHCl_3$ was added to sterilize.

Plate Lysate Preparation: Lysate dilution was added to 300 µL of indicator cells + 3 mL of top agar and poured onto LB plates and incubated at 37° C for 24 hrs. Plates showing distinct plaque formations but mostly lysed were selected for lysate preparation. 10 mL of TN buffer was added to the surface of the plate and incubated for an additional 24 hrs at 4° C. The TN buffer was then removed and along with underlying top agar and mixed vigorously before centrifuging at 12 K RPM at 4° C for 20 min. The supernatant was decanted and 20-40 µL of $CHCl_3$ was added to sterilize.

Immunity Determination Assay: This was employed to generate a λ*imm21* lysate to serve as the wild type (wt) control for λF7. A λ*imm21* lysogen, LE392, was centrifuged at maximum speed at 4° C for 20 min and the supernatant was collected and streaked onto W3101. Two plaques were then placed into TN buffer and were used to create a plate lysate. The lysate was titred on W3101 at 1.29 x 10^9 pfu/mL. To test phage 21 immunity the lysate was streaked onto a λ*imm21* lysogen, W3899(λF7) and λ*imm21* lysogen, W3101(λcI857) and observed for plaques. λimm21 yielded lysis on W3101 (λcI857), but not on W3899(λF7) indicating that the infecting phage carried phage 21 immunity.

Lysogenic Inductions: A fresh overnight culture of lysogen was diluted 100 fold in LB + Ap, and grown to OD_{600} = 0.2 - 0.6 at 30° C. The flask was then heated at 65º C for 15 s and quickly transferred to 42ºC water bath with aeration until complete lysis was observed (OD_{600} of 0.05 or less). The lysate was then placed on ice for 10 min before being centrifuged for 20 min at 15 K RPM. The supernatant was decanted and 20-40 µL of $CHCl_3$ was added to kill any remaining cells.

Phage titering: A 1/100 serial dilution series was prepared in TN buffer. Next 100 µL of lysate dilution was added to 300 µL of indicator cells + 3 mL of top agar and poured onto LB plates and incubated between 30 and 40° C for 24 hrs. Plaques were counted and plaque number was then multiplied by the dilution factor to determine the lysate pfu (plaque forming unit) titre (pfu/mL).

2.2.5 Phage Filtering and Concentration

Primary lysates (10-20 mL) were clarified of any cell debris (as above) then further filter purified by passaging through a 0.4-micron filter. In some cases, lysates were further purified by adding lysate to an Amicon Ultra-15 Centrifugal Filter, then centrifuged at 5 K x g at 4° C for 15-30 min. After centrifugation the filtrate was removed. Protein concentration (Protein at A_{280}) was then determined by Nanodrop 2000 (Bio-Rad, Mississauga ON). Filtration was performed to both purify and concentrate whole phage lysates and remove any potential free gpD::eGFP monomer in preparation for protein analysis.

2.2.6 Functional Immunity Marker Rescue Assay

Three hundred microlitres of homoimmune lysogen and 10 µL of lysate was added to 300 µL of indicator cells + 3 mL of top agar and poured onto LB plates (with or without antibiotic) and incubated at 30° C for 24 hrs. Next, a toothpick was used to capture a small amount of donor lysogen, which was then stabbed into phage cell mix overlay. Plates were incubated at 30° C for 24 hrs and observed for lysis spot formation. Any lysis that developed was due to the presence of homologous recombination between the donor lysogen and the recipient phage replacing the deficient allele (marker rescue) or the immunity region (FI Assay) and these were picked with a Pasteur pipette and stored in TN buffer for further screening.

2.2.7 Semi-quantitative phage titration

An indicator cell overlay was prepared on agar plates as described above. A matrix was drawn on the plate to indicate an array of phage at an incremental dilution series (10^{-1} – 10^{-4}) of each phage, prepared in TN buffer. Next 10 µL of each phage dilution was transferred with a pipette to the spot on the corresponding matrix and the plate was incubated at 30° C for 24 hrs. After incubation, the plate was examined for the presence/absence of plaques and relative extent of lysis. In the cases where individual plaques were visible within the lysis spot, plaques were counted and titer was determined. This assay was used to determine best dilutions to carry out full plate titration assays.

2.2.8 Cell Viability (Titration) Assay

Overnight cultures of cells were grown at 30° C and diluted 100 fold in fresh 10 mL of LB broth and grown at 25° C until OD_{575} = 0.4 - 0.5. A dilution series was prepared in TN buffer and each cell was

plated on both LB + antibiotic plates when pertinent. Plates were incubated overnight at 30°, 32°, 35° and 37° C. Colonies were then counted and multiplied by the dilution factor to determine the cell titer at that temperature (cfu/mL) and divided by the total number of cells initially present to determine the relative viability.

2.2.9 Complementation Assays

Full genomic length phage λF7, carrying the *Dam15* mutation, is incapable of packaging on a nonsuppressor host W3101, but the mutation is suppressed on strain BB4 that possesses two AS mutations (SupE, SupF). λF7 grows equally effectively as its D^+ counterpart on this strain, and is conventionally considered to confer "100%" relative efficiency of plating (eop = 1). λF7 was plated at varying dilutions on strains at 30, 32, 35, 37, or 39° C and eop was scored against BB4 to determine relative plating efficiency of the tested phage. Relative plating efficiencies were then divided by that on BB4 (100%) to derive the eop. Relative eop was determined as a ratio of λF7 eop divided by λ*imm*21 eop at each tested temperature. This strategy was employed to derive an eop for the experimental phage preparations that is independent of plating differences of λ due to temperature or other confounding variables.

2.2.10 Fluorescence (eGFP) Assays

Overnight cultures of cells were grown in LB + antibiotic at 30° C. Cultures were diluted 10 fold in fresh LB + Ap and grown for 24 hrs at experimental temperatures before measuring A_{575}. Each cell sample was then diluted to a titre of 1 x 10^9 cfu/mL in TN buffer and 1 mL was transferred to a 24-well cell culture plate and observed under GFP filter (Excitation = 470 nm, Emission = 535 nm).

Qualitative Fluorescence analysis of host cells: Overnight cultures were grown in LB + Ap at 30° C then diluted and grown at varying experimental temperatures. Each cell sample was then diluted to a titre of 1 x 10^7 cfu/mL in TN buffer and 1mL was transferred to a 24-well cell culture plate and observed under an eGFP filter (Excitation = 470 nm, Emission = 535 nm). Background fluorescence was corrected against an $eGFP^-$ control strain.

Qualitative Fluorescence analysis of EGFP-decorated phage: Lysates were diluted to a titre ranging between 1 x 10^3 - 1 x 10^8 pfu/mL in TN buffer and 1 mL was transferred to a 24-well cell culture plate and observed under a GFP-specific filter (Excitation = 470 nm, Emission = 535 nm). Background fluorescence was corrected against an $eGFP^-$ control strain.

2.2.11 Immunoblotting

Immunoblot experiments were conducted using rabbit anti-gfp polyclonal antibody (gift of Dr. B. Moffatt, University of Waterloo). Samples were mixed with loading dye and denatured by boiling for 10 min, and placed on ice and centrifuged. A total volume of 20 μL was electrophoresed with a range of 100-200 ng of total protein in each. Samples were run along side a GFP standard ranging from 10 pg/μL to 100 ng/μL as positive standard then separated by 15% SDS-PAGE. After electrophoresis the gel was placed in transfer buffer (48 mM Tris, 39 mM glycine, 20% (v/v) methanol, 0.0357% (w/v) SDS, pH 9 to 9.4) for 10 min. The protein was transferred to a nitrocellulose membrane at 20 V for 45 min using a Trans-Blot® SD Semi-Dry Transfer Cell (Bio-Rad, Mississauga ON). The membrane

was then stained with Ponceau S stain (0,2% w/v) by shaking for 10 min and de-staining in dH_2O until bands were visible. The stain was then removed by shaking in 1X PBS buffer until the stain (and bands were no longer visible). The membrane was then placed in PVA for 30 s to block, and then washed in PBS/milk/Tween for 10 min. The membrane was then incubated at 4° C overnight in PBS/milk/Tween plus $1/30^{th}$ dilution of primary rabbit anti-GFP antibody. After incubation the membrane was washed three times for 10 min in PBS/milk/Tween and then the secondary AP conjugate antibody (anti-rabbit) was added at a 1:2000 and incubated for two hrs, rinsed three more times with PBS/milk/Tween for 10 min then a final rinse in PBS was performed for five min. To detect bound antibody the membrane was placed in a pool of ECF and then visualized with a Typhoon imaging system. A second membrane was blocked with TBST for one hour at room temperature and incubated with primary antibody (1:30) for one hour at room temperature and washed three times for 10 min with TBST and then incubated with a different secondary antibody (gift from Dr. Michael Beazely, University of Waterloo) in TBST for one hour at room temperature and then washed again three times and the bands were detected with SuperSignal West Pico Chemiluminescent substrate and visualized on a Kodak imaging system.

2.2.12 Sequencing (λ*Dam15*)

A 10 mM dilution of the KS1 forward and KS2 reverse sequencing primers (Sigma-Aldrich, USA) were prepared in sterile molecular grade water and used to PCR amplify the *Dam15* allele. A standard gradient PCR was performed using *Phusion* high fidelity DNA polymerase to determine the optimal Tm (65, 61.4, 57, and 55° C) for the primers. A standard three-step PCR cycle was then performed at optimal Tm (61.4° C) to amplify the gpD sequence. λF7 phage lysate was used as the template for all PCR cycles. PCR products were then purified from a 0.8% agarose gel via QIAquick Gel Extraction kit (Qiagen, Toronto ON) and sent to University of Waterloo, Department of Biology Core Facility as well as the York University Automated DNA Sequencing Facility for sequencing. Cycle sequencing reactions were done with BigDye Terminator on the Applied Biosystems 3130xL DNA Sequencer.

2.2.13 DNA Manipulation

Plasmid Extraction and Purification: Purification of plasmids was conducted using Promega Wizard Plus SV Miniprep DNA Purification System (Promega, Madison WI), described here in brief. Cells (1.5 mL) were pelleted (all centrifugation steps were performed at ~12K RPM) for 10 min then re-suspended in 250 µL of re-suspension solution. Next, 250 µL of lysis solution was added and the tube was inverted 4 times to mix. Next, 10 µL of alkaline protease solution was added and the tube was once again inverted to mix and incubated for 5 min. Finally, 350 µL of Neutralization Solution was added and the tubes were inverted to mix, then centrifuged for 10 min at room temperature. A spin column was inserted into a collection tube and the cleared lysate was decanted into the spin column, and then centrifuged for 1 min. To wash 750 µL of wash solution was added and the tube was centrifuged for 1 min. A second wash was performed using 250 µL of wash solution and then a final centrifugation step was performed for 2 min to remove any excess wash. The DNA was then eluted by adding 40 µL of sterile molecular grade water to the column and centrifuging for 1 min into a sterile 1.5 mL microfuge tube and then adding an additional 40 µL of water and performing a second spin into the same tube.

Gel Extraction of DNA Fragments: DNA fragments were extracted via QiaQick Gel Extraction Kit (Qiagen, Toronto ON). Briefly, the DNA fragment was excised from the agarose gel and dissolved in Buffer QG at 50° C. Next the mix was spun through a QIAquick spin column and 0.5 mL of Buffer QG was again added and spun through the column to remove any residual agarose. The filter was then washed with 0.75 mL of Buffer PE and centrifuged for an additional 1 min to remove all wash, before the column was placed into a clean 1.5 mL microcentrifuge tube and DNA eluted by spinning 40 µL of sterile molecular grade water through the column.

DNA ligation: NEB Quick Ligation kit (New England Biolabs, Whitby ON) was used for all ligations. A minimum of 50 ng of vector DNA was combined with a 3-fold molar excess of insert. To this mixture a 10 µL of 2X Quick Ligation Buffer and 1 µL of Quick T4 DNA Ligase was added and the solution and the volume was adjusted with ddH2O to a final volume of 20 uL and mixed. The tube was then incubated at room temperature (25° C) for at least 2 hrs before it was used to transform JM109 or DH5α cells.

Quality Assurance: To ensure that the plasmid construct was correct, a simple nucleic acid digestion was performed. The pPL451 plasmid was digested by *Hpa*I and pPL451 *gpD::eGFP* and pPL451 *gpD* were double digested by *Hpa*I and *Nco*I. For all digestions approximately 500 ng of DNA was digested and visualized.

Chapter 3 Results and Discussion

3.1 Strain and Construct Selection and Characterization

3.1.1 Sequencing of λ*Dam15*

The bacteriophage utilized as the carrier in all phage display experiments was λ F7 (λ*imm21Dam15*). This phage possesses two important differences versus wild type λ: 1) it possesses the immunity region of phage 21, and as a heteroimmune phage it is not sensitive to the λ cI repressor and is therefore capable of growth on a λ lysogen, or cell expressing *cI* repressor; 2) the λF7 phage carries an amber mutation in the major capsid gene *D* that is necessary to compact full-length λ genome into the capsid and provide structural integrity. The phage is unable to grow on a wild-type *E. coli* K-12 strain, can make plaques on particular amber suppressor mutant strains.

I first sought to determine the exact location of the point mutation in the λ*Dam15* allele by DNA sequencing of the PCR amplified sequence. The derived sequence was then compared to wild-type gpD (Accession number NC_001416.1). The amplified 333 bp *Dam15* gene is shown in Figure 6. The amber mutation was localized to the 204th bp of *D*, converting the 68th CAG (glutamine) codon, to an amber stop (TAG) codon. In a nonsuppressor cell the presence of the amber mutation will be read as a stop codon and result in a truncated and non-functional gpD that is essential to package strains full length λ DNA and hence phage viability. Growth of D*am15* phage on various suppressors will result in the substitution of a amber stop codon for an amino acid. While only SupE strains will insert glutamine at the 68th codon restoring the native sequence, SupD will substitute a serine residue to produce a gpDQ68S allele and SupF will substitute tyrosine to produce a gpDQ68Y allele. The efficiency of plating data below agrees with historical literature, which found that the *supE* suppressor, encoding glutamine in place of the amber codon (restoring the native sequence) was the most effective in restoring viability of λF7 (Mikawa, Maruyama & Brenner 1996).

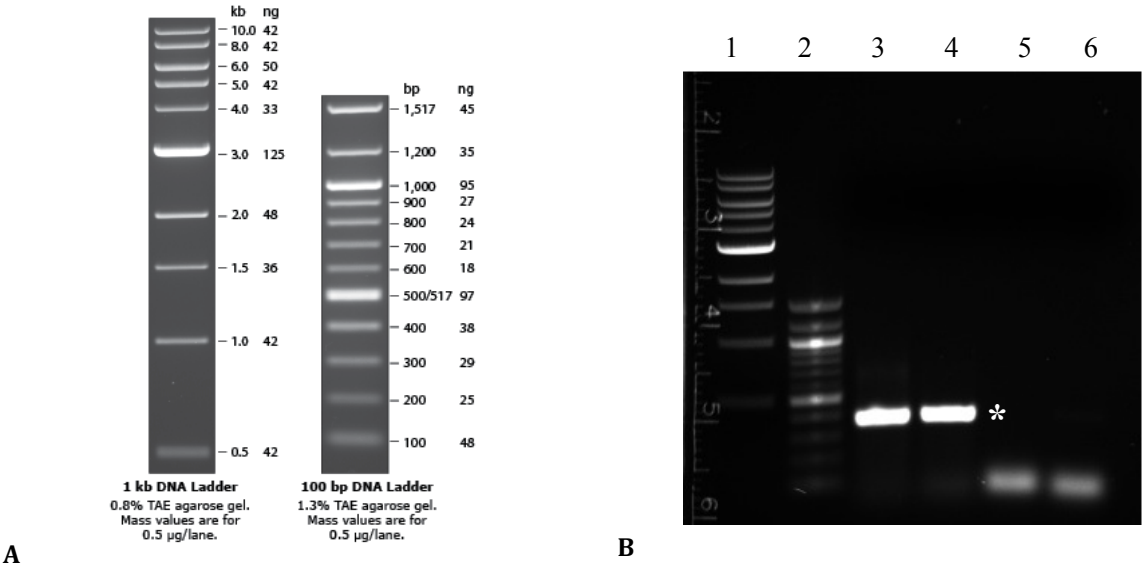

Figure 6: Sequencing of λD*am15*

A: 1kb and 100 bp DNA ladder reference chart (New England Biolabs). **B:** Lane 1: 1 kb ladder; Lane 2: 100 bp ladder; Lane 3-4: Amplified 333 bp D*am15* allele from λF7*; Lane 5: non-functional PCR product; Lane 6 PCR negative control.

3.1.2 Genetic Screening of Phage and Bacterial Candidates

As many of the phage and bacterial strains that were utilized in this work were acquired from other labs, making it essential to first perform appropriate diagnostics on these strains to ensure that their phenotype agreed with their documented genotype. Each phage was diluted and three different concentrations were plated on four well known experimental bacterial strains of *E. coli* K-12. Lysis (amount of clearing) was scored on each strain qualitatively as either no detectable lysis (-), evidence of lysis (+) minor lysis (++) or full lysis (+++). The results shown in Table 5 indicate that both λF7 and λ*cI857* were unable to grow on their respective lysogens (λimm21 and λ, respectively) as expected due to homoimmunity. λF7 was also unable to grow on the Sup^{-} (W3101) strain, due to the inability of this wild-type strain to suppress the D*am15* mutation. As expected, λimm21 (D^{+}) that has no packaging constraints, showed consistent growth across all strains. Finally, both λF7 and λimm21 demonstrated equivalent unimpeded growth on the double suppressor strain, BB4 (*supF58 supE44*). The confirmation of these phenotypic characteristics was essential to ensure that all work was done with the proper genotypes taken from a variety of different sources (see Table 3) and that downstream experiments could be performed with confidence.

Table 3: Genetic Testing of Bacterial and Phage Strains

	Nonsuppressor[3]			Suppressor[3]			W3101 (λc*I857*)[4]			W3899 (λF7)[4]		
Phage Conc.	10^{-9}	10^{-7}	10^{-5}	10^{-9}	10^{-7}	10^{-5}	10^{-9}	10^{-7}	10^{-5}	10^{-9}	10^{-7}	10^{-5}
λD^{-}[2]	-	-	-	-	++	+++	-	-	++	-	-	-
λD$^{+}_{1}$[2]	++	+++	+++	++	+++	+++	++	+++	+++	++	+++	+++
λD$^{+}_{2}$[2]	-	++	+++	-	++	+++	-	-	-	-	++	+++

[1] - = no detectable lysis, ++ = slight lysis, +++ = Full lysis

[2] λD^{-} = F7, λD$^{+}_{1}$ = Imm21, λD$^{+}_{2}$ = *cI*857

[3] Nonsuppressor = W3101, Suppressor = BB4

[4] W3101 (λ*cI*857) and W3899 (λF7) are both lysogens

3.1.3 Characterizing λF7

In order to further characterize λF7 it was necessary to determine optimal growth temperature and reversion frequency. To ascertain optimal growth temperature, λF7 was grown on a double suppressor (BB4) at various temperatures. Reversion frequency was established by growing λF7 on a nonsuppressor strain (W3101) at various concentrations and then examining plates for the presence of plaques.

3.1.3.1 Effect of Temperature on λF7 Viability

Coliphage grow best at mammalian body temperatures between 37-39^{o} C. Not surprisingly, a slight change in λ (D^{+}) and λ (D^{-}) titres at various temperatures was observed on the respective permissive hosts (Sup^{+}). λ*Dam15* is non-viable on the Sup$^{—}$ strain regardless of the temperature at which the strain is grown, and therefore this data was omitted. Table 4 summarizes the data of the titres observed at 30° C, 37° C and 42° C for the λ D^{+} and D^{-} derivatives. The table values are expressed as the efficiency of plating (eop) with the optimal growth temperature of 37^{o} C set to one, to show the subtle differences in phage viability at temperatures above and below optimal temperature.

Table 4: Effect of Temperature on λF7 Viability

Temperature (°C)	λD^{-} Titre [1,2]	λD^{+} Titre [1,2]
30° C	0.52	0.55
37° C	1.00	1.00
42° C	0.19	0.96

[1] Titres are eops based on use of BB4 as 100% plating efficiency

[2] λD^{-} = F7, λD^{+} = *cI*857

3.1.3.2 Calculating λF7 Reversion Frequency on Sup⁻ Strain

As a general rule, it can be expected that revertants to point mutations occur at a frequency of ~10^{-6}. To determine the best concentration to plate λF7 on the Sup⁻ strain (W3101), in the absence of revertants, λF7 was plated at various concentrations. Concentrations where no plaque formation was observed are indicated by n/a in Table 5.

Table 5: λF7 Titre on sup- strain (W3101) and various concentrations

Dilution of λF7 plated (phage/mL)	Titre (pfu/mL) on W3101
10	480
100	700
10^{-3}	n/a[1]
10^{-4}	n/a[1]

[1]Indicates the absence of plaques being observed on agar plates at the specified phage concentration.

3.1.4 Isogenic Suppressor Construction

The ability of a mutant strain to suppress a conditional amber mutation is conferred by a second site mutation in a tRNA gene that is capable of reading a UAG stop codon and inserting an amino acid in its place. To ensure isogenicity and that suppression of the amber mutation was entirely conferred by the amber suppressor, a series of amber suppressor genes were transduced into the nonsuppressor, W3101 background. Suppressor alleles were transferred from donor strains by linking each to a Tn*10* Tc^R marker. A two-step transduction process transferred genes, whereby a marker was first linked to the suppressor allele, then the suppressor allele plus Tc^R marker was transferred to the recipient nonsuppressor strain. Table 6 displays the expected gene linkages for each of the suppressor strains and the observed linkages that were seen during the transduction process. While *supE* and *supD* transfers agreed reasonably with expected linkages, *supF* linkage of *fadR613::*Tn*10* to the *tyr58* allele was observed to be farther apart than expected (<10% vs 43% expected). This difference could be attributable to an unrecorded insertion between the two genes in *supF* donor strain, or more likely, due to the limited number of transductants obtained (8) by which to score percent linkage. Indicated in the table are also the locations of both the suppressor mutation and the Tn*10* marker. These locations were critical in the initial design of marker linkages due to the limited packaging capabilities of the general transducing phage P1 at ~100 kb or approximately two min of the *E. coli* genome. Linkage further than this distance exceeds the length of packaging capabilities of P1 and would render co-transduction of the marker and the allele in tandem unattainable. In order to screen to ensure that the sup^+ allele was co-transduced with the Tc^R linkage marker, λF7 was plated on all Tc^R candidate strains, to determine whether it was capable of growth on the transductant. If the suppressor gene was not transferred, then the strain would remain a nonsuppressor and no plaques would be observed.

Table 6: Isogenic Suppressor Construction

Suppressor Mutation	Mutation Position (min)	Linked Marker	Marker Position	Expected Linkage	Observed Linkage	Distance from marker (min)
SupE (*glnV44*)	14.99	*crcA280::Tn10*	14.14	57.5%	50%	0.85
SupF (*tyr58*)[3]	27.74	*fadR613::Tn10*	28.06	43.0%	<10%	0.32
SupD (*serU132*)	44.01	*uvrC279::Tn10*	42.91	45.0%	37.5%	1.1

[1] Two different phages were used in the transduction experiments. The first was p1kc (Titer = 1.34 x 10^9) and the second was p1rev6 (Titer = 1.10 x10^9)

[2] # of transductants ranged from 8 to 200

[3] The supF strain that was employed in the final transduction already contained a Tet^R linked gene and therefore only one transduction was required to transfer both genes

3.1.5 Efficiency of Plating of λ*Dam15* on Isogenic Suppressor Derivatives (37° C)

To determine the eop of the isogenic suppressor strains at 37° C, λF7 was plated on each. The eop was then determined by dividing by the titre on each strain by that obtained on BB4 and then by the eop yielded by the D^+ phage control, λimm21. The results are shown in Table 7. Overall, the presence of a suppressor does not appear to restore a significant level of viability (results are the percentage efficiency as compared to the positive control phage λ*imm21*). This will be an important finding to compare when looking at the efficiency of plasmid-mediated complementation below.

Table 7: Efficiency of Plating of λ*Dam15* on Isogenic Suppressor Derivatives (37°C)

Bacterial Host Cell[1]	Efficiency of plating (eop)[2]
W3101	1.92 x 10^{-6}
W3101 supD	<1.13 x 10^{-5}
W3101 supE	0.09
W3101 supF	0.19

[1] N =3, each strain was plated for 3 separate trials

[2] eop's were scored using BB4 as the 100% plating efficiency standard

3.1.6 Discussion

The ability of gpD to accept fusions of large peptides and proteins and lambda's high infectivity has given λ an advantage over the traditional use of filamentous phage for display. Assembly of the λ capsid is accomplished in two steps: 1) prohead assembly; and 2) DNA packaging. During DNA packaging there is a large scale, irreversible, conformational change of the prohead, where there is an increase in volume and stability. During packaging, when only gpE is present, the capsid shape is

transformed from being more rounded to its final icosahedral structure with the subsequent binding of gpD to each face. The gpD protein is described as "thimble-shaped" with protrusions that are arranged in trimers once bound to the prohead. The trimer itself is shaped as a hollow triangle with rounded sides where the "bottom side" binds to the capsid. The "top" ends are relatively hydrophilic and exhibit both positive and negative charges, while the "bottom" is hydrophobic. The N-terminus likely governs interactions with gpE as it is situated near the interface. This conclusion is supported by the fact that if the N termini of gpD is truncated no viable progeny are produced. Furthermore, since the N-terminus sits at the interface of gpE/gpD, and the fact it still accepts fusions, suggests that it either underlies the trimer, connecting it to the capsid, remaining exposed to accept fusions, or it is threaded across the interface so it can still display fusions on the outside. The gpE and gpD proteins interact at three-fold sites of the capsid surface lattice forming twenty icosahedral facets in total (Yang et al. 2000, Sternberg, Hoess 1995, Mikawa, Maruyama & Brenner 1996).

It is important to understand the structure and function of gpD when assessing its ability to act as an appropriate fusion partner and determining whether to exploit an N or C terminal fusion. The gpD protein is thought to be a good fusion partner for several reasons. First, it does not contain any cysteine residues, which eliminates the misplacement of disulfide bonds under oxidative conditions, which may lead to misfolding and aggregation with the fusion partner. Secondly, gpD lacks enzymatic activity, which is important when discussing fusions, where in eukaryotic cells, activity may interfere with cellular signal transduction. The gpD protein is also stable at elevated temperatures for long periods of time and can remain soluble for prolonged periods of time at these increased temperatures (Forrer, Jaussi 1998). It is characteristics like those above coupled with a long history of phage display that has made gpD an ideal candidate to employ as a fusion partner throughout the remainder of this study.

Upon sequencing the *Dam15* allele of λF7, the location of the amber stop mutation was localized to the 68th residue of the gpD 110 a.a. protein. The presence of this stop codon also indicates the truncation size of gpD when λF7 is grown on a nonsuppressor strain of *E. coli*, which renders the phage non-viable. In determining the sequence of the stop codon, I concluded that the SupE strain would restore the sequence and hence, would be expected to be the most efficient at suppressing the *Dam15* mutation. This finding agrees with previous findings of Mikawa et al. (1996) who observed that a SupE strain (TG1) showed the strongest suppression activity of the *Dam15* mutation.

All phage strains tested were unable to grow on their respective lysogens (λF7, λ*cI857*, and λ*imm21*) as expected, ensuring heteroimmunity between λ and λF7 (λ*imm21Dam15*) phages and that λ*imm21* and λF7 were indeed homoimmune. Despite the expectation that λF7 would be unable to grow on the nonsuppressor (W3101) strain, the confirmation of this phenotype was also critical to the downstream applications. Many wild-type strains vary in their ability to impart a Sup^{-} phenotype and identifying a Sup^{-} host that strongly inhibits λ*Dam15* phage propagation was paramount to developing Sup^{+} derivatives. The phage D^{+} counterpart to λF7, λ*imm21*, showed consistent growth across all strains, confirming that no other factors were modulating λF7 efficiency of plating. λF7 and λ*imm21* also both grew equally well on the double suppressor strain, BB4 (*supF58 supE44*); an important finding as this strain was to serve as the positive bacterial control in forthcoming experiments and as the 100% efficiency of plating (eop) marker in subsequent relative eop plating experiments.

λF7 (D^-) had the highest titrre when grown on a suppressor strain at 37° C. The reduced eops at lower temperatures could be attributed to poorer adsorption and infection efficiency of this phage that thrives in the natural environment of 37-40° C or they could also be caused by temperature-related changes to *E. coli* receptor expression producing suboptimal phage binding. The exponentially lower ($<10^{-4}$) eop of λF7 on the Sup^- host (W3101) is due to the inability of this strain to confer suppression of the amber mutation within the essential late structural capsid gene *D*, resulting in a truncated and nonfunctional gpD product, yielding non-viable phage. Any plaques seen here can be attributed to intragenic reversion mutations that restore gpD functionality, expected at $\sim 10^{-6}$ frequency.

A general transduction strategy was employed to construct an isogenic suppressor set, eliminating any additional mutations that may have confounded growth and viability results between allogenic sup^+ donor strains. Each transduction was successful but, in the case of *supF*, the observed linkage was found to be considerably lower than the expected gene linkage to the Tc^R marker. While there is a possibility that the donor strain has experienced an insertion between the two linked genes, dropping the co-transduction frequency, it is more likely that the observed linkage was due to the relatively low number of transductants that was isolated. A very low number of transductants were also observed for *supE*, which may be justified by the fact that the suppressor gene is situated very close to the integration site of λ, *attB*, which has been documented to make transduction of this gene particularly difficult in the case that the donor strain is a λ lysogen, which may induce the phage upon transduction to the recipient (Inokuchi et al. 1979).

Interestingly, λF7 formed very small plaques on W3101 *supD* compared to D^+ λ*imm21* plaques on the same cells. Viability of λF7 was also very poor on this suppressor and much closer to that of the Sup^- strain than it is to the other two suppressor siblings. This indicates that W3101 *supD* is a very poor suppressor and much of the gpD Q68S protein that is produced is either poorly integrated into the gpD translated product, or the Q68S protein possesses very poor gpD functionality. This may be attributed to the fact that the inserted serine in the place of a glutamine, which is a much larger and polar amino acid, does not possess the necessary size or chemical attributes to properly substitute for glutamine. This poor substitution for gpD function is a welcomed addition to the *sup* group as it provides an important dimension to the project in balancing nonfusion gpD allele incorporation vs gpD::eGFP inclusion; allowing more fusions to be incorporated per phage capsid than the stronger suppressors. In contrast, both *supE* and *supF* show much higher levels of suppression and therefore phage viability, with *supF* performing slightly better than that of *supE*, which was surprising in that it would be expected that the most effective suppressor would be that that restores the native codon (Mikawa, Maruyama & Brenner 1996, Normanly et al. 1986).

3.2 Construction of temperature-regulated *D* and *D::eGFP* expression plasmids

3.2.1 Construction and Characterization of the pKS Plasmid series

The pKS1 plasmid, placing the *D::egfp* under temperature-sensitive repressor (c*I857*) control of the strong λ P_L promoter, was manipulated to create pKS2 by removing the *egfp* gene. The final plasmid

contains the wild-type λ*D* gene in addition to the final 36 bp from the 3′ end of the eGFP gene. A *Kpn*I digest was used to remove the eGFP gene leaving the beginning of the linker that sits just downstream of gpD until the *Kpn*I site found at the 3′ end of the eGFP gene. Figure 7 shows a schematic of the eGFP removal from pKS1, leaving the D gene with the linker. The downstream region of the *D* gene after being cut with *Kpn*I was sequenced as 5′-GGTACCGCGGGCCCGGGATCCACCGGATCTAGATAA-3′, this sequence concludes with an ochre stop codon, eliminating the concern of it being read through if an amber stop codon was in its place.

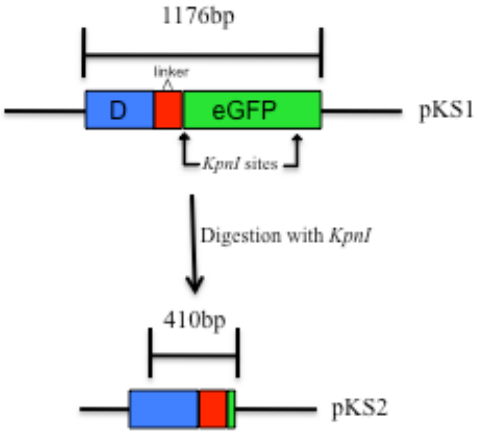

Figure 7: Construction of the pKS2 gpD plasmid

Schematic representation of the construction of pKS2, blue is the gpD gene, red is the linker, and green is the eGFP gene. The initial fragment was 1176 bp, which comprises gpD::linker::eGFP. After digestion by *Kpn*I the final fragment was 410 bp and was comprised of the gpD gene and 36 bp of the 3′ end of the eGFP gene. The downstream eGFP bp additions are 5′-GGTACCGCGGGCCCGGGATCCACCGGATCTAGATAA-3′, with the stop codon being TAA (ochre). The *Kpn*I site is underlined in the sequence above.

3.2.2 pKS1 Transformation Verification

To confirm that the transformed plasmid carried the correct sequence plasmid DNA a simple nucleic acid digestion was performed (Figure 8).

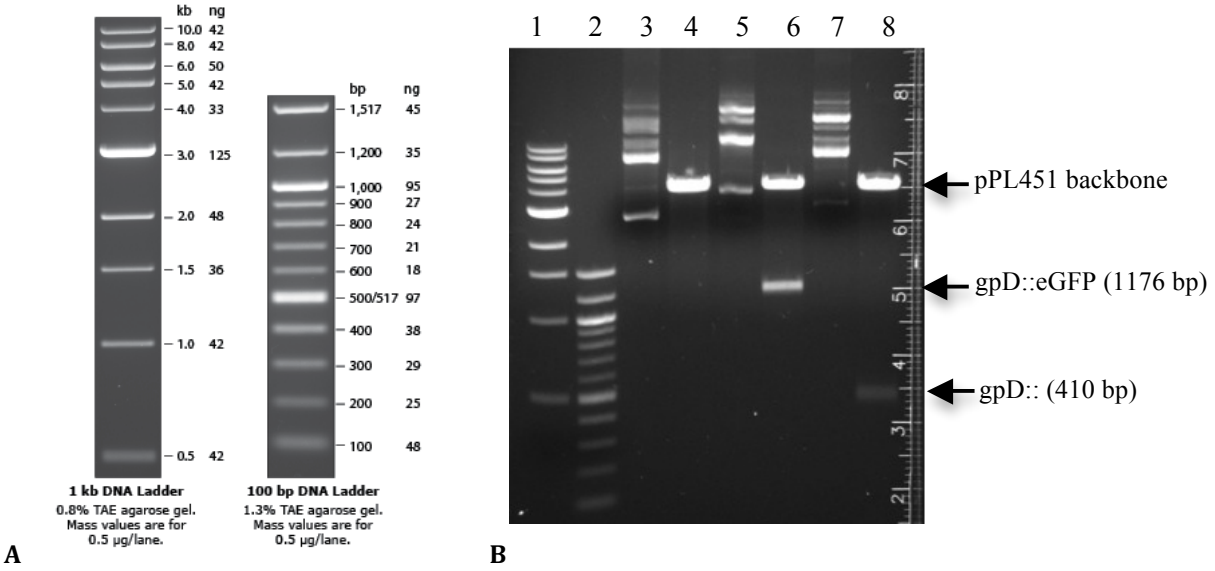

Figure 8: pKS1 Transformation Confirmation by Digestion

A: 1 kb and 100 bp DNA ladder reference (NEB). **B:** Plasmids extracted from the suppressor cells were digested to yield the presence of *D::eGFP* or *D*. Lane 1 and 2 are a 1 kb and 100 bp DNA ladder respectively; Lanes 3, 5 and 7 are uncut pPL451, pKS1 and pKS2, respectively. Lane 4: pPL451 digested with *Hpa*I; Lane 6 and 8: pKS1 and pKS2 double digested by *Hpa*I and *Nco*I. In Lane 6 and 8, *D::eGFP* and *D* can be observed at approximately 1176 and 410 bp, respectively. For all digestions 500 ng of DNA was analyzed in each case.

3.2.3 Analysis of gpD Complementation

To determine the level of gene *D* expression under various temperature conditions, the nonsuppressor strain W3101 was transformed with the pKS2 plasmid. Since gpD is an essential protein to package full length λ genomes, the ability to properly package and produce viable particles relies upon *in trans* complementation for the phage-borne *Dam15* mutation by the gpD fusion proteins expressed from pKS2. As expected, at increasing temperatures, complementation for *Dam15* by plasmid-encoded *D* increased, with optimal results seen at 37° C. Complementation results for each temperature tested are presented in Table 8. Relative eop was determined based on plating results on the double suppressor (BB4) at the same temperature.

Table 8: Complementation of the λ *Dam15* mutation *in trans* via expression of *D* from pKS2

Temperature (°C)	Efficiency of Plating (eop)[1]
32° C	5.10×10^{-4}
35° C	5.60×10^{-4}
37° C	1.0[2]
39° C	1.0[2]

[1] averaged data from 3 separate trials

[2] eop was either identical or higher than that achieved on the double suppressor strain BB4

3.2.4 Assaying toxicity of *D::EGFP* expression in host cells

It was important to ensure that plating efficiencies of λ*Dam15* phage on cells harbouring the pKS1 plasmid were not confounded by potential toxic effects of pKS1-mediated *D::gfp* over-expression within the nonsuppressor strain, W3101. To test this, the efficiency of plating of W3101 carrying the plasmid backbone was grown at a variety of temperatures and compared to the same strain carrying pKS1. To examine the plasmid expression toxicity, pKS1 and pPL451 transformants were assayed for viability at various temperatures. Cells were plated on both LB and LB + antibiotic plates and the relative cell viability eop was determined by dividing the pKS1 cell titre by the backbone titre. Results indicated little difference in eop between antibiotic and non-antibiotic scenarios at all temperatures tested (Table 9). Interestingly, larger colonies were observed at temperatures of 35° C and above, but no remarkable toxic effect of the *D::egfp* fusion expression was observed.

Table 9: eGFP Expression Effect on Cell Viability

Temperature	W3101 [pKS1][3]	Efficiency of Plating (eop)	W3101 [pKS1][3]	eop
RT (22-25° C)	1.83 x 10^8	1[1]	2.20 x 10^8	0.78
30° C	1.33 x 10^8	0.67	2.64 x 10^8	0.84
32° C	2.22 x 10^8	1[1]	2.60 x 10^8	0.88
35° C[2]	1.01 x 10^8	060	2.54 x 10^8	0.89
37° C	1.45 x 10^8	0.65	2.31 x 10^8	0.90

[1] eop slightly greater than 1.

[2] Larger colonies were observed at temperatures of 35° C and above

[3] Column 2 was plated on LB + Ampiciilin and the Column 4 were plated on LB

3.2.5 Fluorescence Assays

3.2.5.1 Determination of cellular expression of eGFP

Plasmid pKS1 was constructed in order to provide varying levels of eGFP expression, controlled by a temperature-sensitive λ c*I857* repressor during infection by λF7. To better observe the activity of pKS1 under various temperatures, imaging was performed using a Kodak imaging system with the appropriate GFP filters. Cellular cultures of W3101 (pKS1) and W3101 (pKS2) were titred to 1 x 10^9 pfu/mL after which the qualitative level of eGFP expression was observed by placing 1mL of lysate into a cell culture plate and then viewing the fluorescence on a gel doc equipped with a GFP filter. Since all cultures are derivatives of W3101, the original strain was used to demonstrate basal expression (Figure 9).

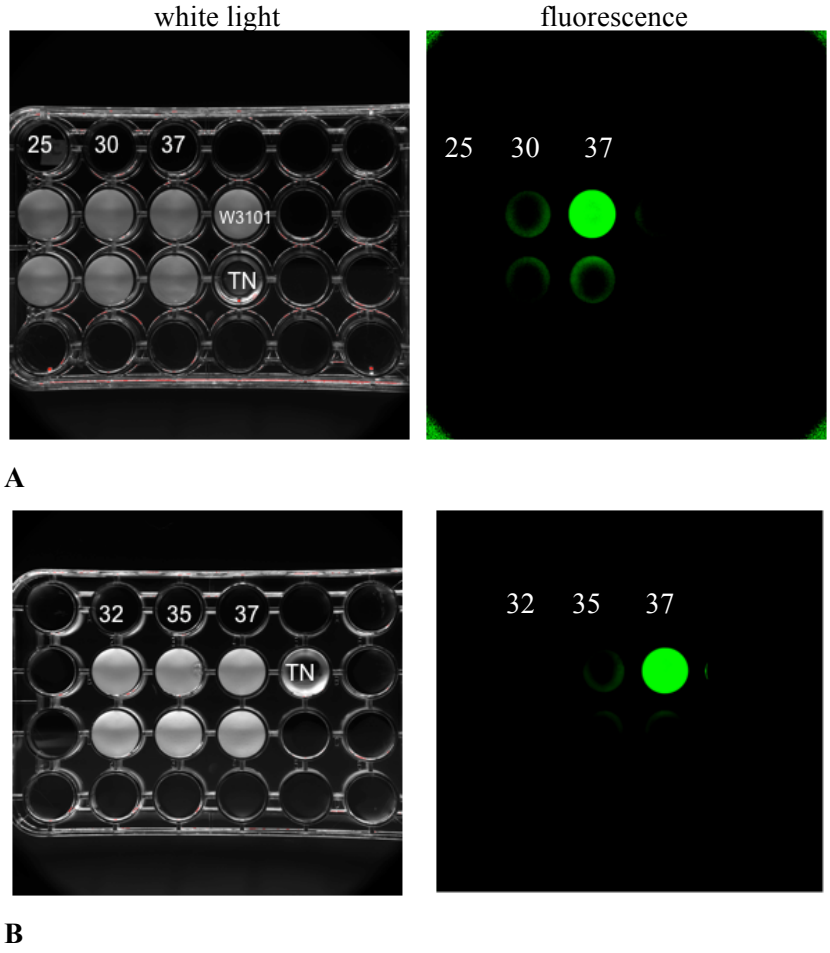

Figure 9: Cellular expression of eGFP (25-37°C)

A: Relative cellular eGFP protein expression at 25, 30 and 37° C (left to right). Experimental W3101 [pKS1] (top), and control W3101 [pKS2] (bottom) to adjust for background signal. **B:** Relative cellular eGFP protein expression at 32, 35 and 37° C (left to right). Bacterial cells as above. W3101 was used as the cell control and TN buffer was also included to ensure that media alone did not produce a signal. TN buffer was placed in a single well and used as an overall control since lysates were diluted in TN, yielding no fluorescence. Initially three temperatures were selected based on the theoretical dissociation temperature of the cI*857* repressor (A). When fluorescence was only observed at 37° C and no gradual signal was detected, activity was reconfirmed with a second experiment utilizing a more sensitive temperature range to determine if a more precise level of expression could be observed when smaller increases in temperature were used to detect *eGFP* expression (B).

3.2.6 Discussion

It was important to determine whether in the absence of a suppressor, a plasmid-mediated approach could supply enough gpD to generate not only viable but also fluorescent phage. As expected, the eops for phage complemented with pKS1 (*D::eGFP*) were lower than that of pKS2 (*D*) likely due to the hindrance to folding imposed by the fusion to eGFP.

After plasmid construction (pKS2) and confirmatio, it was important to ensure that the level of expression was under control of the c*I857* repressor as expected.. As the temperature increases the repressor becomes more labile and there should be an increase in gpD transcription and therefore increased levels of gpD produced and incorporated into assembling phage; optimal incorporation is expected at 37° C.

As shown in Table 8, there is a significant difference in the degree of complementation at 35° C versus 37° C. This finding is not surprising as the λ repressor retains considerable functionality at 35^{o} C, but drops to 1% at 37^{o} C. Not only did complementation increase as temperature increased, as expected, but in addition, the eop at both 37 and 39° C was 100% of that compared to λD*am15* grown on the double suppressor BB4, indicating that full functionality can be restored via plasmid-mediated *in trans* complementation in the absence of any suppression. Zanghi et al. (2005) performed a plasmid-mediated *in trans* complementation for gpD into a *D*-deficient λ and showed that when *D* was expressed, phage readily grew.

Previously, Sternberg and Hoess (1995) showed that recombinant gpD protein could be added to the phage capsid *in vitro* and incorporated into phage using *in trans* complementation. This study also showed that fusion proteins could not occupy all gpD sites on the capsid as phage were still sensitive to EDTA, which indicates the occurrence of empty gpD sites. When phage lack gpD are exposed to EDTA, they are unable to assemble correctly and are therefore nonviable. When this same experiment was performed using a plasmid expressing wild-type gpD, the phage were EDTA resistant. Phage are affected by EDTA because it acts as a chelating agent. These agents are proposed to remove counter ions (Mg_2^+) that are required during phage multiplication and help to balance the negative charges of DNA phosphates. When these ions are removed from solution (by EDTA), phage are inactivated. This inactivation is likely caused by a disruption of the head shell when DNA expansion occurs. Therefore, when phage are lacking capsid proteins, they are even more sensitive to treatment with EDTA and are unable to assemble unless less than a full length genome is present (Wendt, Feiss 2004).

Similar to Sternberg and Hoess, Mikawa et al. (1996) also demonstrated that gpD could be supplied *in trans* via plasmid complementation. This group determined that the plasmid copy number (level of expression) also affected the viability of D^- phage when grown on a nonsuppressor strain, where a low copy plasmid supplying gpD showed weak phage resistance to EDTA; gpD supplied by a high copy plasmid made phage almost completely resistance to EDTA and phage viability was close to that of the phage being grown on a suppressor positive strain (91.3% recovery). In addition, they also determined that fusion proteins supplied by a plasmid caused phage to be more sensitive to EDTA than if they were grown on hosts expressing native gpD. This is consistent with the conclusion that when only fused protein is supplied, not all gpD sites are occupied (Mikawa, Maruyama & Brenner 1996).

In order to determine the effects of over expression of eGFP on overall viability of the bacterial cell, all strains that carried pKS1 were grown at various temperatures and compared with the same host containing just the backbone plasmid (pPL451). Taken as a whole, no discernable differences were seen when cells were grown on antibiotic and only a slight difference in titre was observed when comparing to backbone only. These findings suggest that there was only a very minor toxicity effect generated by any level expression of *D::eGFP* from pKS1, although very minor, the trend of decreasing toxicity relative to the plasmid backbone suggests that over-expression purports some toxicity to the cell as temperature (and expression) increases.

GFP has been displayed on *E. coli*, yeast, hepatitis B, baculovirus, T7, adenovirus, and many other biological entities (Velappan et al. 2010). In order to test the ability of GFP to be detected within bacterial species, Pinheiro et al. (2008) chromosomally integrated a single copy of wild-type GFP or a modified *gfp* gene using a transposon into a strain of *E. coli* and *Salmonella*. Visualizing using a simple UV light (366 nm), they were able to show that the strains carrying the *gfp* cassette were easily differentiated from their non-fluorescent parental strains, and in addition cells remained viable, displaying the strongest fluorescence after 48 h incubation (as opposed to 24 h, incubations performed at 37° C). These levels were also compared and were akin to plasmid-borne expression system. They also found that when the construct was under the control of c*I857*, cells grown at 42° C after integration of a single copy, did not exhibit any detectable fluorescence after 3-5 h. The authors speculated that fluorescence could be potentially observed after longer periods of incubation from the single gene, but the metabolic stress on the cell being grown at such a high temperature likely prevents visible levels (Pinheiro et al. 2008). These results may make a case for growing the cells for longer periods of time (48 hr) in order to achieve maximal levels of fluorophore expression, but this is not advantageous when attempting to maximize phage titres as they peak after only a few hours (liquid lysate) or at the very most after a 24 hr incubation (plate lysate). These details are also important to consider when examining cellular expression evidence at high temperatures over prolonged periods as well as when examining the presence of fluorescent signal. In addition, when comparing the results in the next section, differing optimal eGFP, phage and cellular expression and growth conditions may also have an impact on the final phage decoration.

Interestingly, only the 37° C pKS1 culture showed any strong eGFP expression, compared to the more gradual expression profile that was expected, based on λ c*I857* repressor stability. Even when the temperature range was decreased, similar results were observed (compare Figures 9A and 9B). These results suggest that there is a threshold for c*I857* repressor binding at a qualitative level; there is no incremental increase in eGFP expression as temperature rises from 30° C to 37° C, but rather a surge of expression between 35° C and 37° C. However, this is difficult to confirm since the use of a gel doc filter is not very sensitive and low levels of expression are hard to detect due to the presence of considerable background. These data also agree with the complementation data discussed above where the greatest levels of complementation (and fluorescence) were seen at temperatures above 35° C (at 37° C and 39° C). The complementation data allow for a greater level of sensitivity though and present a repressor profile that most closely reflects the traditional functionality of c*I857* where temperature's effect is gradual and not resembling of an on/off switch (Figure 9).

Loman et al. (1990) examined the use of the c*I857* temperature-inducible repressor for the expression of heterologous fusion genes. They were able to determine that cells were repressed at 29°

C but not at 32° C, as was conventionally thought.. Furthermore, at the upper end of the induction scale, 42° C, not only does downstream expression occur, but intracellular insoluble aggregates and inclusion bodies may form in addition to the increased presence of proteases that are encoded by heat-shock genes induced at 42° C. Loman et al. (1990) concluded that the relative downstream expression is a result of both temperature and the induction period. For example, they detected protein after 2hrs at 32° C and the amount detected increased as temperature increased, but at 6hrs the accumulation peaks at 36° C, meaning that after long periods of incubation, the accumulation of protein is greater at lower temperatures. This can be explained by the fact that the rate of protein synthesis is still greater than the rate of proteolysis at these lower temperatures. At temperatures above 36° C, the proteolysis offsets the gain from protein synthesis due to increased repression and overall protein production was lower than that obtained after 2 h or that obtained by lower temperatures over the same induction period (Lowman, Bina 1990). These facts informed my choice for the temperature range that was chosen for the cellular and phage experiments and suggests that the mid-range, and optimal phage temperature (37° C), will provide the greatest eGFP expression and create an environment for maximal gpD::eGFP production.

Villaverde et al. (1993) also examined the c*I857* inducible repressor at temperatures between 30 and 42° C using a plasmid-based system that expressed β-galactosidase as an indicator of gene expression from the regulated promoter. They found that no gene expression was detected at temperatures below 32° C, except through analysis by Western Blot, where a very slight band was observed at 28° C. These findings agree well with the results obtained by Loman et al. (1990). This group also found a lack of linearity between temperature and product yield, where at temperatures up to 36° C the repressor was not denatured very efficiently. They also found that over long incubation periods (>20hrs), temperatures below 42° C (38° C, 40° C), showed nearly constant values, whereas at 42° C, lower than expected levels were observed, which they also attributed to cell death. In their experiments, the ideal temperature for induction (repressor denaturation) was 42° C, whereas for greatest yield of protein product, a temperature of 40° C was more appropriate (Villaverde et al. 1993). Finally, it is widely known that wild-type GFP folds very inefficiently at temperatures above 25° C, leading to insoluble protein and the absence of fluorescence. Even mutated forms of GFP, such as eGFP, still fold very inefficiently at experimental temperatures such as 37° C. In order to assess the reporter capability of GFP, Scholz et al. (2000) compared the expression of a GFP mutant to that of the *lacZ* gene. Through their experiments they were able to determine that expression of *gfp* was almost identical to that of *lacZ* demonstrating that *gfp* can be effectively used to quantify gene expression *in vivo*. One important determinant this group uncovered was the presence of an inner filter effect that limits the range of fluorescence intensities, where reliable reporting of GFP molecule number is no longer possible. This effect seems to occur in scenarios that produce high concentrations of GFP, where there is then either self-aggregation of fluorescence, increased overlap of absorption and emission spectra or a higher total absorbance of cells expressing GFP. They also realized that certain GFP molecules exhibit maximum fluorescence at different excitation and emission wavelengths and since the filter that was used in these experiments only provided a single excitation and emission, it could have decreased the sensitivity of the visual fluorescence (Scholz et al. 2000). These previous findings represent important considerations impacting the data shown here, with respect to expression environments and factors that influence fusion expression and display. These studies contrast the use of an inducible repressor and a downstream fluorescent translational fusion.

The two variables together however, can counteract each other—at extreme temperatures, non-optimal protein expression is achieved, but both seem to be in agreement that a temperature such as 37°C, will give rise to the greatest expression over long incubation periods, consistent with the complementation and cellular data presented here. These points along with the narrow temperature specific release of the c*I857* repressor give insight into why a sudden surge of expression was observed in the data presented here, and the fact that some recorded values are slightly off trend as all of these factors may not be acting consistently.

3.3 Bi-dimensional genetic approach to the control of *D::EGFP* expression by λ lytic phage display

3.3.1 Assaying suppression and complementation of the *Dam15* mutation

I next assessed the effect of both the suppressor type and a c*I857* activity on the level of gpD::EGFP decoration of λF7. To determine the capability of each suppressor to suppress the *Dam15* mutation and the temperature-regulated *D::eGFP* expression plasmid to complement for the mutation, I measured λF7 viability under permissive and non-permissive conditions. Each assay was paralleled by the negative control plasmid, pPL451, to ensure that the plasmid backbone was not influential on phage viability.

Table 10: Efficiency of Plating of λ*F7* on [pPL451] and [pKS1] on different suppressing hosts at various temperatures

Host Strain[1]	**30° C**	**32° C**	**35° C**	**37° C**
W3101 [pPL451]	4.06×10^{-6}	4.98×10^{-6}	1.83×10^{-4}	1.76×10^{-6}
W3101 [pKS1]	1.22×10^{-4}	1.79×10^{-4}	7.89×10^{-5}	2.21×10^{-4}
W3101 supD [pPL451]	8.82×10^{-5}	6.52×10^{-5}	1.50×10^{-5}	9.45×10^{-6}
W3101 supD [pKS1]	8.07×10^{-5}	4.93×10^{-4}	9.75×10^{-3}	4.93×10^{-4}
W3101 supE [pPL451]	0.031	0.12	0.075	0.025
W3101 supE [pKS1]	0.41	0.18	0.045	0.13
W3101 supF [pPL451]	0.010	0.103	0.042	0.041
W3101 supF [pKS1]	0.046	0.15	0.025	0.13

[1] N = 2, each eop is averaged from two separate trials

[2] All experiments were performed using λD*am15* (λF7)

The basis of the bi-dimensional decoration strategy infers that different suppressors will suppress the *Dam*15 mutant phage λF7 to varying degrees based on the functionality of the substituted amino acid for the amber UAG codon as each suppressor in reality imparts a different peptide variant of gpD. The ability of the host strain to suppress the *Dam15* mutation and incorporate wild-type D protein into the capsid provides the basis for the first dimension of decoration control.

The second dimension is based upon the expression level of *D::eGFP* expressed from the pKS1 plasmid, which is regulated by the temperature-sensitive c*I857* repressor (Table 10).

A significant increase in eop was not observed across temperature for any of the suppressor or nonsuppressor strains, suggesting that the presence of the *in trans* fusion peptide does not complement well for the D*am15* mutation. The most significant change in eop was observed for the strongest suppressors (SupE and SupF). This result could be expected since the presence of no wild-type gpD in the nonsuppressor and low suppression in supD could negatively impact phage assembly and viability when not all gpD sites are occupied and there is no or a weak presence of wild type D. This is confirmed when examining the nonsuppressor, which showed no change across temperature. The SupD was close behind displaying the weakest suppression, with many orders of magnitude lower suppression being observed as compared to SupE and SupF, but there does appear to be more noticeable difference across temperature, with 35 and 37° C showing the greatest difference (100-fold). This finding suggests a synergy between the gpDQ68S derivative generated by SupD suppression of the *Dam15* mutation and the gpD::eGFP fusion expressed at these higher temperatures. Overall, the presence of a strong suppressor allowed for the greatest viability, approaching that seen on BB4 but an order of magnitude lower. This is likely due to the fact that the BB4 reference strain is a double suppressor (SupE SupF), while SupE and SupF each only possess a single suppressor gene. Having two suppressor genes greatly improves the chance of producing a functional gpD protein. In addition, due to such low viability, it was very difficult to determine titres for W3101 and SupD since phage viability was greatly affected by the lack of suppression and potentially the increased presence of fusions per capsid. The data above suggest that the degree of complementation and the degree of suppression can greatly impact the eop data, which is most evident at the extreme temperatures, where theoretically one could be more dominant than the other (suppression at lower temperatures and complementation at higher temperatures). The data does support this when examining the increase in eop when using the strong suppressors at low temperatures where complementation would be all but absent due to a high level of repression. There is also a slight trend towards an increasing eop as temperature rises in the weak suppressor (SupD) and nonsuppressor (W3101), but viability may also be counteracted by the lack of wild type D being integrated into the capsid.

A few data points deserve special comment: SupE 30° C and 35° C for SupE and SupF. These results do not follow the general expected trends. This could be due to the low number of trials that were performed (N=2). New results by our group demonstrates that an increase in eop is clearly observed as temperatures rise, the greatest values are achieved at lower temperatures for strong suppressors (SupE, SupF) and when observing the weak and nonsuppressor (SupD and W3101) the maximal eop is achieved at 37° C (see Appendix A for Table 2) (Nicastro, Sheldon, El-zarkout, Sokolenko, Aucoin, Slavcev unpublished). The discrepancy between this study and the new data could be attributed to improved lysate preparation, particularly with respect to shortened induction times that maximize *D::eGFP* expression.

3.3.2 Determination of qualitative phage decoration with eGFP by Fluorescence

I next sought to qualitatively assess the fluorescence of phage constructed under a high *D::EGFP* expression in various suppressor hosts. Assays were performed to visualize the fluorescence of

gpD::EGFP-decorated phage passaged at 37° C through the suppressor or nonsuppressor strains carrying pKS1. Figure 10 shows the fluorescence of phage grown on each suppressor strain as indicated by the letter that appears in the leftmost well of the row. The phage dilution that appears above the top wells indicates the titre of each column. Fluorescence was then compared, where a noticeable signal was only observed for SupD and the nonsuppressor at high titres (10^8, 10^7 and 10^8 respectively), with a significantly stronger signal being observed for SupD. This result is an underestimation since a smaller volume was loaded as compared to the other samples (1 mL vs. 5 mL), the actual relative fluorescence would be even greater when examining total phage per well (equal volume).

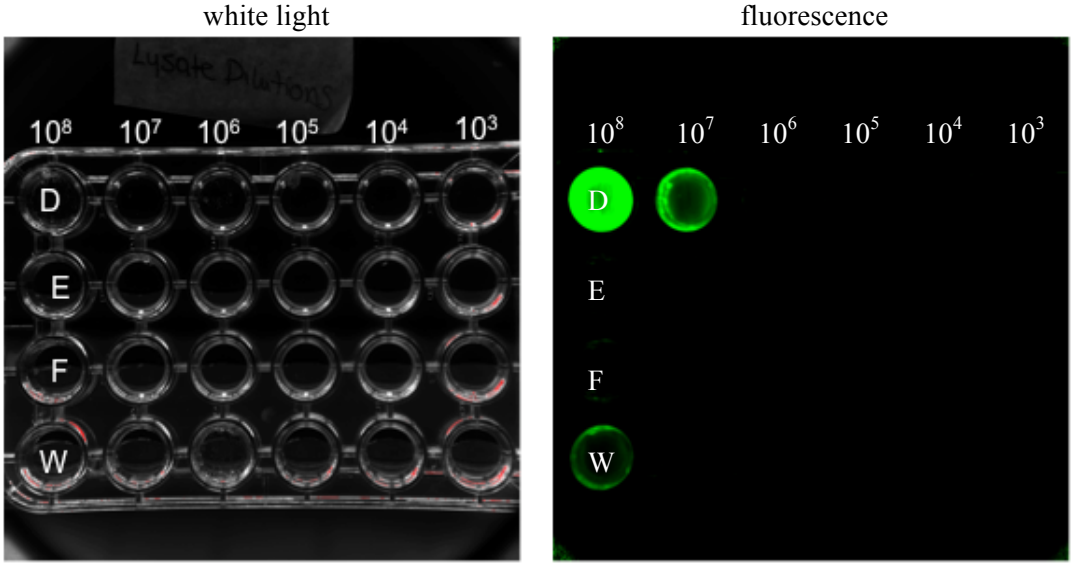

Figure 10: Level of eGFP expression across titre

All samples were prepared using λF7. Each row left to right is a single suppressor strain as indicated by the letter that appears in the leftmost well of the row. The number that appears above the top wells indicates the titre of the lysate in each column (top to bottom). Each whole lysate was diluted to 1 x 10^3 pfu/mL, then 5 mL of each sample was loaded to the corresponding well and the relative visualized fluorescence was compared. All lysates were prepared at 37° C. For W3101 supD [pKS1] 10^8 only 1 mL instead of the usual 5 mL was loaded.

A comparison was then made of the effect of temperature on fluorescence, (Figure 11) where lysate titres were standardized and compared when expression of gpD was off (30° C) and on (37° C). Only the SupD and the nonsuppressor showed any noticeable level of fluorescence at either 30 or 37° C. The result observed for the nonsuppressor at 37° C was expected as gpD was only supplied as the gpD::eGFP fusion. The results achieved for SupD on the other hand were less expected, especially for 30° C, as fluorescence observed here would indicate leaky expression of c*I857* at low temperatures. This leakiness was however not seen in the nonsuppressor. This finding supports previous evidence that the presence of weak suppression may confer a more appropriate environment for maximum decoration of fused protein as opposed to the lack of suppression and wild-type gpD. This model supports the difference seen between SupD and the nonsuppressor preparations at 30° C, where the

lack of any wild-type D could decrease phage viability enough to eliminate any signal. It was difficult to visually compare the level of decoration since the standardization titre had to be set at 1 x 10^7 pfu/mL as a lowest common denominator, as a higher titre was difficult to achieve for SupD preparations.

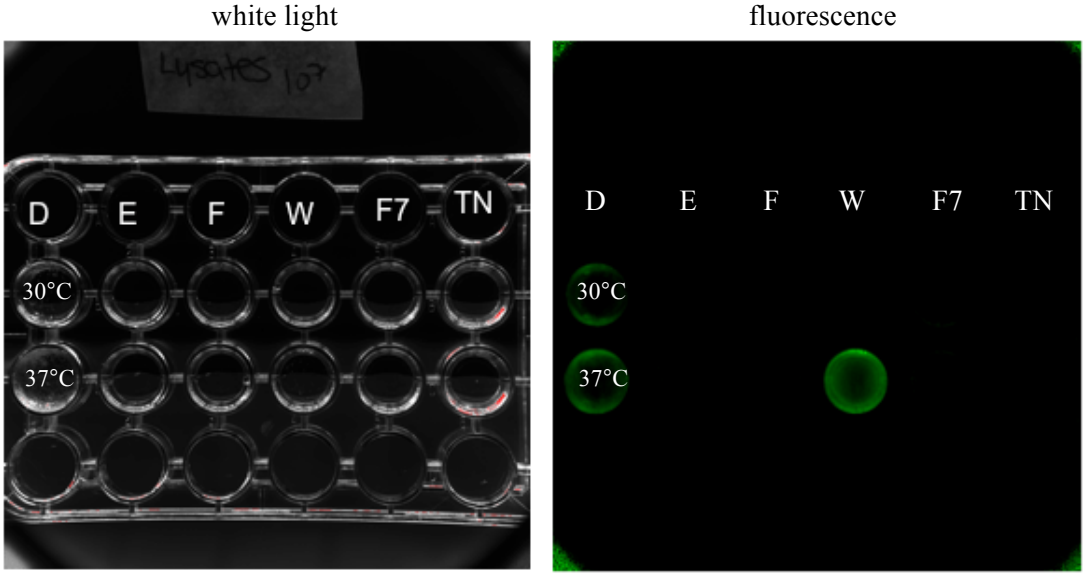

Figure 11: Effect of temperature on eGFP decoration

A comparison between the effects of temperature on fluorescence. Lysates of λF7 were prepared at 30° C (top) and 37° C (bottom) and standardized to 1 x 10^7 pfu/mL on various suppressors. The letter in the top row indicates the suppressor strain used to prepare the lysate. λF7 lysate grown on BB4 and TN buffer were used as controls and were only placed in the single well.

3.3.3 Discussion

SupD suppression of the *Dam15* mutation proved to confer the lowest viability to λF7, supported by the fact that plaques generated by λF7 were tiny, indicating a low burst size too. However, this mutant strain provided a superior gpD::eGFP decoration environment for λF7 as evidenced by the highest level of relative fluorescence. SupE and SupF were found to be essentially equal in their ability to suppress the D*am15* mutation, which was also surprising given the difference between glutamine and tyrosine in chemical structure. This difference may impact size and polarity, and is even more surprising since the insertion of glutamine agrees with the native polypeptide sequence of λ *D*. SupE was previously found to be the best suppressor of this mutation substituting glutamine at the stop codon, while supF substitutes tyrosine, a far bulkier and polar amino acid. Great variation in eop of λ*Dam15* on the wild type (Sup$^-$) and suppressor derivatives was observed. It is important to note that complementation by the *D::eGFP* plasmid cannot be measured in suppressors by eop assays, but rather by changes in the cellular ratio of λ gpD to gpD::eGFP and varying degrees of phage decoration. Across temperatures eop's did not change much for both the nonsuppressor and SupD except at 35° C and 37° C where there appeared to be a hundred-fold difference as compared to

suppression alone. When examining the stronger suppressors it is evident that at lower temperatures viability is not compromised. New unpublished data by our group indicates that the optimal temperature for decoration of λF7 by gpD::eGFP when passaged through SupD and the nonsuppressor appears to be 37° C. Furthermore, since complementation of the *Dam15* mutation by *D* and *D::eGFP* is quite efficient at higher temperatures, as indicated by the signals produced by SupD and the previous cellular data indicating rates of expression, the results attained with the nonsuppressor strain are unexpected. They further suggest that a 100% fusion decoration strategy is not ideal for maximal viability and that assembly is impacted in the absence of wild-type gpD (Nicastro, Sheldon, El-zarkout, Sokolenko, Aucoin, Slavcev unpublished).

Taking into consideration the results seen in Figures 10 and 11 the increased fluorescence observed for SupD preparations, despite these lower titres, could be due to lower eop yields arising from interference in phage adsorption due to high levels of decoration. Again, the difference in SupD over Sup^{-} supports the case that the presence of some (very few) gpD or similar derivatives provides the optimal scenario with respect to phage viability and phage decoration. This is corroborated by new data generated by our group (Table 2 of Appendix A) (Nicastro, Sheldon, El-zarkout, Sokolenko, Aucoin, Slavcev unpublished).

When attempting to achieve high-density display, many factors may contribute to success. The results of the assays here suggest that the maximum level of e*GFP* decoration cannot be achieved by the gpD::eGFP fusion alone, and performs best in the presence of the gpD Q68S protein. There is evidence to indicate that mosaic strategies may be the most effective in achieving high-level display in lytic display systems. High-level Soc expression in T4 results in inclusion body formation that is lethal to the host. A soluble form of Soc is rapidly degraded by proteolytic activity (Forrer, Jaussi 1998). Zucconi et al. (2001) looked at the high-density display capabilities of λ and its ability to display large proteins on its capsid as compared to other phage such as T7. This inherent flexibility makes λ a much more desirable fusion partner. Correspondingly, T7 is designed to display fusions at a low density for a reason related to the phage assembly process, and density of the hybrid capsid protein depends on protein size. This work also reported that λ is not only capable of displaying large proteins via gpD fusions, but can do so at a density where approximately 90% of the incorporated D protein is a fusion (Zucconi et al. 2001). Yang et al. (2000) also tested a variety of gpD fusions with a maximum size of 425 amino acids, fusing them to either terminus; all were able to complement a gpD mutation. Even though these fusions all required sizeable linkers, they were also able to show that the fusions occupied most, if not all binding sites. However, they did indicate that it is likely that a certain degree of proteolysis did occur, that would in turn generate some wild-type gpD to be displayed at some sites *in vivo* (Yang et al. 2000).

The optimal temperature (37^{o} C) to best complement λF7 with D expressed from pPL451 was the temperature at which almost all c*I857* repressor activity is eliminated and expression of the fusion is directed by the λ P_L promoter. Interestingly, and unexpectedly, phage grown on SupD expressing *D::eGFP* proved to be the most highly decorated, exceeding even that of the nonsuppressor, originally intended to be a positive control for decoration. This finding was surprising since theoretically phage can only be decorated by the *D::eGFP* protein due to the lack of *Dam*15 suppression in this strain. However, even a ten-fold phage reduction (10^7 Sup D vs 10^8 W3101) exhibited a greater fluorescent signal. A possible explanation for this result is the possible difference

in eGFP functionality versus eGFP decoration, where over-decoration may result in improper folding and fluorophore functionality, or signal quenching do to the close proximity of fluorophores (Dai et al. 2008).

Display of superfolder GFP (sfGFP) on the capsid of a phage has been previously explored using different filamentous phage display vectors (Velappan et al. 2010). In this study the authors assessed correct folding and display of sfGFP through fluorescence and antibody recognition. They found that there was little correlation between phage fluorescence and a positive antibody (ELISA) test (Velappan et al. 2010). Further studies were then performed to examine the antibody binding of eGFP. In regards to this study, it will be interesting to note if a similar trend in the level of expression exists (through Western Blotting) as it does with the recently discussed eop and fluorescent data. Dai et al. (2008), utilized T7 as a display vehicle and assessed its ability to correctly display GFP-based cytoplasmic proteins that were know to be poorly expressed by traditional phage display. This study concluded that fusions confirmed to be present on the phage surface (via Western Blot) do not necessarily fold correctly. They also determined that the fluorescence of free protein was higher than that of displayed protein. This was attributed most likely to quenching due to an interaction between the two fused proteins (Dai et al. 2008). These caveats are important to consider when examining the results of this research study. Since no steps were taken to eliminate free protein from solution, monomeric protein (gpD::eGFP) could contribute to the qualitative results, due to its presence in the lysate adding to visualized fluorescence. That aside, the level of expression should be the same in each host strain since the plasmid is identical and this additional fluorescence should be eliminated as background.

Other single-molecule fluorescence techniques have been employed to count fluorescent proteins per phage and determine display levels. Methods that can distinguish between soluble and phage-bound fluorescent proteins directly have proved more accurate for quantifying display levels than bulk methods, which contain non-infectious phage and soluble protein. Two such methods that have been employed when examining the number of GFP molecules present on T7 are fluorescence correlation spectroscopy (FCS) and photon antibunching (Dai et al. 2008). In addition, there has also been a study published recently using fluorescence-activated cell sorting (FACS) to quantify the number of eGFP molecules present on λ. This type of analysis allows for a much greater discrimination of phage populations and will allow for greater analysis of sub-populations and determinations of a true numerical difference when varying environmental conditions are applied (Sokolenko et al. 2012).

3.4 Assessing eGFP phage decoration

3.4.1 Whole Lysate Filtration

Since the *D::GFP* fusion is plasmid encoded and can be expressed at high levels by thermal induction (Figure 3), much of which may not be incorporated into assembling phage, the possibility of free protein in the cell lysate contributing to phage lysate fluorescence had to be addressed. To purify lysates and remove any contaminating protein, protein analysis data was collected following centrifugal filtration of whole lysates through three different molecular weight cut off filters. Titres of

lysates were measured before and after processing (Table 11) to ensure that filters were maximized to capture large gpD::eGFP molecules, while allowing phage passage. In addition, absolute protein concentration of each filtrate was measured to assess how much free protein had been filtered. The process by which lysates were membrane filtered is shown below (Figure 12).

While the 100 KDa filter allowed passage of ~400 phage per mL, the 50 kDa filter appeared optimal to remove residual protein without compromising any loss of phage when comparing the titres of different samples that were analyzed using various molecular weight cut offs. Results indicated that the ideal filtration optimization appeared to be with a 50 kDa filter. The 100 kDa filter used for the λF7 phage that was grown on W3101 supD [pKS1], which generated filtrate of 4 x 10^2 pfu/mL. Lysates were filtered in order to remove residual cytoplasmic gpD::eGFP monomers, which were retained through filtration with the 10 and 30 KDa filters.

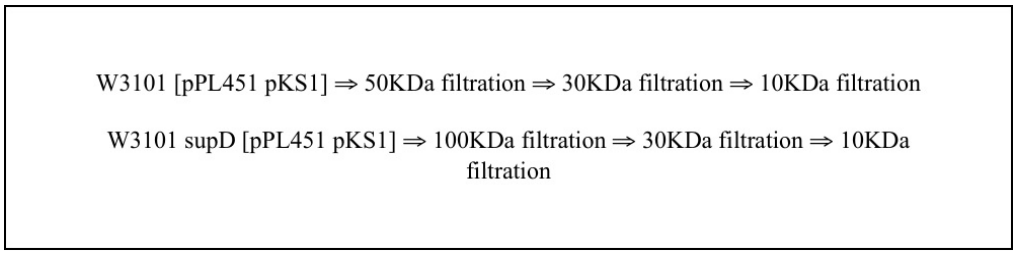

Figure 12: Lysate filtration of EGFP decorated λ*Dam15*

Filtration process taken with each lysate in preparation for protein analysis.

Table 11: Whole Lysate Filtration for Protein Analysis

Phage Lysate	**Initial Titre (pfu/mL)**	**Final Titre (pfu/mL)**	**Filter MWCO[1] (KDa)**	**Protein Conc. of Filtrate OD_{280} (mg/mL)**
W3101 [pKS1]	7.00 x 10^7	2.2 x 10^8	50	19.502
W3101 sup*D* [pKS1]	4.00 x 10^7	2.0 x 10^7	100	16.930
W3101 [pKS2]	9.90 x 10^8	2.5 x 10^{10}	50	21.116
W3101 [pKS1]	n/a	< 1 x10^2	30	6.435
W3101 sup*D* [pKS1]	n/a	4 x 10^2	30	9.572

[1]MWCO = Molecular Weight Cut Off

[2]The flow through from use of the 30KDa filter was also refiltered with a 10KDa filter and the concentrations were W3101 [pKS1] = 9.648 mg/mL and W3101 supD [pKS1] = 10.212 mg/mL

After filtration of the flow-through from W3101 [pKS1] and W3101 SupD [pKS1], filtrates were observed under eGFP filters alongside their whole lysate counterparts. There was a decrease of fluorescence for the Sup^{-} [pKS1] strain and strong presence of fluorescence for the W3101 SupD [pKS1] strain. Both strains were then further filtered using a 30 kDa and 10 kDa filter and the resulting filtrates flow through were compared with the first and noted to yield a similar result to the initial filtration. This data agrees with the results from Table 11 above, as filtrate flow through from the later strain (SupD) contained phage at approximately 4 x 10^2 pfu/mL post filtration whereas the W3101 [pKS1] did not yield any viable phage.

Figure 13, shows the comparison of primary lysate fluorescence to lysate filtrate. The level of fluorescence was standardized using λF7 as the negative control background signal. The filtrate of the W3101 SupD [pKS1] phage preparation through the 100 kDa filter exhibited detectable fluorescence at 2 x 10^7 pfu/mL. The fluorescence signal should be primarily due to gpD::eGFP monomers within the whole lysate.

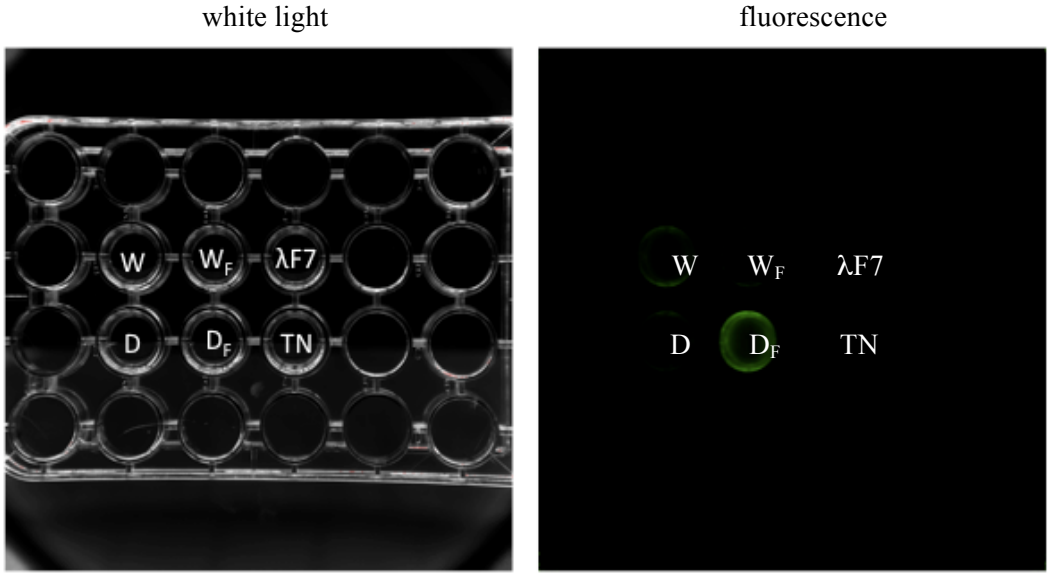

Figure 13: Comparison of fluorescence from filtered and unfiltered lysates

Comparison of fluorescence between prefiltered lysates and filtrates. Each phage preparation is labeled indicated by the strain on which the lysate was grown. Subscript F indicates post filtration. λF7 and TN were used as a phage and buffer control, respectively.

Next, the levels of fluorescence observed from the lysate filtrates were compared. Figure 14 shows a comparison of the both filtered phage pre and post 30 kDa and 10 kDa size exclusion filtering. Only the pre 30 kDa lysate for SupD showed any signal, indicating that it was the only lysate that contained a significant amount of eGFP assuming that free monomeric gpD::eGFP was retained by the 30 kDa filter. The background level of fluorescence was determined by the use of a control phage grown on W3101 [pKS2].

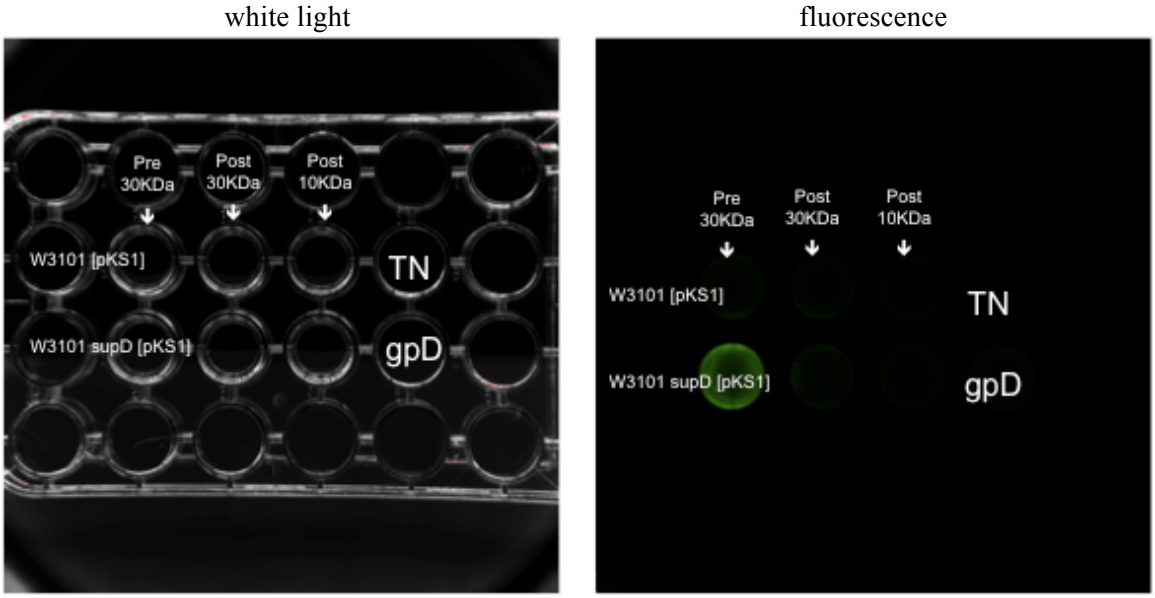

Figure 14: Fluorescent signal from lysate filtrates

A comparison of collected lysate filtrates. Top row: W3101 [pKS1] preparations. Bottom row: W3101 SupD [pKS1]. Column 1: Flow through from before the 30 kDa filtration; 2: Filtrate following 30 kDa filtration; 3: Filtrate following 10 kDa filtration. Background level of fluorescence was determined based on W3101 [pKS2 (pD^{+})].

3.4.2 Western Blot Analysis

The GFP fluorescence assays suggest that λ F7 passaged through SupD expressing *D::egfp* provided the strongest decoration of λ phage by gpD::eGFP. However, it is important to note that fluorescence is related to protein function, and may not parallel the actual fusion protein insertion. For instance, over- decoration may result in quenching, steric hindrance or other unidentified hindrance of functionality, as mentioned in above sections regarding GFP. To determine actual eGFP density per phage, immunoblotting was conducted on phage lysates passaged through the two highest fluorescence yielding strains under induced conditions (37^{o} C): Sup^{-} and SupD, both carrying the inducible *D::eGFP* [pKS1] plasmid. Proteins were separated electrophoretically by size, then immunoblotted using a polyclonal primary anti-GFP antibody and stained by two different approaches (Figures 15 and 16). The intensity of the eGFP band at 33 kDa from SupD [pKS1] following filtration via 30 kDa filter was observed to be remarkably stronger than that of W3101 [pKS1] when the same amount of whole protein is loaded. This finding suggests that SupD [pKS1] phage preparation may confer a greater eGFP decoration capacity to the λF7 phage. Figure 15 shows the presence of gpD::eGFP within the filtered lysates that is decorating the phage. The predicted size of the upper polypeptide is consistent with gpD::eGFP, while the lower band migrated at a rate consistent with the size of native eGFP. As a polyclonal antibody was used for detection, it is possible

that this lower polypeptide is due to cross-reactive staining of a different phage protein, but this is unlikely. The lower polypeptide more likely represents a derivative generated during the sample boiling step of the immunoblot protocol or could potentially been caused by proteases within the host cell that have caused the breakage before samples were prepared. In either case the linker between gpD and the fused eGFP represents a weak point in the modular protein that results in dissociation between the two components.

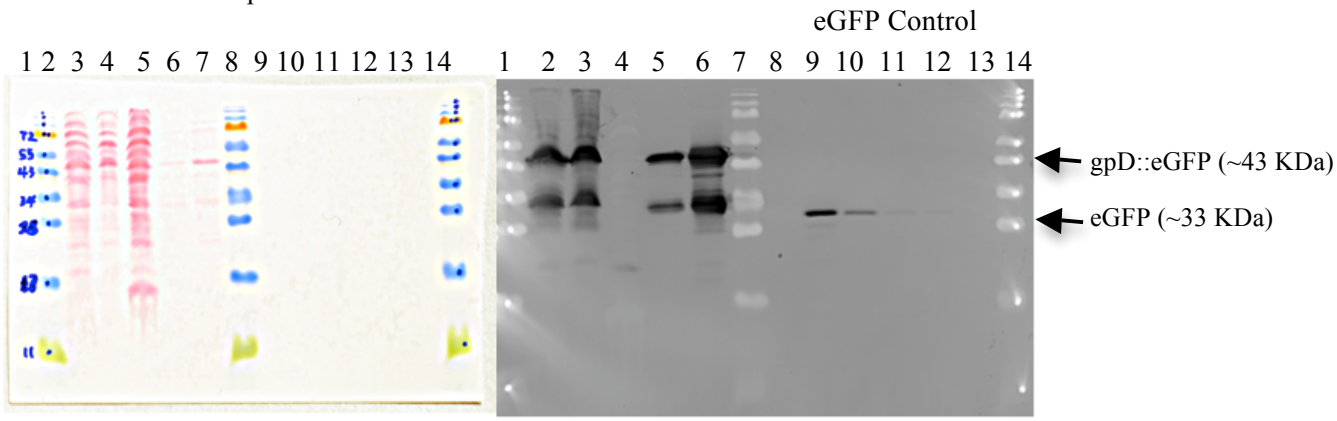

Figure 15: Fusion gpD::eGFP decoration of λ*Dam15* phage passaged through Sup⁻ and Sup+ *D::eGFP* expressing strains.

Lanes 1, 7, 15: size markers. L2: W3101 [pKS1], L3: W3101 *supD* [pKS1]. L4: W3101 [pKS2], L5 and 6: Filtrate from the initial samples filtered with a 30 kDa filter. L8: blank. L9 - 14: eGFP standard at 50 ng, 10 ng, 1 ng, 50 pg, and 100 pg respectively. For lanes 2, 3, and 4, 200 ng of absolute protein was loaded. For lanes 5 and 6, 100 ng of absolute protein was loaded. Membrane image shown on left, stained with Ponceau S; membrane image on right, detection by fluorescence.

The filtrates following passage through a 10 KDa exclusion filter were analyzed in a similar blot (Figure 16). Once again, the level of eGFP decoration observed upon passaging of the λ*Dam15* phage through the W3101 *supD* [pKS1] strain was qualitatively much greater than that seen on W3101 [pKS1]. The 10 kDa filtrates lost the lower eGFP band originally observed from the 30 kDa flow through (Figure 15). This may be due to the removal of all dissociated eGFP by the 10 kDa filter, retaining only gpD::eGFP. While this finding likely indicates the presence of gpD::eGFP monomer in the whole lysate, it was not substantial enough to signal notable fluorescence for the control phage (Figures 9 and 10), indicating that in prior qualitative studies the majority of fluorescence observed was indeed conferred by the decorated phage and not free gpD::eGFP fusion protein.

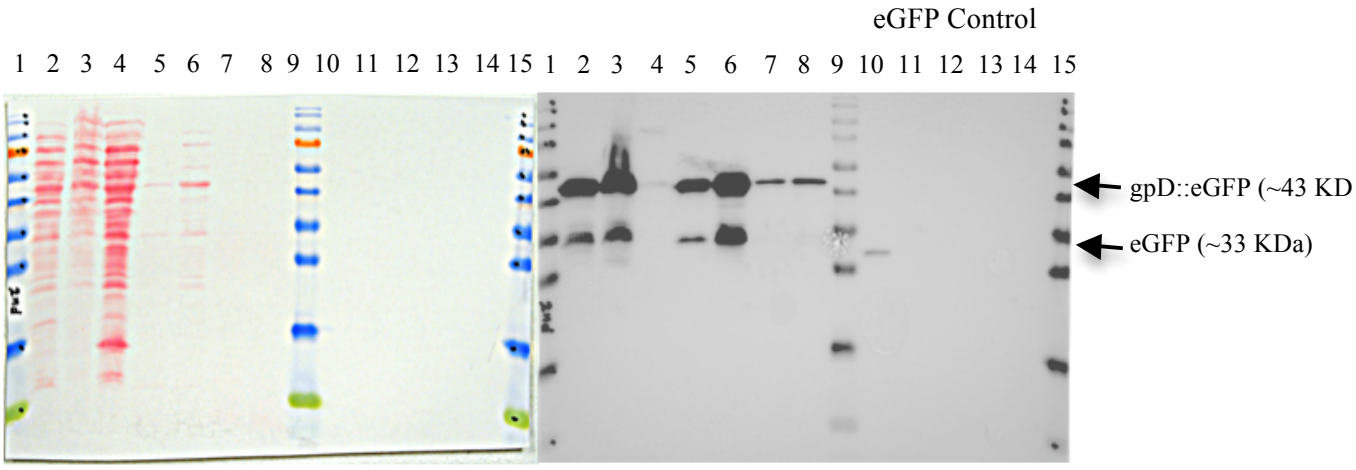

Figure 16: Protein analysis of gpD::eGFP monomer present within the sup⁻ and sup+ filtered lysates

Lanes 1, 9, 15: size markers. L2: W3101 [pKS1], L3: W3101 *supD* [pKS1]. L4: W3101 [pKS2], (negative control for eGFP). L 5 and 6: Flow through from the initial samples filtered with a 30 kDa filter. L10 - 15: eGFP standard at 50 ng, 10 ng, 1 ng, 50 pg, and 100 pg respectively. For lanes 2, 3, and 4, 200 ng of absolute protein was loaded. For lanes 5 and 6, 100 ng of absolute protein was loaded. Lanes 7 and 8 are 10KDa filtrates of W3101 [pKS1] and W3101 supD [pKS1]. As in Figure 15, the left image of Figure 16 is the membrane stained with Ponceau S and the right image is detection by fluorescence. For lanes 7 and 8 100ng of absolute protein was loaded.

3.4.3 Discussion

In solution, λ gpD exists as a monomer even at very high concentrations, and trimer formation of native or fusion D proteins only occurs through cooperative binding; it is facilitated by λ gpE during prohead assembly (Hayes, Gamage & Hayes 2010, Yang et al. 2000). With this in mind, in order to eliminate the majority of free gpD and gpD::eGFP in solution before immunoblotting was performed, phage lysates were filtered through size exclusion columns. Here, titers were compared between pre and post-filtered lysates to determine whether phage were being filtered as well. A study by Vaccaro et al. (2006) involves purifying phage particles first by standard PEG precipitation, before capturing viable phage by affinity-purification using an anti-V monoclonal antibody. The purpose of the additional step was to eliminate free recombinant gpD from solution since it is also precipitated by PEG with phage particles. A similar intention was desired in this study through the use of filtration, rather than through the use of antibodies.

A fluorescent signal was evident in the flow through after passage through the 30 kDa filter, which may indicate that this size exclusion treatment did not remove free gpD::eGFP from the lysate, or that another cleaved species of eGFP was present upon preparative treatment, since this size of filter should capture gpD::eGFP monomers.

Similarly to the fluorescence assays, two distinct bands were noted in all assays of decorated phage or filtrates. The 43 kDa protein denotes gpD::eGFP, while the smaller identified species (~33 kDa) aligns with a cleaved eGFP. This could be a possible point of cleavage or breakage as, there is only a short linker that separates gpD and eGFP and during the SDS and boiling process or within the

host cell at the hand of proteases, the two proteins could separate through a break of this linker. More specifically, there is also a Lon protease cleavage site at this location as well, that may cleave at high temperatures. This may also be responsible for the two distinct bands that are observed here. Interestingly, the filtrate from the 10 kDa filter retains only gpD::eGFP, eliminating the smaller species, which should occur, since the fragment is 33 kDa.

GFP has proven to be a suitable fusion protein and reporter. In addition, certain mutants have shown to be relatively stable in the presence of some proteases and protein denaturing solutions such as 1% SDS, where studies have observed that it also does not lose its fluorescence (Aoki et al. 2003). Fused GFP species were observed to migrate to different positions, where the molecular mass of the fused polypeptide was lower than that of the nonfused counterpart. This result may be caused by the β-can structure of GFP, where the structure is not destroyed by SDS and the mobility of GFP is slow and the fused protein moves more quickly (Aoki et al. 2003). In addition, the fluorescence intensity of GFP can increase or decrease depending on the polypeptide that is fused. Here, the expression level was not consistent with observed fluorescence, which depends on the amount of the active form present. Aoki et al. (2003) further speculated that the amount of active form depends on the hydrophilicity of the fused polypeptide where there is a positive correlation between fluorescence and hydrophilicity. Velappan et al. (2010), in their work with display of stable GFP on filamentous phage, were able to apply a commercially available monoclonal antibody that recognized a conformational epitope destroyed by SDS and boiling. The use of a similar antibody could provide insight into whether or not an active or inactive form of eGFP is present in solution after SDS treatment and boiling.

To quantify the amount of protein and therefore the number of fusion proteins per phage Gupta et al. (2003) and Vaccaro et al. (2006) used densitometric scanning of a Western blot to determine that the total copies of fusion protein per phage particle was approximately 400 gpD fusions/phage. Here, the N-terminal comprised 48.8% of recombinant gpD proteins, while the C-terminal constituted up to 88.4%. This application extends the utility of immunoblotting to density quantification of gpD::eGFP fusions present on each phage capsid. Since, we were unable to determine the exact amount of protein (gpD and eGFP) as lysates also contain phage structural proteins, this method may prove useful since it would not consider the additional protein content that is present within the lysate that is not eGFP.

3.4.4 Conclusion

By immunoblotting filtered lysates, additional insights were garnered with respect to density of fused protein on the capsids of decorated phage constructs. Firstly, when phage lysates were filtered to remove gpD::eGFP monomers in solution, a significant level of fluorescence was observed in the flow through, indicating that monomers were present and they contributed to the overall fluorescence observed in previous experiments. Through the use of an eGFP-specific antibody, the presence of eGFP was confirmed to be present on the phage capsid with two distinct polypeptides appearing on the blot, one the size of gpD::eGFP (43KDa) and the second, eGFP (33KDa) alone. It is possible that this second band was generated through the cleavage of gpD::eGFP, dissociating eGFP from gpD due to breakage of the short peptide linker during SDS treatment or boiling during sample preparation. This additional (lower) band did not exist in flow through samples (that were filtered with a 30 kDa

filter, that would not allow larger phage particles to be passaged), further supporting the above theory. Purification could be dramatically improved through the use of an affinity binding strategy, such as utilizing the major tail protein gpV to avoid the need to filter samples. This would eliminate the potential loss of titre from filtering as well as reduce cellular contamination of unincorporated fusion proteins.

Chapter 4 Conclusions and Future Directions

4.1 Final Conclusions

4.1.1 Overall Objectives and Achievements

The global objective of this research project was to create a bacterial model for the controllable expression of peptides/proteins on the major capsid protein (gpD) of bacteriophage λ. The creation of such a modifiable platform system of phage display could then be geared towards downstream applications such as novel biologic development (vaccines, antimicrobials) and/or targeted gene therapy, to name a few. In order to achieve this objective, two levels of genetic control were applied; a plasmid-mediated temperature inducible repressor (c*I[Ts]857*) governing downstream gene expression, and amber suppression (via SupD, SupE, SupF suppressor alleles) providing different translational derivatives of the major capsid protein with varying levels of functionality.

The novel constructs that were derived from this research include:

1. SupD/E/F bacterial *isogenic* amber suppressor strains
2. The pKS1 plasmid, a multicopy *D::eGFP* expression plasmid governed by the temperature sensitive λ c*I857* that imparts *in trans* gpD::eGFP decoration increasingly as temperature is raised
3. The pKS2, a multicopy derivative of pKS1 deleted for eGFP that expresses wild-type *D*.

The novel scientific results achieved through this research include:

1. Sequencing of λD*am15* allele, indicating a point mutation at 204th bp of *D* converting the 68th residue, glutamine (**C**AG), to an amber translational stop signal (**U**AG).
2. Determination of the relative plating efficiency of each isogenic suppressor strain at various temperatures. As expected the nonsuppressor did not support viability of the λ*Dam15* phage, and the Q68S allele generated by λ*Dam15* growth on the *supD* showed very poor functionality compared to gpDwt (*supE*) and gpDQ68Y(*supF*).
3. Expression of λ *D* from pKS2 was able to nearly completely complement for the D*am15* mutation at induced temperatures, while observed complementation in this work from pKS1 (*D::eGFP*) was far lower than its D$^+$ counterpart.
4. Expression of *D::eGFP* and *D* from pKS1 and pKS2 respectively, at temperatures showing high-level expression of D::eGFP was not toxic to the bacterial cell.
5. Regulated expression of *D::eGFP* from pKS1 in combination with varied D allele functionality conferred by various amber suppressor strains led to different levels of λ capsid decoration by both wild-type and fused gpD. gpDwt (*supE*) and Q68Y (*supF*) alleles demonstrated comparable and best functionality as gauged by restoring viability of λ*Dam15* phage.
6. Greatest eGFP decoration of phage was observed in phage passaged through the nonsuppressor and *supD* strains expressing *D::eGFP* from pKS1 at the inducing temperature

of 37° C. These constructs also appear to affect phage viability, where the presence of increased levels of fused protein impacts the ability of phage to assemble appropriately.

7. Western blotting confirmed the presence of eGFP fused to gpD as well as the presence of a second species that may be attributed to proteolytic cleavage or breakage of eGFP from gpD.

4.1.2 Supporting Literature

4.1.2.1 Amino vs. Carboxyl Fusions and the Presence of Suppression

The λ gpD protein is tolerant of a wide variety of protein and peptide fusions to its amino and carboxy terminal ends, providing great flexibility for phage display. Pavoni et al. (2004) constructed a tumor cDNA display library employing N-terminal fusions to gpD in order to prevent the selection of out-of-frame fusions. Since the N-terminal fusion was upstream of gpD, if it was out-of-frame, the fusion would not be expressed because the downstream gpD would also be out-of-frame and therefore unable to assemble appropriately within the phage capsid. As such, the recombinant phage would be decorated solely with wild-type gpD (Pavoni et al. 2004, Minenkova et al. 2003). This study also utilized the λKM8 and λKM10 phage constructs, which were based on KM4 phage which can accept inserts of up to 3 kb in length without disturbing lambda packaging (Minenkova et al., 2003). The use of an N-terminal fusion and an engineered phage created an excellent environment for easy assembly of chimeric phage. However, N-terminal fusions, to eGFP prevented its proper folding and therefore fluorescence would not be possible. Our construct has similar properties to the KM phage, in that a two-gene system is employed, although our fusion is plasmid-mediated and controllable in nature. When the phage was first designed, Pavoni et al. (2004) also determined as did Zucconi et al. (2001) that the number of fusion proteins displayed on the capsid surface varied depending on the length and a.a. composition of the foreign sequence and when these fusions were expressed at the C-terminus a very high incorporation rate could be achieved; a similar situation exists for N-terminal fusions. Neither of the studies above mentioned a reduction in phage viability or an effect on phage assembly with the peptides they attempted to fuse (Minenkova et al. 2003, Zucconi et al. 2001). These are however important considerations in that they give insight into the affect the fusion has on the ability for D to retain functionality and thus, for phage to assemble properly and form viable phage particles.

To further examine differences between the N and C termini of gpD in conferring decoration on λ, Vaccaro et al. (2006) created fusions to a functional scFv antibody (anti-CEA) to λ's gpD. Human carcinoembryonic antigen (CEA) is an oncofetal glycoprotein known to be over-expressed in several tumour types. In order to create these fusions, they also utilized the KM phages, λKM8 (N-terminal) and λKM10 (C-terminal), which contain a double gene D system and a flexible linker between the fusion peptide and gpD. The genomic copy of D contains an amber mutation, where the second copy, used for fusions, has a unique cloning site at either the N or C-terminal respectively. When phage carrying a fusion are grown on an amber suppressor, chimeric phage that display both the fusion and wild-type D are produced (Vaccaro et al. 2006). While the phage described by Vaccaro et al. are similar to those generated by the system constructed here, *i.e.* chimeric phage are created when a fusion is cloned into either phage genome, poor control exists in their system imparted only by the crude competition between suppressor generated gpD_{wt} and constitutive production of the fusion allele.

When comparing the N and C-terminal fusions, the carboxy- fusions presented with unusually small plaques, which suggested that the large scFv protein was compromising phage assembly. In addition, titres derived from a single plaque for this phage were also significantly lower than that seen for the N-terminal fusion and unfused λKM8 and λKM10, where the average was 10^6 PFU per plaque as compared to 10^3 PFU per plaque for the C-terminal fusion (Vaccaro et al. 2006). These results show similar trends to this work when a *supD* suppressor or nonsuppressor was employed. These observations suggested that the presence of D::eGFP at high densities might inhibit phage assembly, corroborated by the reduced plaque size and lower titres of this prep as compared to those grown on stronger suppressors. Santini et al. (1998) also observed a similar result where fusion of large protein domains to gpD significantly reduced the titre of phage when grown on Sup^{-} strains, indicating that incorporating wild-type D protein is preferential for proper assembly, and that the use of suppressor strains is advantageous.

Vaccaro et al., (2006) also performed phage stability assays, via immunoscreening, and observed that 1-5% of plaques generated by C-terminal fusions were larger in size and negative for the assay and the C-terminal fusions also had a lower titre as compared to the N-terminal fusions. After further investigation, it was discovered that these plaques were in fact mutants and contained frame shift mutations or stop codons within the scFv gene. This additional evidence further supports the inefficient display of the antibody as a C-terminal fusion and its effect on phage assembly. Tiny plaques observed in this work when phage were grown on *supD*, may indicate the presence of revertants or mutants that are seen because the lack of suppression is disadvantageous to phage assembly and growth. Interestingly enough, this was not observed when phage were grown on a nonsuppressing strain, as would be expected. Furthermore, the N- and C-terminal fusions also varied in their fusion density, where the C-terminal was composed of a greater percentage of recombinant protein than the N-terminal. These data agree with the previous observations regarding stability and phage assembly, further confirming that a portion of the phage must consist of wild-type gpD (Vaccaro et al. 2006). The significant disparity in percentages also presents a strong case for the success of high-density display at the C-terminal. It is important to note, that the presence of a suppressor, may also contribute to the overall density, since the integration of some wild-type gpD increase phage viability. Even though this study determined that an N-terminal fusion to a scFv antibody gives rise to normal plaques, with comparable efficiency to that of the wild type, they have a lower antibody display density. This may be due to a reduced interaction at the gpD-binding site with gpE and therefore lower incorporation efficiency, while still retaining the higher viability. Here we observe a trade-off that exists between N and C-terminal fusions, where increased phage viability is inversely proportional to incorporation efficiency. A similar conclusion was also arrived at by Yang et al. (2000) when N-terminal fusions to gpD were examined. The higher display density exhibited by the C-terminal fusion indicates that the presence of a large protein disrupts phage assembly (not in the same manner as N-terminal fusions, because a higher incorporation is observed) thereby decreasing phage viability due to the overloading of recombinant protein, causing the lower PFU and higher mutation rate. Interestingly, they report that this C-terminal phenomenon was not observed in previous studies where recombinant protein was incorporated with wild-type gpD again suggesting the role of wild type gpD in improving incorporation of the fusion. These studies did mention that low yields and decreased phage viability were observed when there was a greater incorporation of

fused protein, most likely due to the presence of a strong suppression (the source of the fusion protein) (Mikawa, Maruyama & Brenner 1996, Maruyama, Maruyama & Brenner 1994).

4.1.2.2 Foundational Data for this Research Study

Close examination of the principal research that forms the basis of the studies reported in this thesis reveals additional consistent observations. Maruyama et al. (1994) initially investigated the use of suppression as a control mechanism for the display of fusion proteins on the surface of λ. They used the λfoo vector that expressed a truncated form of λ's major tail protein, gpV (mutants had been shown to exist where up to one third of the protein is missing), a short linker and an in-frame coding sequence. Phage grown on a suppressor strain produced full-length gpV with a fusion at the C-terminus. Fusions created using this system included *E. coli* β–galactosidase and plant *Bauhinia purpurea* agglutin. Again, when grown on strong suppressor strains, smaller plaques were observed. This result was not observed when comparing the parent (λfoo) or growth on weaker/nonsuppressor strains. The authors hypothesized that "large amounts of chimeric fusion protein produced by the strong suppressor, inhibit phage assembly". Further evidence to support the effect on phage assembly is the observed low yield of fusions present on the phage surface, where the majority of phage had no incorporation and only 1% had 3 or more fusions. A final important observation was the residual read-through of the amber stop codon, where trace amounts of fusion were noted when phage were grown on nonsuppressor strains.

From these prior experiments, some similarities and incremental improvements can be observed in the results presented in this thesis. For the constructs described in the paragraph above the level of suppression fully controlled the presence of fused protein and therefore, the stronger the suppressor the greater the level of expression of the gpD allele. Initially, it was found that large C-terminal fusions created distinctive plaque sizes and impacted phage assembly but may not influence yield, since gpD exists in a much greater density than gpV. In addition, the chance of residual read-through was greatly reduced with the existence of an ochre stop codon within the eGFP sequence, which does not allow for residual read through after the fusion, since only amber suppression is being conferred by the amber suppressor host cells. Furthermore, due to the reverse construction of this system, where suppression supplies the gpV fusion, rather than wild type, it does not as easily allow for the presence of wild type gpD, which may have contributed to the reduced phage viability and smaller plaques. Again, the ability to control the number of fusions, on the phage capsid appears to impact phage assembly and phage viability.

Following the use of the tail protein as a fusion candidate, two separate groups studied the use of gpD for fusions at the same time. Sternberg and Hoess (1995) studied N-terminal fusions, and Mikawa et al. (1996) looked at both N and C-terminal fusions to gpD. The former used the Cre-*lox*P site-specific recombination system to incorporate fusion plasmids directly into λ, whereby phage then contained both a wild-type D (when grown on a suppressor) and the fusion protein was supplied by the integrated plasmid (Sternberg, Hoess 1995).

Both studies demonstrated that protein could be fused to the phage capsid *in vitro* utilizing plasmid-mediated *in trans* complementation. Both studies also showed an inability to achieve a scenario where all gpD sites on the capsid were occupied by fusion proteins as phage were still

resistant to EDTA, indicating empty gpD sites. Sternberg and Hoess (1995) also used a plasmid expressing wild-type *D* reporting similar results to those described here, where they were able to restore phage viability via complementation from the *D*-expressing plasmid. In addition, the concept of polyvalency was raised, and the ability to use such a system for gene delivery where surface decoration could be achieved *in vitro* or *in vivo*. Moreover, Mikawa et al. (1996) showed that plasmid copy number does affect the level of expression and therefore ability to complement and by supplying only fused protein at high levels phage are still sensitive to EDTA, indicating again not all sites are occupied by fused protein (Mikawa, Maruyama & Brenner 1996, Sternberg, Hoess 1995). In this work, plasmid copy number was not used as an approach to control decoration and a high copy plasmid was employed for all constructs, but this may be of interest in future studies where multiple fusions could be incorporated simultaneously into a phage capsid. The manipulation of plasmid copy number could provide a third dimension of control.

Mikawa et al. (1996) developed a system where a peptide/protein could be fused at either the N or C-terminus of gpD. Genetic (amber) suppression was used to control the proportion of chimeric protein decorating the phage capsid. Using this system, they examined gpD fusions of β–lactamase, the IgG-binding domains of the *Staphylococcus aureus* protein A and β–galactosidase (β–gal). They noted that N-terminal fusions of Protein A and β–gal, yielded low recovery on a nonsuppressor host, indicating that the phage assembly and viability is affected by chimeric gpD fusions in the absence of native gpD. Interestingly, when passaged through a strong suppressor alone, this study revealed a greater than 100% recovery of original titre, suggesting that suppression may in fact be more or equally as effective as *trans* complementation and may incorporate proteins just as efficiently. As mentioned and illustrated previously, the availability of unfused molecules increases viability in combination with their fused counterparts compared to fused molecules alone (Mikawa, Maruyama & Brenner 1996). In my work, I also noted a higher recovery of phage carrying both unfused and fused gpD compared to unfused alone. This may suggest that 100% decoration of λ by gpD fusions cannot result in functional phage, and there is still a need for some wild type gpD in achieving optimal phage assembly. The results shown here indicate that the highest fusion density occurs through the combination of the fused gpD and a poorly functioning gpD derivative, such as gpDQ68S (SupD), thus allowing the incorporation of some unfused gpD allele, and a large portion of fused protein, as seen in this study with the supD strain. This argument is further confirmed when comparing the supD incorporation to that of both the strong suppressor (SupE and SupF) and the nonsuppressor strains, where increased viability is conferred by the strong suppressor but a low ratio of fused to unfused molecules was observed.

In addition, when a wild-type λ *imm21* (D^+) phage was plated on cells carrying the fusion plasmid, fusions were also incorporated into the capsid, not just wild-type gpD, which further suggests that plasmid-mediated complementation has the capacity to compete effectively with the incorporation of wild-type gpD within the cytoplasm during phage assembly (Mikawa, Maruyama & Brenner 1996). This is an important observation when attempting to determine what the efficiencies of incorporation are when comparing suppression and incorporation of various gpD derivatives compared to that of the fused gpD allele expressed from a temperature-regulated plasmid.

Like Sternberg and Hoess (1995), this group also constructed their own phage vectors, which in this case were modeled after λfoo, a vector that utilizes a truncated form of λ's major tail protein,

gpV, a short linker and a fused protein, where phage grown on a suppressor strain produce full-length gpV with a fusion at the C-terminal. One of these vectors contained an N-terminal fusion (λfooDn) and the second, a C-terminal fusion (λfooDc). Once Protein A was incorporated, and phage were grown on different suppressor strains, they noted that both phage were capable of binding to a corresponding antibody (BSA) when the phage was passaged through a strong suppressor. The same phage (λfooDc) decorated with β–gal was used to estimate the number of fusions per phage as compared to the original λfoo. As expected a greater number of fusions were observed on a stronger suppressor (34.3 vs. 2.3) and both showed a greater efficiency to that of λfoo (Mikawa, Maruyama & Brenner 1996). This is important to note when considering the use of a display system for downstream applications, in that there must be a certain number of fusions present on the capsid in order to elicit any response, to provide utility toward any application.

The Maruyama (1994) and Mikawa (1996) studies used constructs where an amber stop codon was located upstream of the gpV/gpD fusion modulating total fusion protein incorporated on the capsid. As such, the level of decoration was dependent on the strength of suppression supplied by the host bacterial Sup^+ mutant through which the phage was passaged. Overall, these initial studies provided a great foundation and premise for this body of work while also providing preliminary insight into some of the challenges that would be faced and complications that needed to be overcome. To build on this foundational work we sought to construct a novel display platform that uses multiple levels of control—1) amber suppression that supplies various unfused gpD derivatives; and 2) temperature regulated complementation of the gpD fusion. Utilizing the C-terminal of the gpD molecule allowed for high-density display, where the highest level of phage decoration was when high expression of the D fusion was combined with the poorest functioning gpD derivative (SupD).

4.2 Future Directions

4.2.1 Downstream Applications of this Research

The intended downstream applications of this research are the construction of multivalent phage vaccines and/or the development of vehicles for phage-mediated targeted gene therapy. These applications exhibit the two endpoints of the spectrum of phage surface display control. Vaccination would expectedly be most effective if display saturation was reached, whereas targeted transgene delivery applications would require a high-level of specificity in targeting unique receptors of appropriate cells, where fewer and controlled fusions would be preferable. The use of this system to create a novel procedure for phage vaccine development will first be discussed followed by the practicality for use in gene therapy. Advantages of using phage in vaccine design include:

- Feasibility of producing them rapidly in large scale for minimum cost
- Non-infectivity toward an animal host, safety (phage can be genetically or physically inactivated)
- Stability (wide range of temperature and pH)
- Natural adjuvant activity
- Ability to target APCs and induce both cellular and humoral immunity (Hayes, Gamage & Hayes 2010)

4.2.1.1 Use of Phage in Vaccine Development

The use of filamentous phage in development of vaccines was explored by Bastien et al. (1997), who employed phage fd to display a chimeric protein with a proven protective epitope (G glycoprotein) against RSV. This study showed that mice acquired complete resistance to a viral challenge by the lack of virus in their lungs and high levels of RSV-specific antibodies. In addition, the level of antibody was only slightly lower than that seen when mice are immunized with whole RSV virus. This study also first showed that a recombinant phage can be selected directly from a random peptide library and used directly in protection assays (Bastien, Trudel & Simard 1997).

March et al. (2004) first used λ as a DNA vaccine when they immunized mice with λ particles encoding either eGFP or hepatitis B surface antigen (HBsAG) in the commercially available λ expression vector λ-gt11 (Agilent Technologies, Mississauga ON). In order to create this non-traditional DNA vaccine, expression cassettes containing DNA from eGFP or HBsAG were cloned into λ-gt11 under the control of a eukaryotic promoter. The DNA was then packaged *in vitro* by the phage and propagated in *E. coli*. Finally, recombinant phage containing the DNA were injected into mice. Here the expression system allowed the DNA to be protected by the phage until safely within the cell. These particular constructs did not display the protein on the phage surface (March, Clark & Jepson 2004). Both of these modified DNA vaccine constructs were able to elicit an immune response in mice that were specific to eGFP and HBsAG, but results were inconsistent, suggesting that by displaying antigens on the surface of the phage, rather than a DNA solely format is a more specific and effective approach for phage vaccination. Recently, Thomas et al. (2012) developed a λ vaccine using a combination of *cis* (via recombination) and *trans* (plasmid-mediated) phage display to further show that peptide immunization is superior to genetic immunization, where proteins elicited a far stronger immune response at physiological pH in higher primates and humans than genetic vaccination in the absence of an adjuvant, where *cis* complementation indicates that the gene product is derived from the same gene and *trans* complementation indicates that the gene product is derived from a different gene. In addition, they also developed a divalent subunit vaccine, that was a hybrid of both a DNA and a peptide vaccine which was far more superior than the solely peptide vaccine creating two separate fusions to gpD, one with GFP and the other TAT protein (protein transduction) from HIV1. Both fusions were constructed to the C terminal of gpD and a short linker was placed between the two protein domains and these were displayed on the phage surface in tandem. The same phage that lacked display of these two proteins was used as the DNA vector for comparison. Similar to the system shown here, the plasmid expressing the fusion was inducible by IPTG (Isopropyl β-D-1-thiogalactopyranoside) and the recombineered genome was passaged through a SupF host. All immunization groups observed a primarily humoral response and they also found that λ itself acted as an endogenous adjuvant, where the phage displaying the two peptides again outperformed the non-displaying DNA vaccine (Thomas et al. 2012). One incremental improvement seen in the system constructed for this research study is that the temperature-inducible promoter does not require the addition of any chemical inducers, but rather just a change in temperature, which simplifies the preparation process.

A second lambda-based vaccine was also developed by Hayes et al. (2010) that was slightly more advanced than the prior. In this construct multiple fusions to the C-terminal of gpD were made; one where four immunodominant regions of the porcine circovirus capsid were fused (D-CAP), a

second with GFP (D-GFP) and a third with SPA tag protein. (D-SPA). SPA is a C-terminal tag that is used to purify a target protein with its corresponding antibody (Zeghouf et al. 2004). Interestingly, the D-GFP and D-CAP fusions could be expressed constitutively without compromising host viability, whereas D-SPA expression reduced cell viability by >50-fold. These results suggest that not all fusions are well tolerated. Termed "recalcitrant" such fusions prevent protein oligomerization and the formation of trimers during phage assembly and therefore display fewer D-fusion proteins. Overall, this group was successful in creating three different D-fusions, where the D-GFP was highly fluorescent, the D-SPA was recognized by a FLAG monoclonal antibody and the D-CAP construct was able to elicit both an antigen-specific cellular and humoral response in pigs. One important note to make though, is that once these constructs were integrated into a lambda display particle (LDP) both LDP-D-GFP and LDP-D-SPA did not induce a useful antibody response suggesting that *in vivo* they would not elicit a sufficient immune response (Hayes, Gamage & Hayes 2010, Gamage, Ellis & Hayes 2009). With the ability to control the number of fusions present, the chance of encountering recalcitrant fusions would be decreased. Despite the lower number of fusions per phage, cell viability would be improved.

The issue of "recalcitrant" protein display was explored in detail by Zanghi et al. (2005) who developed a mosaic expression approach where λ was decorated by both wild-type and recombinant proteins in tandem to circumvent the issue of recalcitrance. This system utilized two separate plasmid constructs that contained different origins of replication and selectable markers, that were co-transformed into a gpD-deficient λ lysogen. When only the recombinant plasmid was expressed no viable phage could be recovered, indicating that the fusion must somehow interfere with assembly or prevent formation of stable phage particles. Mosaic phage titres were very similar to that of wild-type phage, where the slight reduction could be attributed to plasmid attributes—mainly copy number and protein expression (Zanghi et al. 2005). With the presence of two plasmids that theoretically have consistent expression and fusion capacities, the level of control is still quite limited. In contrast, employing an independent second dimension of control such as that conferred by suppression, imparts differences in rates of incorporation due to functionality that can generate greater variability in decoration.

This group next expanded on this design by using the same construct design to simultaneously fuse proteins to both the head and tail of λ. The proteins that were tested were intended to increase phage-mediated gene transfer into mammalian cells. In order to utilize phage during gene transfer, phage will need to be able to overcome multiple intracellular barriers such as "cell attachment, cytoplasmic entry, endosomal escape, uncoating and nuclear import". Using this strategy, multiple peptides could be displayed in tandem, with each function to circumvent a separate barrier. During this process they were also able to determine that the number of fusions per phage particle was roughly 400 copies for gpD and 100 copies for gpV (Zanghi et al. 2007). In addition to using a system like this to overcome intracellular barriers, this system could potentially be employed to target intracellular pathogens, where the lower density display would presumably be employed for ligand interaction and receptor-mediated endocytosis, while a higher density display could be used to target the pathogen specifically.

A more recent and commercial example of phage display employed λ phage scaffold decorated with HIV-1 envelope protein gp140 via *in vitro* complementation. The immune response

elicited was then compared to that of soluble gp140. This strategy was employed because in their native state, envelope spike proteins are sparsely present on the virion and the ability to increase their density on the phage capsid, would in theory generate an increased immune response. Phage were decorated with a mixture (different molar ratios) of gpD:gp140 and wild-type gpD protein. Like Zanghi et al. (2005) and Hayes et al. (2010), Mattiacio et al. (2011) also discovered that phage were "recalcitrant" and not stable when decorated completely or with a 20-fold molar excess of fusion protein. Further to this, they also determined that some fusion proteins could stabilize phage particles even when they occupy only a fraction of the gpD binding sites. It was determined that the number of fusions incorporated into the capsid was 30 copies of Env trimers per particle. In regards to immune response, the authors did not observe an increased response to the decorated phage as compared to the conventional protein (Mattiacio et al. 2011). This shortfall may have been circumvented by the system described here, whereby utilizing a weak suppressor could have increased the number of fusions per particle. This in turn could have elicited a stronger immune response than what was observed with the conventional protein. Each of these groups also executed codon optimization in developing their constructs. This allowed for more efficient protein expression and decreased the homology of fusions to native λ sequences, thus decreasing the potential for homologous recombination between alleles (Zanghi et al. 2005).

4.2.1.2 Use of Phage in Gene Transfer

An early use of filamentous phage for gene transfer and delivery was first reported by Hart et al. (1994). In this study, phage fd was employed to display a cyclic-binding peptide sequence via translational fusion to major coat protein pVIII. This N-terminal fusion was shown to bind to cells and be efficiently internalized where competition and cell binding assays, staining and different forms of microscopy detected cell binding. Approximately 300 copies of fusion protein were present per phage (Hart et al. 1994). The same peptide sequence was then fused to the major tail protein. hypothesizing that λ is a more suitable candidate for transfecting mammalian cells. The double stranded DNA genome of λ would be more effective in cell transfection compared to single-stranded filamentous phage DNA that would need to be converted to double-stranded. These modified phage were shown to transfect mammalian cells at a remarkable frequency as compared to the control counterparts that showed no significant interaction with cells. (Dunn 1996).

Lankes et al. (2007) expanded the application of lambda as a gene or vaccine delivery vector by executing phage-mediated gene transfer *in vivo*. They constructed recombinant λ particles encoding firefly luciferase, in order to visualize gene delivery in real-time via the use of bioluminescence imaging (Xenogen IVIS system). They also determined that pre-immunization of mice with wt λ, a few weeks before immunization with recombinant phage conferred increased luciferase expression compared to unprimed control mice (Lankes et al. 2007). They next fused a $\alpha_v\beta_3$ (CD51/CD61) receptor integrin-binding peptide to gpD to increase its uptake by receptor-mediated pinocytosis. This integrin was chosen because it is known to play a role in the binding/internalization of a number of mammalian viruses and it also has been previously used to enhance the targeting of modified virus vectors to dendritic cells, a particularly useful accessory cell target for a vaccine vector. Through the use of this recombinant phage, the study showed an increased internalization versus a nonfused phage, where internalization was decreased in a dose-dependent

fashion; similar to findings by Vaccaro et al., (2006) who noted a similar decrease in internalization upon addition of competitor protein, indicating a receptor-mediated process. The recombinant phage outperformed the control cells both *in vitro* and *in vivo*. In addition, there was a 100-fold increase in the efficiency of phage internalization into integrin positive cells vs. control cells, but only about a 3-fold increase in the level of phage-mediated gene expression, suggesting that an increase in internalization does not correspond to a comparable increase in delivery of genetic material. Overall, this study provided a proof-of-concept for the use of recombinant phage to increase the gene transfer *in vivo* and also provides compelling argument for the use of phage in transgene delivery (Lankes et al. 2007)

Sapinoro et al. (2008) further explored pre-immunization as an approach to increase the uptake of recombinant phage, termed *antibody-dependent enhancement*. In concept, as "virus-specific antibodies fail to completely neutralize virus infectivity, the opsonization instead permits the more efficient infection of susceptible host cells such as monocytes and macrophages". The group's goal was to develop an *in vitro* model for this phenomenon in mammalian cells by bacteriophage λ vectors and determine their mechanisms. Since it is known that this effect can be mediated through cellular receptors specific for the Fc portion of IgG, the group used a cell line expressing human Fc gamma receptor (FcγR) receptor. The conclusions of this study indicated that antibody-dependent enhancement of phage-mediated gene transfer requires a receptor on the surface of target cells. In addition, prior immunization with wild-type phage results in more efficient phage-mediated gene expression in live mice and this increased transduction is undertaken through a receptor-mediated endocytic mechanism rather than through phagocytosis (Sapinoro et al. 2008).

Overall, the system created by this research study has many advantages for use in development of downstream vaccines and targeted gene therapy approaches. When undertaking a vaccination approach high-density display may be preferable as functionality of the fused protein may not be critical. In contrast, an application such as targeted gene therapy relies upon ligand interaction and proper folding/function of the fusion to improve cell specificity or enhanced endocytosis. The ability to control the number of fusions provides power and flexibility to cater mosaic phage to different scenarios and needs. Moreover, the ability to control the number of fusions and gpD molecules could reduce the chance of recalcitrance and improve viability. Finally, this system can further be expanded to generate multiple fusions, and polyvalent therapeutics.

4.3 Future Experimentation (Next Steps)

In order to further increase the likelihood and applicability of this research moving forward, necessary future experimentation is outlined below. During the preparation of this thesis, new work in our lab has been carried out that addresses many of the next steps indicated here. In progress or complete work directly related to the future steps outlined here has been inserted into Appendix A with description.

1. Additional plating experiments to confirm the viability of phage and varying levels of D:GFP expression; more effective means of phage preparation are required due to the occurrence of low titres when using traditional lysate preparation methods (CsCl, PEG precipitation, large volume batch cultures).

- Table 2 of Appendix A shows a continuation of this work. As noted in my work here, the greatest viability (eop) was again observed for the strong suppressors grown at low temperatures and 37° C is the ideal temperature for growth on a weak (SupD) or nonsuppressor strain. These additional results follow the same trends as those observed during the initial experimentation of this study.

2. Determination of a more effective way to quantify the number of GFP fusions present per phage capsid under varying conditions. This may include the use of an antibody-based approach (ELISA, Western Blot) or potentially the use of a more specific measurement instrument such as Fluorescence Activated Cell Sorting (FACS), FCS or photon antibunching. Once a more effective measurement of fusions can be determined, further experiments can be designed to determine if phage are viable and if populations are heterogeneous or homogenous.
    - To compare fluorescence of phage from various preparations, flow cytometry experiments were performed for SupE (Sokolenko et al. 2012) as well as other strains (Table 4 of Appendix A). As expected the weak suppressor (SupD) and the nonsuppressor strains again show the highest level of decoration. In addition, for all species examined, the greatest decoration was recorded at the optimal temperature of 37° C, which is on point, with all previous studies.
3. Further investigation into inner filtering when high-density display is achieved with GFP. If this phenomenon is observed, qualitative fluorescence measurements may need to be adjusted (Scholz et al. 2000).
    - This work has yet to be completed, but further fluorescent work through the use of FACS has continued to follow expected trends. This being said, there could still be an underestimation of the level of fluorescence emitted by each phage particle. Because more quantitative approaches have been taken to count the number of fusions per phage, this potential phenomenon becomes more relevant in helping to determine if fusion-to-fusion interactions occur between and within phage particles, which could be very useful information when employing alternative fusions for downstream applications.
4. Supplementary exploration into the supD expression system, as the use of this cell and a mosaic approach (fusion and wild-type) may be the most effective way to achieve nearly 100% display with fusions, when large recalcitrant proteins are desired for display.
    - This work has yet to be completed, but will pose an interesting task and a very important one in determining the future potential of this work and how relevant it will be to specifically the development of vaccines. Further exploration into the ability for high-density (maximal display) becomes a very important caveat to the development of vaccines and the ability to elicit an appropriate immune response. In relation to this, it will also be important to further explore this specific expression, as it will not only help to indicate the level of display possible, but may also give insight into any restrictions that exist as to the type and size of peptide/protein that can be fused to gpD as traditional recalcitrance may be able to be eliminated for some fusions.
    - Tables 5 and 6 in Appendix A show sizing of phage grown on different strains. Interestingly, when phage are complemented with wild type gpD, all suppressor strains are relatively the same size, whereas the nonsuppressor strain is significantly larger,

which may be because no suppressor is present and therefore gpD is incorporated more efficiently, with no effect on assembly or viability. Correspondingly, when size comparisons are made between decorated phage (Table 6), considerable differences are seen not only between phage preparations on the various suppressors strains, but as expected, particles are much larger than their non-decorated counterparts. As in this work, 37° C again confers the ideal temperature for fusion, regardless of bacterial strain, but unlike the wild type complementation, the SupD and nonsuppressor strain phage preparations lead the pack, with once again, the nonsuppressor showing the greatest diameter.

5. Forrer and Jaussi (1998), produced a His-tagged derivative of gpD, they named gpHD. This fusion partner is seen to be able to mediate optimal translation initiation while reducing inclusion body formation and protein degradation, making it an ideal fusion partner for high-level expression of soluble heterologous protein in the cytoplasm of *E. coli*. The authors believe in order to do this gpHD acts as a "cytoplasmic anchor", allowing its fusion partner more time to fold which decreases the likelihood of aggregation and degradation (Forrer, Jaussi 1998). Similar incremental improvements could be made to future gpD fusion constructs taking into account advantageous modifications that increase the functionality and create optimal conditions for each individual fusion protein.
    - In addition to exploring other incremental improvements to optimize this system, it is also important to explore appropriate applications and fusion partners as eGFP was employed for exploration and optimization purposes only. One application currently being characterized in our lab is the expression of *S. aureus* endolysin on the phage capsid to serve as a bacteriolytic therapeutic against Staphylococcal infections.

Appendix A Supplementary Data

The data below is supplementary and is part of a current paper that is in draft form within our lab.

Nicastro, J., Sheldon, K., Kaur, T., Aucoin, M., and R.A. Slavcev*. 2013. Construction and development of a fine-tuned lytic phage display system. *Applied Microbiology and Biotechnology.*

Table 2. Variable amber suppression and complementation of the *Dam15* mutation

Strain [1] / Plasmid [2]	**Relative efficiency of plating (eop) [3]**				
	30° C	**32-33 ° C**	**35 ° C**	**37 ° C**	**39-40 ° C**
Sup-	nd	nd	nd	1.92×10^{-6}	nd
pD⁻	4.06×10^{-6}	5.0×10^{-6}	$3.1x\ 10^{-6}$	1.7×10^{-6}	2.0×10^{-6}
pD^{+}	7.5×10^{-6}	3.2×10^{-5}	2.1×10^{-4}	0.15	0.93
pD::eGFP	7.5×10^{-6}	2.0×10^{-5}	2.0×10^{-5}	0.02	0.01
SupD	nd	nd	nd	1.13×10^{-5}	nd
pD⁻	8.8×10^{-5}	6.5×10^{-5}	1.5×10^{-5}	9.5×10^{-6}	2.3×10^{-5}
pD::eGFP	4.9×10^{-5}	1.8E-5	8E-5	0.09	0.05
SupE	nd	nd	nd	0.09	nd
pD⁻	0.04	0.11	0.07	0.03	0.08
pD::eGFP	0.1	0.04	0.02	0.07	0.03
SupF	nd	nd	nd	0.19	nd
pD⁻	0.01	0.01	0.04	0.04	0.03
pD::eGFP	0.1	0.13	0.06	0.07	0.05

[1] Derivatives are W3101 background.

[2] Derivatives of CI857 temperature regulated expression plasmid pPL451.

[3] All eop determinations from a minimum of three assay and determined using BB4 (SupE, SupF) as the 100% control.

Table 4. Estimated average eGFP molecules per phage.

Strain (+/- Plasmid) [1]	Estimated eGFP/phage [2]			
	30°C	**35°C**	**37°C**	**39°C**
Sup⁻ [pD::eGFP]	n/a	44 ± 2	115 ± 6	61 ± 10
SupD [pD::eGFP]	86 ± 19	127 ± 5	147 ± 33	142 ± 25
SupE [pD::eGFP]	46 ± 15	53 ± 5	77 ± 1	69 ± 1
SupF [pD::eGFP]	65 ± 1	69 ±	89 ± 2	69 ± 5

[1] all strains are derivatives of W3101.

[2] fluorescence measurements were divided by those derived from λF7 grown on that strain. Values in parentheses denote calculated number of functional eGP fusions per phage interpolated from eGFP purified protein fluorescence calibration curve.

[3] Phage preparation on W3101[pD] at 37°C expressing gpD_{wt} *in trans*

Table 5. Sizing of λ *Dam15* phage grown on suppressor strain series

Strain [1]	gpD Allele	Relative size difference [2]
Sup⁻ [3]	gpD_{wt}	1.1 ± 0.2
SupE	gpD_{wt}	1.0
SupD	gpDQ68S	0.3 ± 0.1
SupF	gpDQ68Y	0.6 ± 0.3

[1] All strains are derivatives of W3101

[2] A minimum of three runs of triplicate determinations of size determination from DLS were divided by size determinations for phage generated of W3101 *supE*, conferring the D_{wt} allele decoration of λ*Dam15* phage in absence of complementation.

[3] Phage preparation on W3101[pD] at 37°C expressing gpD_{wt} *in trans*

Table 6. Sizing of λ *Dam15* phage variably decorated by gpD::eGFP

Strain [+ Plasmid] [1]	Times (X) increase in phage diameter [2]			
	30°C	**35°C**	**37°C**	**39°C**
Sup⁻	nd	nd	n/a	nd
Sup⁻ [pD::eGFP]	n/a	2.2 ± 0.5	5.5 ± 0.8	3.5 ± 0.9
SupD	nd	nd	0.3 ± 0.03	nd
SupD [pD::eGFP]	0.8 ± 0.1	1.2 ± 0.7	3.1 ± 1.5	1.8 ± 0.2
SupE	nd	nd	1.0 ± 0.1	nd
SupE [pD::eGFP]	0.9 ± 0.2	1.0 ± 0.1	1.7 ± 0.2	1.2 ± 0.2
SupF	nd	nd	0.67 ± 0.3	nd
SupF [pD::eGFP]	1.0 ± 0.3	1.3 ± 0.2	1.6 ± 0.6	1.0 ± 0.3

[1] Lysate produced on strain at respective temp. All strains are derivatives of W3101.

[2] A minimum of three runs of triplicate determinations of size determination from DLS were divided by size determinations for naked phage grown on each of the Sup strains. Comparisons are for phage grown on SupE in absence of complementation.

[3] nd, not done

References

Ansuini, H., Cicchini, C., Nicosia, A., Tripodi, M., Cortese, R. & Luzzago, A. 2002, "Biotin-tagged cDNA expression libraries displayed on lambda phage: a new tool for the selection of natural protein ligands", *Nucleic acids research,* vol. 30, no. 1362-4962; 15, pp. 78.

Aoki, T., Tahara, T., Satoh, K., Fujino, H. & Watabe, H. 2003, "General properties of GFP-display, an electrophoretic analysis for single amino acid changes in target polypeptides.", *Analytical Biochemistry,* vol. 317, no. 1, pp. 107-115.

Bastien, N., Trudel, M. & Simard, C. 1997, "Protective immune responses induced by the immunization of mice with a recombinant bacteriophage displaying an epitope of the human respiratory syncytial virus", *Virology,* vol. 234, no. 1, pp. 118-122.

Benzer, S. & Champe, S.P. 1962, "A change from nonsense to sense in the genetic code", *Proceedings of the National Academy of Sciences of the United States of America,* vol. 48, pp. 1114-1121.

Bernard, H.U., Remaut, E., Hershfield, M.V., Das, H.K., Helinski, D.R., Yanofsky, C. & Franklin, N. 1979, "Construction of plasmid cloning vehicles that promote gene expression from the bacteriophage lambda pL promoter", *Gene,* vol. 5, no. 1, pp. 59-76.

Bratkovic, T. 2010, "Progress in phage display: evolution of the technique and its application", *Cellular and molecular life sciences : CMLS,* vol. 67, no. 5, pp. 749-767.

Breitling, R., Sorokin, A.V. & Behnke, D. 1990, "Temperature-inducible gene expression in *Bacillus subtilis* mediated by the c*I857*-encoded repressor of bacteriophage lambda", *Gene,* vol. 93, no. 1, pp. 35-40.

Brenner, S., Stretton, A.O. & Kaplan, S. 1965, "Genetic code: the 'nonsense' triplets for chain termination and their suppression", *Nature,* vol. 206, no. 988, pp. 994-998.

Brown, E.D. 2004, "Drugs against superbugs: private lessons from bacteriophages", *Trends Biotechnol,* vol. 22, no. 9, pp. 434-436.

Brussow, H. 2005, "Phage therapy: the *Escherichia coli* experience", *Microbiology,* vol. 151, pp. 2133-2140.

Clark, J.R. & March, J.B. 2006, "Bacteriophages and biotechnology: vaccines, gene therapy and antibacterials", *Trends in biotechnology,* vol. 24, no. 5, pp. 212-218.

Coates, A.R. & Hu, Y. 2007, "Novel approaches to developing new antibiotics for bacterial infections", *Br J Pharmacol,* vol. 152, no. 8, pp. 1147-1154.

Curiel, T.J., Morris, C., Brumlik, M., Landry, S.J., Finstad, K., Nelson, A., Joshi, V., Hawkins, C., Alarez, X., Lackner, A. & Mohamadzadeh, M. 2004, "Peptides identified through phage display direct immunogenic antigen to dendritic cells", *Journal of immunology (Baltimore, Md.: 1950),* vol. 172, no. 12, pp. 7425-7431.

Dai, M., Temirov, J., Pesavento, E., Kiss, C., Velappan, N., Pavlik, P., Werner, J.H. & Bradbury, A.R. 2008, "Using T7 phage display to select GFP-based binders", *Protein engineering, design & selection : PEDS,* vol. 21, no. 7, pp. 413-424.

d'Herelle, F. & Smith, G.H. 1926, *The bacteriophage and its behavior,* The Williams & Wilkins Company, Baltimore, Md.

Dokland, T. & Murialdo, H. 1993, "Structural Transitions During Maturation of Bacteriophage Lambda Capsids", *Journal of Molecular Biology,* vol. 233, no. 4, pp. 682-694.

Duckworth, D.H. 1976, ""Who discovered bacteriophage?"", *Bacteriological Reviews,* vol. 40, no. 4, pp. 793-802.

Dulbecco, R. 1982, *Viruses with recombinant surface proteins*, Patent 4593002, United States of America.

Dunn, I.S. 1996, "Mammalian cell binding and transfection mediated by surface-modified bacteriophage lambda", *Biochimie,* vol. 78, no. 10, pp. 856-861.

Dunn, I.S. 1995, "Assembly of Functional Bacteriophage Lambda Virions Incorporating C-Terminal Peptide or Protein Fusions with the Major Tail Protein", *Journal of Molecular Biology,* vol. 248, no. 3, pp. 497-506.

Efimov, V.P., Nepluev, I.V. & Mesyanzhinov, V.V. 1995, "Bacteriophage T4 as a surface display vector", *Virus genes,* vol. 10, no. 2, pp. 173-177.

Eguchi, A., Akuta, T., Okuyama, H., Senda, T., Yokoi, H., Inokuchi, H., Fujita, S., Hayakawa, T., Takeda, K., Hasegawa, M. & Nakanishi, M. 2001, "Protein transduction domain of HIV-1 Tat protein promotes

efficient delivery of DNA into mammalian cells", *The Journal of biological chemistry,* vol. 276, no. 28, pp. 26204-26210.
Forrer, P. & Jaussi, R. 1998, "High-level expression of soluble heterologous proteins in the cytoplasm of *Escherichia coli* by fusion to the bacteriophage lambda head protein D", *Gene,* vol. 224, no. 1-2, pp. 45-52.
Fortuna, W., Miedzybrodzki, R., Weber-Dabrowska, B. & Gorski, A. 2008, "Bacteriophage therapy in children: facts and prospects", *Medical science monitor : international medical journal of experimental and clinical research,* vol. 14, no. 8, pp. RA126-32.
Gamage, L.N., Ellis, J. & Hayes, S. 2009, "Immunogenicity of bacteriophage lambda particles displaying porcine Circovirus 2 (PCV2) capsid protein epitopes", *Vaccine,* vol. 27, no. 47, pp. 6595-6604.
Garufi, G., Minenkova, O., Lo, P.C., Pernice, I. & Felici, F. 2005, "Display libraries on bacteriophage lambda capsid", *Biotechnology annual review,* vol. 11, no. 1387-2656, pp. 153-190.
Geier, M.R., Trigg, M.E. & Merril, C.R. 1973, "Fate of bacteriophage lambda in non-immune germ-free mice", *Nature,* vol. 246, no. 5430, pp. 221-223.
Goodman, H.M., Abelson, J., Landy, A., Brenner, S. & Smith, J.D. 1968, "Amber suppression: a nucleotide change in the anticodon of a tyrosine transfer RNA", *Nature,* vol. 217, no. 5133, pp. 1019-1024.
Gorski, A., Miedzybrodzki, R., Borysowski, J., Weber-Dabrowska, B., Lobocka, M., Fortuna, W., Letkiewicz, S., Zimecki, M. & Filby, G. 2009, "Bacteriophage therapy for the treatment of infections", *Current opinion in investigational drugs (London, England : 2000),* vol. 10, no. 8, pp. 766-774.
Gorski, A. & Weber-Dabrowska, B. 2005, "The potential role of endogenous bacteriophages in controlling invading pathogens", *Cellular and molecular life sciences : CMLS,* vol. 62, no. 5, pp. 511-519.
Gupta, A., Onda, M., Pastan, I., Adhya, S. & Chaudhary, V.K. 2003, "High-density Functional Display of Proteins on Bacteriophage Lambda", *Journal of Molecular Biology,* vol. 334, no. 2, pp. 241-254.
Guzman, C.A., Piatti, G., Walker, M.J., Guardati, M.C. & Pruzzo, C. 1994, "A novel *Escherichia coli* expression-export vector containing alkaline phosphatase as an insertional inactivation screening system", *Gene,* vol. 148, no. 1, pp. 171-172.
Haimovich, J. & Sela, M. 1969a, "Inactivation of bacteriophage T4, of poly-D-alanyl bacteriophage and of penicilloyl bacteriophage by immunospecifically isolated IgM and IgG antibodies", *Journal of immunology (Baltimore, Md.: 1950),* vol. 103, no. 1, pp. 45-55.
Haimovich, J. & Sela, M. 1969b, "Protein-bacteriophage conjugates: application in detection of antibodies and antigens", *Science (New York, N.Y.),* vol. 164, no. 885, pp. 1279-1280.
Hart, S.L., Knight, A.M., Harbottle, R.P., Mistry, A., Hunger, H.D., Cutler, D.F., Williamson, R. & Coutelle, C. 1994, "Cell binding and internalization by filamentous phage displaying a cyclic Arg-Gly-Asp-containing peptide", *The Journal of biological chemistry,* vol. 269, no. 17, pp. 12468-12474.
Hayes, S., Gamage, L.N. & Hayes, C. 2010, "Dual expression system for assembling phage lambda display particle (LDP) vaccine to porcine Circovirus 2 (PCV2)", *Vaccine,* vol. 28, no. 41, pp. 6789-6799.
Hayes, S. & Hayes, C. 1986, "Spontaneous lambda OR mutations suppress inhibition of bacteriophage growth by nonimmune exclusion phenotype of defective lambda prophage", *Journal of virology,* vol. 58, no. 3, pp. 835-842.
Hohn, T. & Katsura, I. 1977, "Structure and assembly of bacteriophage lambda", *Current topics in microbiology and immunology,* vol. 78, pp. 69-110.
Imber, R., Tsugita, A., Wurtz, M. & Hohn, T. 1980, "Outer surface protein of bacteriophage lambda", *Journal of Molecular Biology,* vol. 139, no. 3, pp. 277-295.
Inokuchi, H., Yamao, F., Sakano, H. & Ozeki, H. 1979, "Identification of transfer RNA suppressors in *Escherichia coli*. I. Amber suppressor su+2, an anticodon mutant of tRNA2Gln", *Journal of Molecular Biology,* vol. 132, no. 4, pp. 649-662.
Jechlinger, W., Szostak, M.P., Witte, A. & Lubitz, W. 1999, "Altered temperature induction sensitivity of the lambda pR/cI857 system for controlled gene E expression in *Escherichia coli*", *FEMS microbiology letters,* vol. 173, no. 2, pp. 347-352.
Jepson, C.D. & March, J.B. 2004, "Bacteriophage lambda is a highly stable DNA vaccine delivery vehicle", *Vaccine,* vol. 22, no. 19, pp. 2413-2419.
Jestin, J.L. 2008, "Functional cloning by phage display", *Biochimie,* vol. 90, no. 9, pp. 1273-1278.

Kaiser, A.D. 1966, "On the internal structure of bacteriophage lambda", *The Journal of general physiology,* vol. 49, no. 6, pp. 171-178.
Kalnina, Z., Silina, K., Meistere, I., Zayakin, P., Rivosh, A., Abols, A., Leja, M., Minenkova, O., Schadendorf, D. & Line, A. 2008, "Evaluation of T7 and lambda phage display systems for survey of autoantibody profiles in cancer patients", *Journal of immunological methods,* vol. 334, no. 0022-1759; 1-2, pp. 37-50.
Katsura, I. 1983, "Structure and inherent properties of the bacteriophage lambda head shell , : IV. Small-head mutants", *Journal of Molecular Biology,* vol. 171, no. 3, pp. 297-317.
Kong, B. & Ma, W.J. 2006, "Display of aggregation-prone ligand binding domain of human PPAR gamma on surface of bacteriophage lambda", *Acta Pharmacologica Sinica,* vol. 27, no. 1671-4083; 1, pp. 91-99.
Kropinski, A.M. 2006, "Phage Therapy - Everything Old is New Again", *The Canadian Journal of Infectious Diseases & Medical Microbiology,* vol. 17, no. 5, pp. 297-306.
Lankes, H.A., Zanghi, C.N., Santos, K., Capella, C., Duke, C.M. & Dewhurst, S. 2007, "*In vivo* gene delivery and expression by bacteriophage lambda vectors", *Journal of applied microbiology,* vol. 102, no. 1364-5072; 5, pp. 1337-1349.
Lieb, M. 1966, "Studies of heat-inducible lambda bacteriophage. I. Order of genetic sites and properties of mutant prophages", *Journal of Molecular Biology,* vol. 16, no. 1, pp. 149-163.
Lindqvist, B.H. 2005, "Phage in Display" in Oxford University Press; Second Edition edition (Dec 1 2005), , pp. 686-694.
Liu, J., Dehbi, M., Moeck, G., Arhin, F., Bauda, P., Bergeron, D., Callejo, M., Ferretti, V., Ha, N., Kwan, T., McCarty, J., Srikumar, R., Williams, D., Wu, J.J., Gros, P., Pelletier, J. & DuBow, M. 2004, "Antimicrobial drug discovery through bacteriophage genomics", *Nature biotechnology,* vol. 22, no. 2, pp. 185-191.
Lowman, H.B. & Bina, M. 1990, "Temperature-mediated regulation and downstream inducible selection for controlling gene expression from the bacteriophage lambda pL promoter", *Gene,* vol. 96, no. 1, pp. 133-136.
Makela, O. 1966, "Assay of anti-hapten antibody with the aid of hapten-coupled bacteriophage", *Immunology,* vol. 10, no. 1, pp. 81-86.
March, J.B., Clark, J.R. & Jepson, C.D. 2004, "Genetic immunisation against hepatitis B using whole bacteriophage lambda particles", *Vaccine,* vol. 22, no. 13-14, pp. 1666-1671.
Maruyama, I.N., Maruyama, H.I. & Brenner, S. 1994, "Lambda foo: a lambda phage vector for the expression of foreign proteins", *Proceedings of the National Academy of Sciences of the United States of America,* vol. 91, no. 17, pp. 8273-8277.
Mattiacio, J., Walter, S., Brewer, M., Domm, W., Friedman, A.E. & Dewhurst, S. 2011, "Dense display of HIV-1 envelope spikes on the lambda phage scaffold does not result in the generation of improved antibody responses to HIV-1 Env", *Vaccine,* vol. 29, no. 14, pp. 2637-2647.
Mikawa, Y.G., Maruyama, I.N. & Brenner, S. 1996, "Surface Display of Proteins on Bacteriophage [lambda] Heads", *Journal of Molecular Biology,* vol. 262, no. 1, pp. 21-30.
Minenkova, O., Pucci, A., Pavoni, E., De, T.A., Fortugno, P., Gargano, N., Cianfriglia, M., Barca, S., De, P.S., Martignetti, A., Felici, F., Cortese, R. & Monaci, P. 2003, "Identification of tumor-associated antigens by screening phage-displayed human cDNA libraries with sera from tumor patients", *International journal of cancer. Journal international du cancer,* vol. 106, no. 0020-7136; 4, pp. 534-544.
Moore, S. 2011, *, Sauer: P1vir phage transduction*. Available: http://openwetware.org/wiki/Sauer:P1vir_phage_transduction [2009, June].
Mott, J.E., Grant, R.A., Ho, Y.S. & Platt, T. 1985, "Maximizing gene expression from plasmid vectors containing the lambda PL promoter: strategies for overproducing transcription termination factor rho", *Proceedings of the National Academy of Sciences of the United States of America,* vol. 82, no. 1, pp. 88-92.
Mullen, L.M., Nair, S.P., Ward, J.M., Rycroft, A.N. & Henderson, B. 2006, "Phage display in the study of infectious diseases", *Trends in microbiology,* vol. 14, no. 3, pp. 141-147.
NBRP-Prokaryotes(E.coli) 2009, *, National BioResource Project*. Available: http://www.shigen.nig.ac.jp.proxy.lib.uwaterloo.ca/ecoli/strain/top/top.jsp [2011, February 24].

Nicastro, J., Sheldon, K., El-zarkout, F., Sokolenko, S., Aucoin, M. & Slavcev, R. unpublished, "Construction and Analysis of a Genetically Tuneable Lytic Phage Display System", .

Nicol, C.G., Denby, L., Lopez-Franco, O., Masson, R., Halliday, C.A., Nicklin, S.A., Kritz, A., Work, L.M. & Baker, A.H. 2009, "Use of in vivo phage display to engineer novel adenoviruses for targeted delivery to the cardiac vasculature", *FEBS letters,* vol. 583, no. 12, pp. 2100-2107.

Niwa, M., Maruyama, H., Fujimoto, T., Dohi, K. & Maruyama, I.N. 2000, "Affinity selection of cDNA libraries by lambda phage surface display", *Gene,* vol. 256, no. 1-2, pp. 229-236.

Normanly, J., Masson, J.M., Kleina, L.G., Abelson, J. & Miller, J.H. 1986, "Construction of two *Escherichia coli* amber suppressor genes: tRNAPheCUA and tRNACysCUA", *Proceedings of the National Academy of Sciences of the United States of America,* vol. 83, no. 17, pp. 6548-6552.

Pavoni, E., Vaccaro, P., Pucci, A., Monteriu, G., Beghetto, E., Barca, S., Dupuis, M.L., De Pasquale, C.A., Lugini, A., Cianfriglia, M., Cortesi, E., Felici, F. & Minenkova, O. 2004, "Identification of a panel of tumor-associated antigens from breast carcinoma cell lines, solid tumors and testis cDNA libraries displayed on lambda phage", *BMC cancer [computer file],* vol. 4, no. 1471-2407, pp. 78.

Petrenko, V. 2008, "Evolution of phage display: from bioactive peptides to bioselective nanomaterials", *Expert.Opin.Drug Deliv.,* vol. 5, no. 1742-5247; 8, pp. 825-836.

Pinheiro, L.B., Gibbs, M.D., Vesey, G., Smith, J.J. & Bergquist, P.L. 2008, "Fluorescent reference strains of bacteria by chromosomal integration of a modified green fluorescent protein gene", *Applied Microbiology and Biotechnology,* vol. 77, no. 6, pp. 1287-1295.

Remaut, E., Stanssens, P. & Fiers, W. 1981, "Plasmid vectors for high-efficiency expression controlled by the PL promoter of coliphage lambda", *Gene,* vol. 15, no. 1, pp. 81-93.

Ren, Z.J., Lewis, G.K., Wingfield, P.T., Locke, E.G., Steven, A.C. & Black, L.W. 1996, "Phage display of intact domains at high copy number: a system based on SOC, the small outer capsid protein of bacteriophage T4", *Protein science : a publication of the Protein Society,* vol. 5, no. 9, pp. 1833-1843.

Saida, F., Uzan, M., Odaert, B. & Bontems, F. 2006, "Expression of highly toxic genes in *E. coli*: special strategies and genetic tools", *Current Protein & Peptide Science,* vol. 7, no. 1, pp. 47-56.

Santi, E., Capone, S., Mennuni, C., Lahm, A., Tramontano, A., Luzzago, A. & Nicosia, A. 2000, "Bacteriophage lambda display of complex cDNA libraries: a new approach to functional genomics", *Journal of Molecular Biology,* vol. 296, no. 2, pp. 497-508.

Santini, C., Brennan, D., Mennuni, C., Hoess, R.H., Nicosia, A., Cortese, R. & Luzzago, A. 1998, "Eficient display of an HCV cDNA expression library as C-terminal fusion to the capsid protein D of bacteriophage lambda", *Journal of Molecular Biology,* vol. 282, no. 1, pp. 125-135.

Sapinoro, R., Volcy, K., Rodrigo, W.W., Schlesinger, J.J. & Dewhurst, S. 2008, "Fc receptor-mediated, antibody-dependent enhancement of bacteriophage lambda-mediated gene transfer in mammalian cells", *Virology,* vol. 373, no. 2, pp. 274-286.

Sarabhai, A.S., Stretton, A.O., Brenner, S. & Bolle, A. 1964, "Co-Linearity of the Gene with the Polypeptide Chain", *Nature,* vol. 201, pp. 13-17.

Scholz, O., Thiel, A., Hillen, W. & Niederweis, M. 2000, "Quantitative analysis of gene expression with an improved green fluorescent protein. p6", *European journal of biochemistry / FEBS,* vol. 267, no. 6, pp. 1565-1570.

Smith, G.P. 1985, "Filamentous Fusion Phage: Novel Expression Vectors that Display Cloned Antigens on the Virion Surface", *Science,* vol. 228, no. 4705, pp. 1315-1317.

Smith, H.W. & Huggins, M.B. 1982, "Successful treatment of experimental *Escherichia coli* infections in mice using phage: its general superiority over antibiotics", *Journal of general microbiology,* vol. 128, no. 2, pp. 307-318.

Sokolenko, S., Nicastro, J., Slavcev, R. & Aucoin, M.G. 2012, "Graphical analysis of flow cytometer data for characterizing controlled fluorescent protein display on lambda phage", *Cytometry.Part A : the journal of the International Society for Analytical Cytology,* vol. 81, no. 12, pp. 1031-1039.

Steege, D.A. 1983, "A nucleotide change in the anticodon of an *Escherichia coli* serine transfer RNA results in supD-amber suppression", *Nucleic acids research,* vol. 11, no. 11, pp. 3823-3832.

Sternberg, N. & Hoess, R.H. 1995, "Display of peptides and proteins on the surface of bacteriophage lambda", *Proceedings of the National Academy of Sciences of the United States of America,* vol. 92, no. 5, pp. 1609-1613.

Sternberg, N. & Weisberg, R. 1977, "Packaging of coliphage lambda DNA. II. The role of the gene D protein", *Journal of Molecular Biology,* vol. 117, no. 3, pp. 733-759.

Szybalski, W., Bovre, K., Fiandt, M., Guha, A., Hradecna, Z., Kumar, S., Lozeron HA, S., Maher, V.M., Nijkamp, H.J., Summers, W.C. & Taylor, K. 1969, "Transcriptional controls in developing bacteriophages", *Journal of cellular physiology,* vol. 74, no. 2, pp. Suppl 1:33-70.

Thomas, B.S., Nishikawa, S., Ito, K., Chopra, P., Sharma, N., Evans, D.H., Tyrrell, D.L., Bathe, O.F. & Rancourt, D.E. 2012, "Peptide vaccination is superior to genetic vaccination using a recombineered bacteriophage lambda subunit vaccine", *Vaccine,* vol. 30, no. 6, pp. 998-1008.

Twort, F.W. 1915, "An Investigation On The Nature Of Ultra-Microscopic Viruses", vol. 186, no. 4814, pp. 1241-1243.

Vaccaro, P., Pavoni, E., Monteri·, G., Andrea, P., Felici, F. & Minenkova, O. 2006, "Efficient display of scFv antibodies on bacteriophage lambda", *Journal of immunological methods,* vol. 310, no. 1-2, pp. 149-158.

Velappan, N., Fisher, H.E., Pesavento, E., Chasteen, L., D'Angelo, S., Kiss, C., Longmire, M., Pavlik, P. & Bradbury, A.R. 2010, "A comprehensive analysis of filamentous phage display vectors for cytoplasmic proteins: an analysis with different fluorescent proteins", *Nucleic acids research,* vol. 38, no. 4, pp. e22.

Villaverde, A., Benito, A., Viaplana, E. & Cubarsi, R. 1993, "Fine regulation of *cI857*-controlled gene expression in continuous culture of recombinant *Escherichia coli* by temperature", *Applied and Environmental Microbiology,* vol. 59, no. 10, pp. 3485-3487.

Wan, X.M., Chen, Y.P., Xu, W.R., Yang, W.J. & Wen, L.P. 2009, "Identification of nose-to-brain homing peptide through phage display", *Peptides,* vol. 30, no. 2, pp. 343-350.

Wendt, J.L. & Feiss, M. 2004, "A fragile lattice: replacing bacteriophage lambda's head stability gene D with the shp gene of phage 21 generates the Mg2+-dependent virus, lambda shp", *Virology,* vol. 326, no. 1, pp. 41-46.

Witkiewicz, H. & Schweiger, M. 1982, "The head protein D of bacterial virus lambda is related to eukaryotic chromosomal proteins", *The EMBO journal,* vol. 1, no. 12, pp. 1559-1564.

Wurtz, M., Kistler, J. & Hohn, T. 1976, "Surface structure of in vitro assembled bacteriophage lambda polyheads", *Journal of Molecular Biology,* vol. 101, no. 1, pp. 39-56.

Yale University 2011, *, The Coli Genetic Stock Center*. Available: http://cgsc.biology.yale.edu/index.php [2011, February 24].

Yang, F., Forrer, P., Dauter, Z., Conway, J.F., Cheng, N., Cerritelli, M.E., Steven, A.C., Pluckthun, A. & Wlodawer, A. 2000, "Novel fold and capsid-binding properties of the lambda-phage display platform protein gpD", *Nature structural biology,* vol. 7, no. 3, pp. 230-237.

Zanghi, C.N., Lankes, H.A., Bradel-Tretheway, B., Wegman, J. & Dewhurst, S. 2005, "A simple method for displaying recalcitrant proteins on the surface of bacteriophage lambda", *Nucleic acids research,* vol. 33, no. 18, pp. e160.

Zanghi, C.N., Sapinoro, R., Bradel-Tretheway, B. & Dewhurst, S. 2007, "A tractable method for simultaneous modifications to the head and tail of bacteriophage lambda and its application to enhancing phage-mediated gene delivery", *Nucleic acids research,* vol. 35, no. 8, pp. e59.

Zeghouf, M., Li, J., Butland, G., Borkowska, A., Canadien, V., Richards, D., Beattie, B., Emili, A. & Greenblatt, J.F. 2004, "Sequential Peptide Affinity (SPA) system for the identification of mammalian and bacterial protein complexes", *Journal of proteome research,* vol. 3, no. 3, pp. 463-468.

Zucconi, A., Dente, L., Santonico, E., Castagnoli, L. & Cesareni, G. 2001, "Selection of ligands by panning of domain libraries displayed on phage lambda reveals new potential partners of synaptojanin 1", *Journal of Molecular Biology,* vol. 307, no. 5, pp. 1329-1339.